TAMPEREEN TEKNILLINEN YLIOPISTO
TAMPERE UNIVERSITY OF TECHNOLOGY

JUHO TUOMINEN

TESTING OF COORDINATED VOLTAGE CONTROL ALGORITHMS USING REAL TIME DIGITAL SIMULATOR

Master's Thesis

Examiner: professor Sami Repo
Examiner and topic approved by The Faculty Council of Computing and Electrical Engineering 8.5.2013

ABSTRACT

TAMPERE UNIVERSITY OF TECHNOLOGY
Master's Degree Programme in Electrical Engineering
TUOMINEN, JUHO: Testing of Coordinated Voltage Control Algorithms Using Real Time Digital Simulator
Master of Science Thesis, 97 pages
August 2013
Major: Electrical Power Engineering
Examiner: Professor Sami Repo
Keywords: RTDS, Active Voltage Control, Coordinated Voltage Control, Optimization, Software-in-the-loop

Since the use of renewable generation and small generation units is fast increasing in the power network, Distribution Network Operators (DNOs) need to reconsider the ways they are designing and controlling their networks. Traditionally generation units have been connected to the high voltage transmission network, but since many of the new Distributed Energy Resources (DERs), like solar power plants and wind turbines, are located far from the transmission network and at the ends of the distribution network, it is more cost effective to connect them to the distribution network instead. However, the distribution network has not been planned to have generation units connected to it and this can cause multiple problems with both the safe use of the network and the capacity of the feeders connecting the DERs. Coordinated voltage control has potential to solve or mitigate these problems by using the existing network more effectively.

During this thesis two coordinated voltage control algorithms created during the Adine project and the SGEM program were tested using the Real Time Digital Simulator and real distribution network data received from Koillis-Satakunnan Sähkö Oy. The first algorithm is called the rule based algorithm and it reacts to the voltage limit violations by following a pre-set order of rules. Its basic control part controls the tap changer of the primary substation transformer and the real and reactive power set point values of the generators connected into the network. The algorithm also contains a restoring part, which is used to undo the changes of the basic control part when network status allows for it. The other algorithm is called the optimizing algorithm and it uses Matlab optimization function to find the most optimal way to use the same resources as the rule based algorithm uses. The algorithms employ a state estimation of the network using data of the network components and status of the loads and generators in the network.

The algorithms were tested using 12 sequences, during which multiple different variables were changed to test the algorithms reaction to different network states. The results from these simulations are presented in a form of metric values derived from the raw data and as graphs portraying some of the key values, like the network maximum and minimum voltages and the power outputs of the distributed generators. The simulation results affirm that the algorithms do not contain any logical or design errors, but both algorithms could still be developed further. The optimizing algorithm is still missing few functions that have been planned to be part of it and this affects its efficiency in certain situations. In most cases, the optimizing algorithm is performing superiorly compared to the rule based algorithm, but this is mainly because the optimizing algorithm executes all of the control actions simultaneously, whereas the rule based algorithm controls one resource at the time. The rule based algorithm could be upgraded to improve the deduction process and to execute all of the changes at the same time, possibly making it able to compete with the optimizing algorithm in efficiency.

PREFACE

This thesis work was done at the Tampere University of Technology Department of Electrical Engineering between January and August 2013. I would like to offer my thanks to my supervisor, Professor Sami Repo for all of his insightful and friendly replies to my many questions during this thesis. I would also like to thank my co-workers, M.Sc. Ontrei Raipala for his help with the Real Time Digital Simulator and PSCAD and M.Sc. Anna Kulmala for her help with questions related to the algorithms. Last but not the least; I would like thank my father, M.Sc. Taisto Tuominen for all the help and inspiration he has given to me during my studies in the field of science.

Juho Tuominen

23.7.2013

CONTENTS

LIST OF SYMBOLS AND ABBREVIATIONS

δ_i	Voltage angle of the bus *i* [°].
τ	Turns ratio of the transformer.
$C_{curtailed}$	Price of the curtailed real power generation [€/MWh].
C_{losses}	Price of the network losses [€/MWh].
m	Tap ratio of the primary transformer.
N	Turns value of the transformer winding.
P_i	Real power injected in bus *i* [MW].
$P_{active,i}$	Real power of *i*th active resource [MW].
$P_{curtailed}$	Curtailed real power [MW].
$P_{gen,i}$	Real power generated in bus *i* [MW].
$P_{load,i}$	Real power consumed in bus *i* [MW].
P_{losses}	Network real power losses [MW].
$\mathbf{P_i}$	Vector of real powers of the buses.
Q_i	Reactive power injected in bus *i* [MVAr].
$Q_{active,i}$	Reactive power of *i*th active resource [MVAr].
$Q_{gen,i}$	Reactive power generated in bus *i* [MVAr].
$Q_{load,i}$	Reactive power consumed in bus *i* [MVAr].
$\mathbf{Q_i}$	Vector of reactive powers of the buses.
S	Apparent power [MVA].
$\mathbf{u_c}$	Vector of continuous variables.
$\mathbf{u_d}$	Vector of discrete variables.
V_i	Voltage of bus *i* [V].
V_{lower}	Minimum voltage limit value [V].
V_{orig}	Primary substation voltage with tap ratio of 1.0 [V].
V_{upper}	Maximum voltage limit value [V].
$\mathbf{V}$	Node voltage vector.
$\mathbf{x}$	Vector of dependent variables.
x	Vector in the Matlab implementation of the optimizing algorithm, that includes $\mathbf{x}$, $\mathbf{u_c}$ and $\mathbf{u_d}$.
$\mathbf{Y_{bus}}$	Bus admittance matrix.
Z_k	Leakage impedance of the transformer [Ω].
AMR	Automatic Meter Reading is functionality found in new generation energy meters that allows for reading of metering data remotely.
AVC	Automatic Voltage Controller is a relay used to control the OLTC.
AVCO	AVC Operating signal informs the algorithm that the AVC is in middle of changing the substation voltage reference.

AVR	Automatic Voltage Regulator is a device used to control generators output voltage by changing the excitation of the generator winding.
CVC	Coordinated Voltage Control combines multiple active voltage control methods to control the voltage in a certain area of the network.
DER	Distributed Energy Resource is a generator or other active power system component like a controllable capacitor or a reactor located away from the primary substation.
DG	Distributed Generator is a term used for small power generation unit connected to the distribution network.
DIN	DIN rail is a standard type metal rail used for mounting equipment into racks.
DMS	Distribution Management System is the main tool for controlling and monitoring the distribution network and it can include other systems, for example NIS and/or SCADA.
DNO	Distribution Network Operator is a company responsible for the use and development of a distribution network.
IEEE	Institute of Electrical and Electronics Engineers is a professional association dedicated to advancing technological innovation and excellence.
NIS	Network Information System is a system containing information and models of the physical network.
OLTC	On Load Tap Changer is a device used to change transformer windings connection status while transformer is energized.
PID	Proportional-Integrative-Derivative controller is a general control loop feedback device.
PSCAD	Power system simulator program with a visual interface.
RSCAD	Control program for the RTDS.
RTDS	Real Time Digital Simulator is power system simulator developed by RTDS Technologies.
SCADA	Supervisory Control And Data Acquisition is type of a software used to supervise and control automated system, for example a distribution network or a factory system.
SGEM	Smart Grids and Energy Markets is a research program of which this thesis is part of, it is managed by Cleen ltd.
SIL	Software-In-the-Loop is a testing method where software is being tested in a simulator environment while it's being developed.
TCO	Tap Changer Operating signal informs the algorithm that the tap changer is in middle of changing the tap setting.

1 INTRODUCTION

In traditional power distribution networks the power flow is assumed to be unidirectional, because power plants are large and need to be connected to the highest available voltage level to minimize losses during the transfer. This causes the power to always flow down from the transmission network to the distribution network and in the distribution network down from the primary substation towards the consumer. [1]

The increasing penetration of Distributed Energy Resources (DERs) like Distributed Generators (DGs) in the distribution networks force Distribution Network Operators (DNOs) to consider new options for controlling the power flow and voltage levels in their networks. Many DGs are located far from the transmission network and in the far ends of the distribution network, for example coastal or offshore wind farms. Owners of these DGs prefer connecting their resources to the nearest possible network to minimize the connection costs. When a DG is being connected to a weak network, the voltage levels in the end of the network can raise, effectively reducing the amount of generating capacity that can be connected. Since traditional network planning also assumes that there are no controllable resources in the network that could take part in controlling the voltage, the problem of voltage rise is handled by reinforcing the existing network or building a dedicated feeder only for the DG. In many cases these measures cause considerable costs. [1; 2]

An alternative to the passive voltage control strategy mentioned before is to employ active voltage control measures. These can include, but are not limited to, controlling the On Line Tap Changer (OLTC) of the primary transformer to change the voltage levels at the whole area controlled by the tap changer or controlling the real and reactive power output of the DG to change voltage levels locally. These functions can be implemented through Automatic Voltage Control (AVC) relay for the transformer and with Automatic Voltage Regulator (AVR) for the DG. Furthermore, these active voltage control measures can be combined into a one larger system to achieve Coordinated Voltage Control (CVC). [2]

In this thesis two algorithms based on the CVC algorithm that was developed during the Adine (Active Distribution Network) project [3] and SGEM (Smart Grids and Energy markets) program [4] are being tested using Real Time Digital Simulator (RTDS). The optimizing algorithm takes into consideration the cost of curtailing real power production of the connected DG units and the cost of losses when transferring power through network whereas the rule based algorithm only considers the operational limits of the network voltage. Both algorithms are introduced in the Chapter 2. The tests consist of 12 sequences and four separate load cases detailed in the Chapter 5.

2 ACTIVE VOLTAGE CONTROL

The incentive to move towards active voltage control methods is largely caused by the growing popularity of renewable energy and small production units. Traditional large power plants like coal, gas or biofuel burning plants and nuclear fission plants are built as large as possible to lower the cost per produced energy and therefore need to be connected to the high voltage transmission network to minimize the transfer costs. Unlike them, small DG plants are located where ever power is needed or where good conditions for the power generation exist, for example on coastal areas or open sea for the wind turbines or at large open areas or integrated into buildings for the solar panels. There are also many factors limiting the size of the DG plants, like wind conditions, area planning by local authorities or the size of the roof where solar panels are installed. It is often more advantageous to connect these small plants to the distribution network instead of the transmission network, since connection costs are smaller thanks to the lower voltage level, smaller amounts of power being transferred and a shorter distance to the network. [1; 2]

However, this can cause problems if the distribution network is weak. In traditional unidirectional network the power is flowing down from the transmission network connecting the large power plants and into the distribution network and further to the end users located on the distribution feeders [5, p. 1]. Since in this model the voltage is always highest at the primary substation (assuming the distribution network capacitance is negligible) and lowers towards the ends of the feeders, the network maximum voltage can be controlled with an OLTC and capacitor banks installed at the substations or along the length of the transmission line [6, p. 188]. In radial distribution networks the loads are located all around the network. This means that more further from the primary substation the line is located at, less current there is flowing through the cable. This has allowed the DNOs who control rural distribution networks to use smaller and smaller distribution line cable diameters the further they are located from the primary substation and therefore save money on the material costs. [7, p. 612] Urban networks with meshed topology or connections between medium voltage substations are built with constant cable diameter to allow for reserve power flow in case of a fault on the primary feeder.

When a DG is connected to the end of a rural network feeder in a network like the one described above, power flow on the feeder can be reversed, meaning that the power is flowing towards the primary substation instead of flowing away from it. This causes the voltage levels to rise near the DG unit and the network maximum voltage might no longer be located at the primary substation. Feeder current limits might also be

exceeded since the cables are of a smaller diameter in the ends of the distribution network. Only ways to correct these problems using the passive voltage control methods are to either strengthen the feeder connecting the DG unit or to build a new feeder only to connect the DG unit. Both of these actions can be quite expensive as physical changes to the network topology need to be made. [2; 8]

In this "Fit and Forget"-type planning the network is always constructed according to the worst case scenarios of maximum generation and minimum load or minimum generation and maximum load. When generation is at the maximum and consumption at the minimum, the voltage rises near the generation units and is lowest near the ends of the feeders with no generation, making the voltage difference between these two types of locations very large. This makes it hard to control voltages with only OLTC, since both the network minimum and maximum voltages are near their allowed limits. Therefore the network is built strong enough that the voltage stays within the allowed limits in all possible normal situations. This easily leads to situations where the network is much stronger and therefore more expensive than needed 99% of the time. When using active voltage control methods like combining the OLTC with the control of active and reactive powers of the DG units, these costly actions might be avoided. High voltages can be controlled locally by consuming reactive power or by curtailing the real power generation, which in turn allows for more effective use of the OLTC. [1; 8] However, it should be mentioned, that sometimes the problem with integration of a large DG unit to a weak network are the large voltage transients when the unit is connected or disconnected. These transients cannot be prevented with active voltage control methods, but instead should be handled by properly designing the DG unit or reinforcing the network. [9, p. 4]

Active voltage control can also be advantageous in situation where there is a fault in the primary substation transformer or the transmission network feeding the substation. If there is a reserve feeder connecting the network below the primary substation to a neighbouring area, the area below the fault point can be fed from another substation. These reserve feeders, however, are often not built strong enough to handle the whole load of the area. In these cases DG units can be controlled with active voltage control methods to support the area in optimal way, reducing the load on the reserve feeders. If connection to the transmission network is completely lost (fault also on the reserve feeder or no such feeder exists), DG units need to be either disconnected or controlled to support the islanded area. In today's distribution networks, DG units are almost always equipped with an anti-islanding protection, which prevents them from being used to support the islanded area. Since the penetration of the DGs in distribution networks has been low, the standards and laws concerning island operation are outdated and the island control technology is still new and under development. However, island situation control is out of the scope of this thesis. [10; 11]

Active voltage control methods already in use in the transmission network are divided to three levels depending on their response time: primary voltage control, secondary voltage control and tertiary voltage control. The primary voltage control is real-

ized using AVRs of the generators and it reacts in less than a second to correct the voltage in the bus the generator is connected to. Since the primary voltage control only monitors and reacts to changes in the voltage of the bus connecting the DG, it can cause harm for the secondary voltage control, which aims to control voltages in larger area. Action that might be good for the local voltage in the connecting bus might be harmful for the area control. The secondary voltage control changes the reactive power set points of multiple generators with response time of about one minute in order to control the voltage in a single pilot bus (actual or virtual) chosen to represent the area and it can be seen as a precursor for the distribution network coordinated voltage control ideology. The secondary voltage control doesn't work well with radial network topologies, but this is not a problem in transmission network, since it is almost always designed to have a meshed topology. This, however, prevents it from being used in many distribution networks. The tertiary voltage control is used to control the reactive power transfer between various areas in a country scale and it is executed with a time constant varying between 10 and 30 minutes. All of these voltage control levels are normally only associated with the transmission network, since the distribution network traditionally doesn't contain any generation capacity. [12, p. 1-2]

Transmission network owners often aim to minimize reactive power transfer to or from their networks and therefore collect a tariff from excessive amounts of reactive power being transferred. The allowed amount of reactive power transfer is often referred to as reactive power window, since the allowed level of reactive power is dependent on the amount of real power transfer, forming a rectangular shape around the origo in a 2D-system with real- and reactive power axis's.

2.1 Basic principle of voltage control

Today most DG units are aimed to be connected into the network with a unity power factor. However, consuming reactive power can be used to lower the voltage or producing reactive power can be used to increase the voltage in many cases. The curtailment of the real power generation is often seen as a last resort since it is economically bad for the DG owner, but it can be allowed when it enables for a larger amount of DGs to be integrated in the network and the probability of production curtailment realizing is low enough. [8, p. 256]

Active voltage control methods use state estimation and/or measurements to confirm voltage levels at the pilot buses. A pilot bus is a network bus which is chosen to represent some part of the power system that is deemed necessary for voltage control. If voltage limits are exceeded locally, for example in the bus connecting the DG, production units reactive or real power generation can be controlled to restore the voltage within the allowed limits.

The primary substations often have a transformer with an OLTC that can be controlled using an AVC relay to correct voltage levels at pilot buses. The tap changer moves between discrete tap positions and therefore the possible voltage values at the

transformers secondary side are also discrete. In this control method it is assumed that changing the primary substation voltage affects the voltages on all of the feeders and buses the same amount. Although this is not exactly the case, the differences are mostly negligible. OLTC-based voltage control is generally the most favoured amongst the DNOs thanks to its simplicity and prevalence in the already existing systems. [13, p. 2097] Other measures for the active voltage control include controllable loads and switch controlled energy storages, which mostly operate the same way as the DGs with an AVR, and switched shunt compensation equipment, but since these are not included in the algorithms tested in this thesis and are not generally in use in Europe, they are not discussed further.

2.2 Automatic Voltage Regulator

AVR is the system controlling the synchronous machines terminal voltage by regulating the excitation voltage used to generate a flux in the field winding. It can also be placed in the voltage rectifier. Since generators terminal voltage is directly dependent on the excitation voltage of the winding, it is easy to control the terminal voltage by changing the excitation voltage set point. First a voltage reference value for the excitation model must be calculated from the reactive power set point value and the measured reactive power value of the generator. In this thesis this is done using IEEE 421.5 Var Controller Type 2, which is depicted in Figure 2.1.

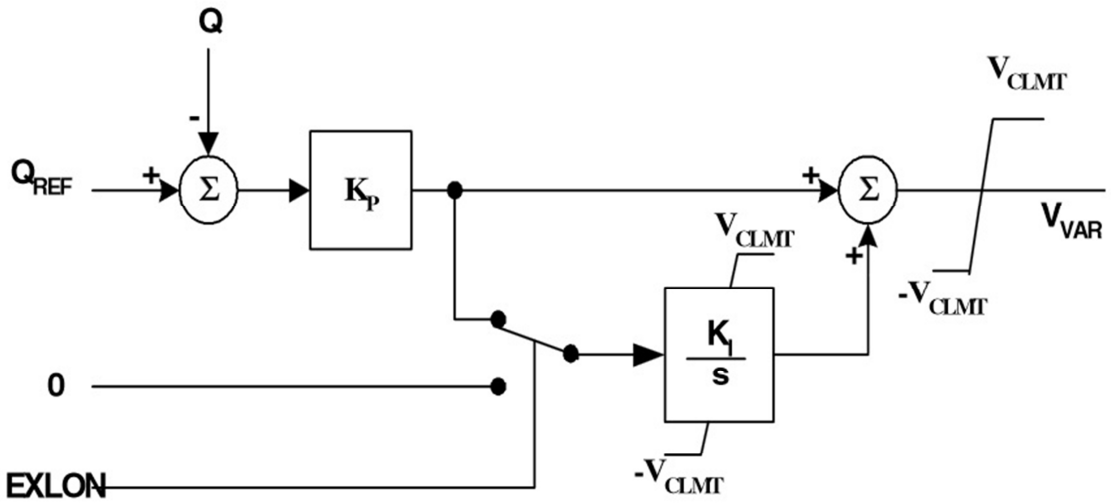

Figure 2.1 *IEEE 421.5 Var Contoller Type 2 model [14, p. 3].*

The measured reactive power of the generator Q is subtracted from the reactive power set point value Q_{ref}. Next the signal goes through gain block K_P and is summed to signal that has been fed through integral gain block K_I/s. V_{CLMT} is the non-windup limit used to keep the voltage reference value V_{VAR} within allowed limits and the EXLON signal switches the integrator block input to 0 when the generator is disconnected. [14]

A general synchronous machine excitation system model is depicted in the Figure 2.2. Reference voltage V_{REF} is the output voltage V_{VAR} from the Figure 2.1.

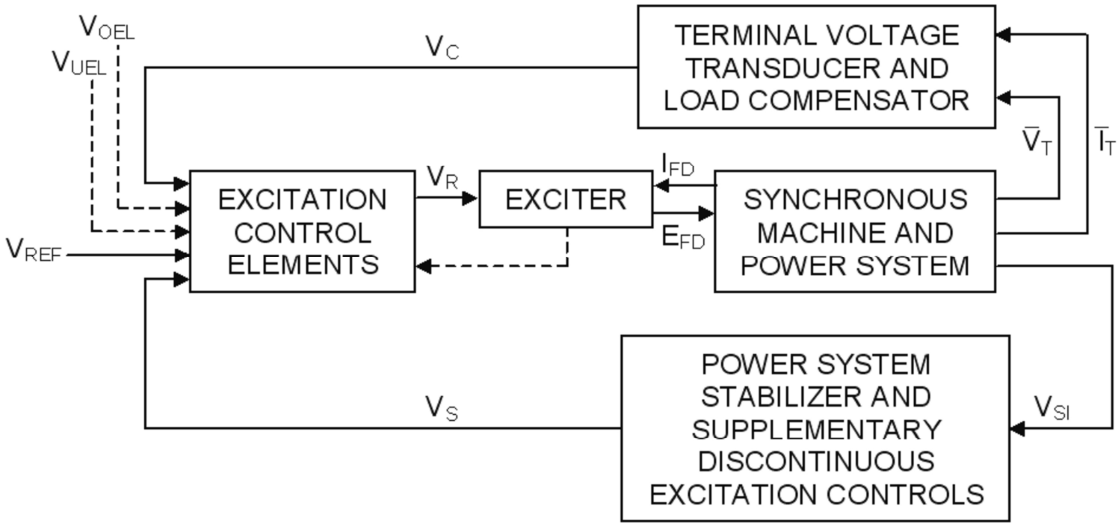

Figure 2.2 *General excitation system model [15, p. 3].*

The excitation control elements-block receives the reference voltage V_{ref} together with the over- and underexcitation limits V_{OEL} and V_{UEL}, the terminal voltage transducer output V_C and the power system stabilizer output V_S as inputs and it outputs the voltage V_R, which is the input for the exciter. Exciter also receives synchronous machine field current I_{FD} as an input and outputs the voltage signal E_{FD} to the synchronous machine model. Synchronous machines terminal voltage $\overline{V_T}$ and terminal current $\overline{I_T}$ are then used as inputs for the terminal voltage transducer. Output V_{SI} is either speed, power or frequency deviation of the synchronous machine and it is used as an input for the power system stabilizer. [15, p. 2-3; 16, p. 387-388]

The excitation system can be either DC-, AC- or Static-type. The generator excitation model used in this thesis is the IEEE AC8B and its design can be seen in the Figure 2.3. This model is used to represent a static voltage regulator applied to brushless excitation system. The excitation control elements-block of Figure 2.2 includes the PID controller and the voltage regulator of Figure 2.3 whereas the Exciter-block includes the excitation part of the Figure 2.3. In the PID controller the reference voltage signal Vref and the stabilizer voltage signal V_S are first summed together and then the generator terminal voltage signal V_C is subtracted from the sum. The outcome signal of these operations is then forwarded to the parallel proportional (PR), integral (IR) and derivative (DR) gain blocks and the outcome signals of these blocks are summed together.

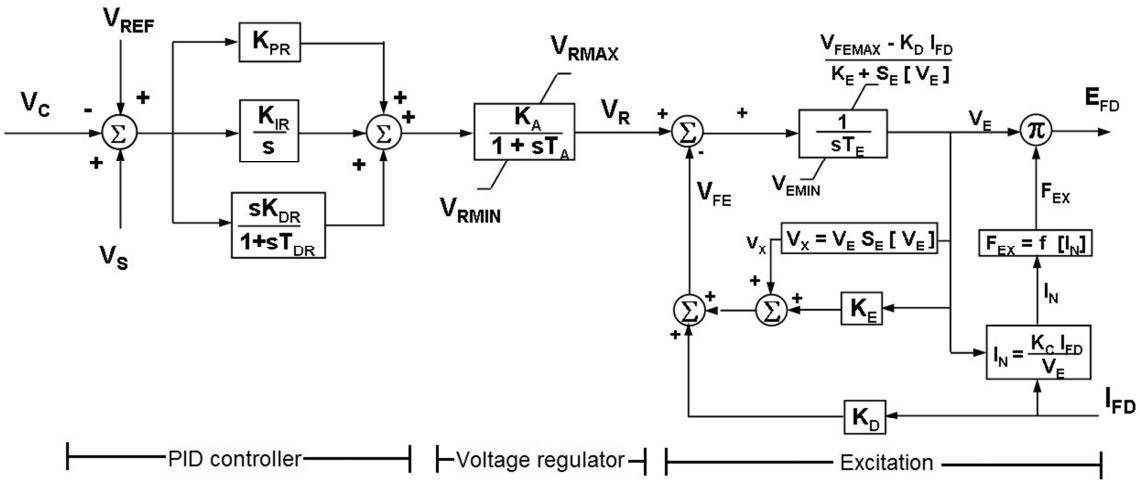

Figure 2.3 *IEEE AC8B excitation model [15, p. 15].*

The PID controller output signal is then forwarded to the voltage regulator, which outputs signal V_R. In the excitation part the voltage signal V_{FE}, which is proportional to exciter field current I_{FD}, is then subtracted from the voltage regulator output signal and the remaining signal is fed to the block that ensures the excitation voltage is between allowed limits. Finally the output signal V_E from this block is used together with the rectifier loading factor F_{EX} to produce the exciter output voltage E_{FD}. [15, p. 14-15; 16, p. 389-390]

2.3 On-Load-Tap-Changer

The OLTC is a mechanical device that can change the tap ratio of a transformer while the transformer is energized. Therefore there is no need to halt the transfer of power through the transformer while the tap position is being changed. The tap changer is often located on the high voltage side of the transformer since the current is smaller on the higher voltage level and therefore it is easier to open the circuit. Basic concept of the tap changer is depicted in the Figure 2.4.

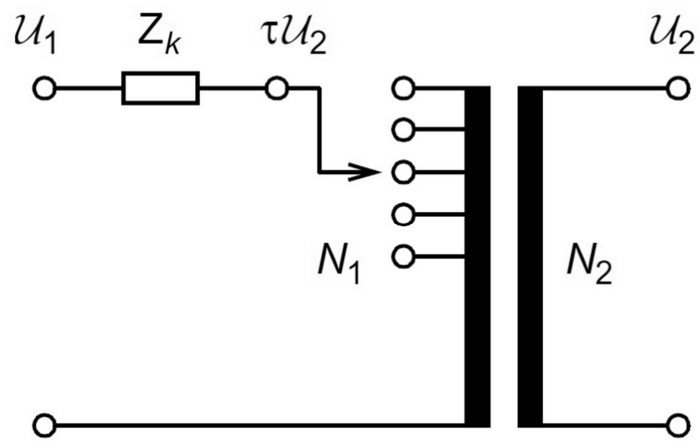

Figure 2.4 *Tap changer basic design [16, p. 391].*

N_1 and N_2 are numbers of winding turns on the high and low voltage sides respectively, Z_k is the leakage impedance of the transformer, τ is the ratio of the winding turns and u_1 and u_2 are the voltage phasors of high and low voltage sides respectively. Relations between the variables are depicted in equations 2.1 and 2.2.

$$\tau = N_1 / N_2 \quad (2.1)$$

$$u_2 = u_1 / \tau \quad (2.2)$$

The leakage impedance Z_k causes a voltage loss when there is a load current in the transformer winding and therefore equation 2.2 does not hold true when transformer is loaded, but this loss can be taken into account in the calculations when the current is known and therefore the basic principle of the tap changer stays valid. In this thesis the primary transformer leakage impedance is set to so small value, that it does not have visible effect to the transformer secondary voltage. The switch changing between the tap positions is depicted with an arrow and it can move up to connect larger part of the winding or down to connect smaller part of the winding. [16, p. 391-392]

The switching equipment of OLTC is situated in compartment filled with oil, air with magneticarc chutes, SF_6-gas or vacuum to avoid arching during the operation of the tap changer [17, p. 30]. Traditionally OLTCs have employed transition resistors as a part of the diverter switch, which breaks the load current when the OLTC is making a switching operation, but lately designs replacing these resistors with thyristors have also been proposed. The main advantages of using thyristors are the smaller conduction losses and the suppression of arching during switching operation. [18]

The OLTC is controlled with an Automatic Voltage Control (AVC) relay. The relay receives the transformer secondary side voltage reference set point V_{set} and the current secondary side voltage value V_{ss} as inputs and outputs either a tap up signal or a tap down signal to the OLTC if a change is needed. The AVC relay realization in the RSCAD is presented in the Figure 2.5.

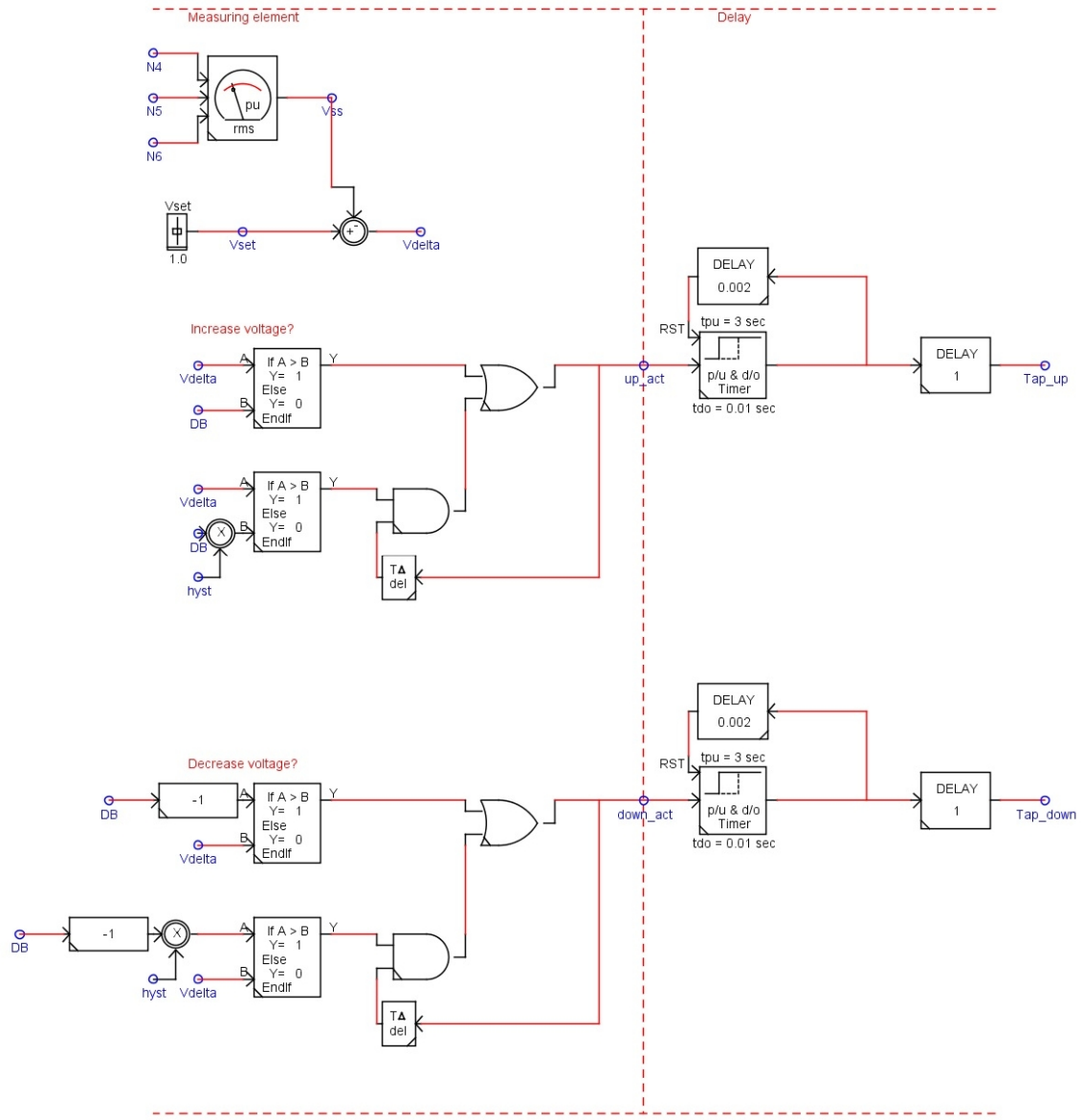

Figure 2.5 *AVC relay in RSCAD.*

Signal V_{delta} is the difference between V_{set} and V_{ss} and it is compared to the deadband value DB. If V_{delta} is larger than the deadband, signal 1 is outputted to the delay element. If this signal stays at value 1 for three seconds, tap up command will be sent to OLTC through one second delay block that is simulating the time it takes for a real tap changer to operate. The three second delay is in place to prevent the AVC relay from reacting to fast transients where the voltage returns to the allowed level fast. In real situations this delay is often 30 s, but since sequences in this thesis are short and changes happen fast, same shortened delays that were used in previous PSCAD simulations are used instead. Hysteresis phenomenon is taken into account with another comparator. If V_{delta} is larger than 0.9 times the deadband value, but at the same time less than the deadband value and during last time step signal 1 was outputted to delay element, signal 1 is again outputted to delay element. The tap down logic works exactly the same way as tap up logic,

but this time the deadband is multiplied by -1 and signal 1 is outputted to the delay element if V_{delta} is smaller than this negative deadband value.

2.4 Coordinated Voltage Control

In CVC active voltage control methods are linked and the most effective action or combination of actions is executed based on the information about the whole distribution network. CVC can be based on simple rules limiting the voltage between allowed values or it can utilize an optimizing algorithm that also considers certain priorities and chooses the scenario with the smallest objective function value. Multiple different priorities can be used as defining factors when choosing the correct actions, for example minimizing the real power curtailment, network losses, tap changer actions et cetera. In most cases voltage levels in the network buses are the primary factor, but other factors can also be taken into account with lower priorities. With more complex algorithms the total costs from all of the voltage control actions could be minimized. [9, p. 2]

The logical place to implement the CVC functionality is Distribution Management System (DMS), where Supervisory Control And Data Acquisition (SCADA) software can be used for both monitoring the network state and for implementing changes to the active resources. The DMS also often includes state estimation functionality and the network topology control, which can be used to give the algorithm the needed information about those network buses which have no active measuring equipment. When CVC is implemented as a part of existing system, it is also easier for the DNOs to adapt to the new technologies available. [19, p. 2]

2.5 Advantages and Disadvantages

With Active Voltage Control the investment costs of the network can be reduced in many cases since the control measures allow more optimized use of the existing network. While implementing control measures to the network is not free, as long as transfer distances are long and the same software can be used in multiple locations, these costs are of a different order of magnitude than those of building new feeders or reinforcing the existing ones. Changing to an actively controlled network requires a change and development of design tools and methods currently used for the network planning, since current tools only consider the extreme cases of minimum load/maximum generation and maximum load/minimum generation and DGs are only seen as static negative loads whose outputs are not dependent on the network status. [9, p. 3; 19, p. 2]

Locally implemented active voltage control measures can operate with only local measurement data, for example, a DG operating in voltage control mode. Most DNOs do not yet allow DGs to operate in the voltage control mode since this can disrupt the voltage control executed with the OLTC if systems are not coordinated with each other. Studies also show that operating in the voltage control mode can be harmful for the loss of mains protection. [20, p. 4] Instead DNOs mostly require DG units to

operate with unity power factor or in some cases in the power factor control mode. [21, p. 478; 22, p. 612] Coordinated voltage control does need information about the voltage levels in every part of the network, but traditionally networks don't contain enough monitoring equipment to have all of these readings. Even when all the meter readings are not available, a state estimation of the network can be used. In Finland DNOs DMS already includes static network data as a part of the Network Information System (NIS) and real-time measurements of key components from primary substations and possibly from MV-network switching stations. When the load curves of the consumers are also known, a good estimate about the voltage levels around the network can be calculated. These load curves have traditionally been generated from the basic data collected from the consumers when they first join the network. Therefore when misclassification of the customer type happens or when the information becomes outdated by changes made to, for example, the heating method or the air conditioning of the building, the load estimation may become inaccurate. [19, p. 2; 23, p. 1755]

With the introduction of the Automated Meter Reading (AMR) equipment to the end users systems, much more information can be obtained. In Finland all DNOs are required by law to install AMR meters to at least 80% of the consumers before the end of the year 2013. [24, p. 1] This will greatly increase measurement data available for the network control. This data can be used to form more accurate load curves for the state estimation purposes as proposed in [23], better taking into consideration factors such as weather, location, season and the time of the day. In the referenced publication comparison is done using pattern vectors that include daily, weekly, monthly and seasonal data instead of just daily load profiles or load-shape factors that are traditionally used. The customers are automatically clustered into groups and each of these groups is represented by a single load curve. Another way to increase the reliability of the state estimation using the AMR is to have the system poll a single AMR meter located at the end of the feeder to receive a real time voltage reading. This data can then be used as a base for the active voltage control and therefore implementing CVC algorithm as part of the DMS has been proposed in multiple papers. This way costs and modifications to the DNOs existing systems could be minimized. [19, p. 2] The existing studies and algorithms are mostly executed with assumption that network is radial and only fed by a single substation. In actual networks ring topologies also exist and network might in some cases be fed by multiple substations. When active voltage control measures are implemented into DNOs systems, these kinds of circumstances must be also considered. [25]

The state estimation used in this thesis's algorithms is based on the one introduced in [26] and further developed in [27]. This state estimator uses branch currents as state variables and is therefore able to use all power, voltage and current measurements available from the network as input for the state estimation. During this thesis's tests all the loads are modelled as static constant power loads in all sequences except Sequence 9, but in real situation these loads most probably would be presented as load curves, which then could be improved using strategically chosen AMR readings from few loads at the ends of the feeders to receive more accurate state estimation of the network. The

state estimator also includes a bad data detection part to remove clearly erroneous input data and has been designed to be able to take into account weather with load temperature dependencies. The state estimator was tested in RTDS tests and in a real life distribution network tests together with a previous version of this thesis's rule based algorithm in [27].

2.6 Algorithms

In this thesis two algorithms used to apply the coordinated voltage control into a radial distribution network are tested. The algorithms have been created as a part of the Adine project between years 2007 and 2010 and further developed in the SGEM program. All information in this subchapter is received from [28].

The rule based algorithm consists of two parts, the basic control and the restoring control. The basic control is activated to correct the voltage levels when the network voltage exceeds its predefined limits and the restoring control is used to return the system to the original state when basic control has operated or the whole network is experiencing high or low voltage levels after, for example, a DG unit has disconnected.

2.6.1 Basic control part of the algorithm

The basic control part of the algorithm is used to keep the network maximum and minimum voltages between their predefined limits when the network state changes and its operating principles are represented in the Figure 2.6. The algorithm is divided into three separate control blocks: Substation voltage control, Reactive power control and Active power control.

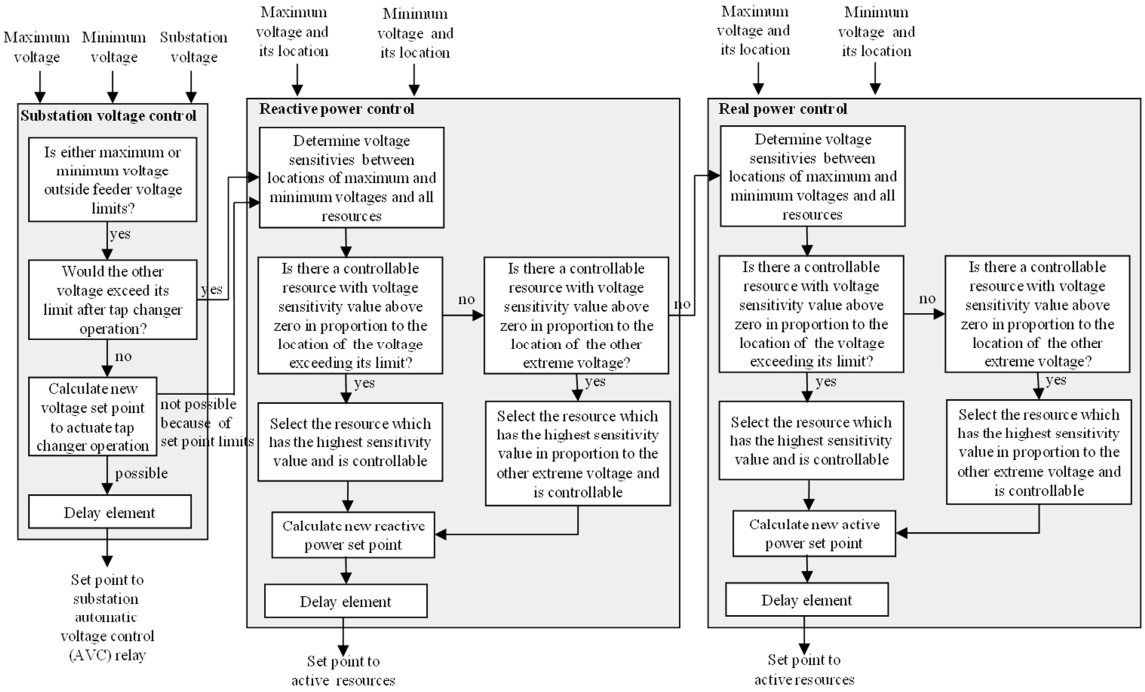

Figure 2.6 *Principle of the basic control part of the algorithm [28, p. 3].*

Basic control is activated when the network minimum or maximum voltage exceeds its pre-defined limits. Algorithm first confirms if the exceeding voltage could be returned within its limits by making the primary substation OLTC change the tap setting and that this operation would not cause the opposite voltage limit to be exceeded. If both of these requirements are met, the algorithm sends a new set point for the AVC relay controlling the OLTC. If either of the requirements is not met, the algorithm will move onto reactive power control.

The reactive power control uses network model data to determine the voltage sensitivities between the maximum or minimum voltage location (whichever is out of its allowed bounds) and all the other network locations. It then confirms if there is an active resource (in this thesis, a controllable generator) that has sensitivity value above 0 that can be used to affect the voltage exceeding its limit. If such resource or resources are found, it selects the one with the highest sensitivity value and that has not yet reached its operational limit and changes its reactive power set point. If there were no active resources that met both of the requirements, the algorithm proceeds to confirm if there are any controllable resources that could be used to affect the other extreme voltage. If such a resource is found, the algorithm calculates a new reactive power set point for this active resource. This action won't correct the exceeding voltage, but it may enable the substation voltage control to take action since the other extreme voltage is brought further away from its limit. If reactive control cannot affect either of the extreme voltages, it activates the real power control.

The real power control works just like the reactive power control does, but it uses active power sensitivities (which are different from the reactive power sensitivities) to find an active resource to control and then sets new active power set point for that resource. If the active power control cannot find a way to make any correcting action, it will output an alert message to the system operator. All control blocks include a delay before applying the new set point values to avoid transient changes from triggering control actions. The voltage needs to exceed its limit for the whole duration of the delay for the set point change to be executed.

2.6.2 Restoring control part of the algorithm

The restoring control part of the algorithm is used to return the voltage and power set points changed by the basic control to their original values when the network situation permits it. It is comprised of three control blocks, just like the basic control, but this time the blocks activate in reverse order. The operating principle of restoring control is represented in the Figure 2.7.

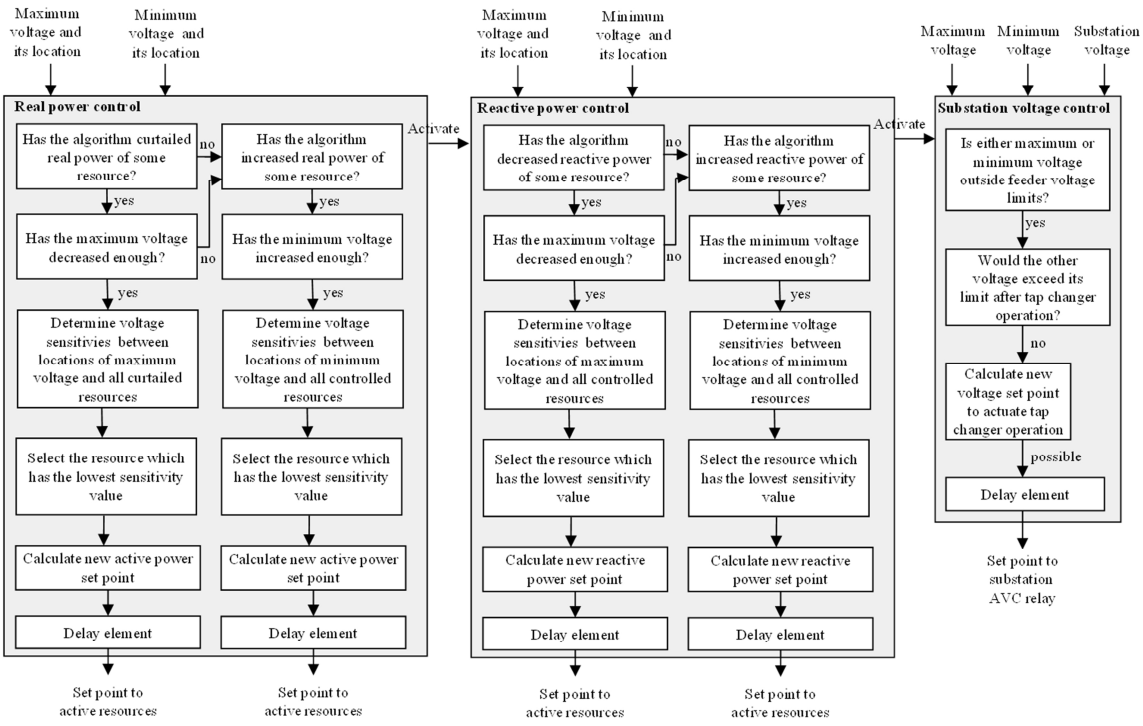

Figure 2.7 *Principle of the restoring control part of the algorithm [28, p. 9].*

The restoring control part of the algorithm starts by determining whether the basic control part has curtailed the real power of any active resource. If it finds such a resource or resources, the algorithm checks whether the network state has changed enough to enable the real power output to be increased again. If this requirement is also met, it will find the resource with lowest voltage sensitivity value in proportion to the network maximum voltage and calculates a new higher real power set point for the active resource in question. If no active resource has been curtailed or if the network maximum voltage has not lowered enough, the algorithm then confirms whether the basic control part has increased the real power generation on any of the active resources. If such a resource or resources are found, the algorithm will check if the network minimum voltage has been increased enough to allow increasing of the real power set point of the resources it found. If it is, the algorithm will use the voltage sensitivities to determine the active resource with the lowest voltage sensitivity value in proportion to the network minimum voltage and calculates new lower real power set point for the active resource in question. If there is no active resource which has had its real power set point changed or if the network state won't allow for a real power restoring action to be taken, the algorithm will activate the reactive power restoring control.

The reactive power restoring control operates with the same principle as the real power restoring control, but using the reactive power values and voltage sensitivities. If there is no active resource which has had its reactive power set point changed or if the network state won't allow for a reactive power restoring action to be taken, the algorithm will activate the substation voltage restoring control. The substation voltage re-

storing control works exactly the same as substation voltage basic control, but usually employs stricter voltage limits.

2.6.3 Control block interaction

If all of the control blocks introduced above would operate independently, multiple of them might be making adjustments to the set point values at the same time. This could lead to them making unnecessary or even harmful changes. To avoid this, a hierarchy has been defined for the control blocks: if a previous block is active, the activation of a new block is prevented with a reset signal. This is illustrated in the Figure 2.8.

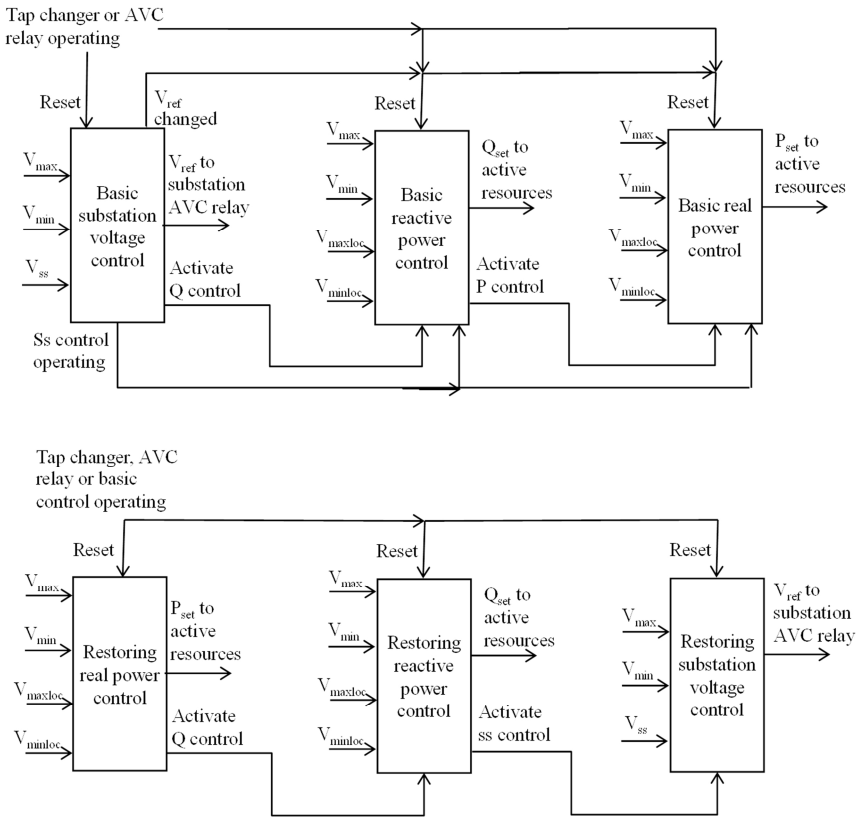

Figure 2.8 *Inputs, outputs and connections between the control blocks [28, p. 12].*

The reset signal blocks the operation of a control block and resets delay counters. When the tap changer or the AVC relay is operating, the activation of the whole algorithm is blocked and when the basic control is operating, the restoring control part is blocked.

2.6.4 Optimizing algorithm

The optimizing algorithm has been developed as an alternative or a supplement to the rule based algorithm. It can either be used alone, to replace the restoring part of the rule based algorithm or together with the rule based algorithm. When it is used alone, it is important to make sure that the iteration always converges and that the algorithms computational time won't be too long.

2.6.4.1 Functions and vectors

The optimizing algorithm is based on a mixed-integer nonlinear programming problem (MINLP) characterized by the following functions:

$$\min f(\mathbf{x},\mathbf{u_d},\mathbf{u_c}) \quad (1)$$

$$g(\mathbf{x},\mathbf{u_d},\mathbf{u_c}) = 0 \quad (2)$$

$$h(\mathbf{x},\mathbf{u_d},\mathbf{u_c}) \leq 0 \quad (3)$$

where $\mathbf{x}$ is the vector of dependent variables. These are the variables of the network that can only be controlled indirectly; the voltage magnitude V and the voltage angle δ. $\mathbf{u_d}$ is the vector of the discrete control variables, like the tap ratio of the primary transformer or the connection status of the capacitors connected to the network. $\mathbf{u_c}$ is the vector of continuously changing variables, the real power P and the reactive power Q of the network nodes.

To solve the optimization problem, vectors $\mathbf{x}$, $\mathbf{u_d}$ and $\mathbf{u_c}$ need be defined along with the objective function $f(\mathbf{x},\mathbf{u_d},\mathbf{u_c})$, equality constraints $g(\mathbf{x},\mathbf{u_d},\mathbf{u_c}) = 0$ and inequality constraints $h(\mathbf{x},\mathbf{u_d},\mathbf{u_c}) \leq 0$. In this algorithm the vector of the dependent variables is defined by following equation

$$\mathbf{x} = [V_1,\ldots,V_n,\delta_1,\ldots,\delta_n] \quad (4)$$

where V_n is the voltage magnitude and δ_n the voltage angle of the nth bus.

The vector of the discretely controllable variables can include tap ratio of the OLTC or the connection status of switches, capacitors, reactors et cetera. In this case it is assumed that the distribution network includes one tap changer at the primary substation transformer and no other discretely controllable components. This is also the predominant case in most European countries. Therefore, the vector of the discrete variables is now

$$\mathbf{u_d} = [m] \quad (5)$$

where m is the main transformer tap ratio.

The vector of continuous variables includes variables that can be directly controlled and which can also get non-discrete values, like the real and reactive power set points of the network nodes. In this algorithm only the real and reactive powers are considered and therefore the vector of continuous variables is defined by the following equation

$$\mathbf{u_c} = [P_1,\ldots,P_i,Q_1,\ldots Q_i] \quad (6)$$

where P_i is the real power set point and Q_i the reactive power set point of the ith active resource.

2.6.4.2 Objective function

The objective function f is formed from the two causes of monetary losses in the distribution network: the network losses and the curtailed production of the real power.

$$f(\mathbf{x},\mathbf{u_d},\mathbf{u_c}) = C_{\text{losses}}*P_{\text{losses}}+C_{\text{curtailed}}*\Sigma P_{\text{curtailed}} \quad (7)$$

In this thesis the price of losses C_{losses} is assumed to be 44.6 €/MWh. This is the average Nordpool Finland spot price during years 2006-2010. The price of the curtailed real power production is the price of the feed-in tariff for the wind power in Finland, 83.5

€/MWh. When considering the losses of the wind power producer, it is necessary to deduct the distribution charge that would be paid to distribution network owner for the transfer of the power. In Finland the maximum value of this charge is 0.7 €/MWh. The lost income due to the curtailment $C_{curtailed}$ is therefore 83.5 €/MWh - 0.7 €/MWh = 82.8 €/MWh.

P_{losses} used in the equation (7) can be calculated as the sum of real powers of all network nodes. In this sum the real power production of the DGs and the real power taken from the transmission network by the primary substation transformer are seen as positive real power and the real power taken by the loads in the network are seen as negative real power. Therefore their sum constitutes for the losses from transfer of the power in the network as seen from the following equation

$$P_{losses} = \Sigma P_i \quad (8)$$

The powers injected to a bus are computed from the following equation

$$\mathbf{P_i}+\mathbf{Q_i} = \text{diag}(\mathbf{V})(\mathbf{Y_{bus}V})^* \quad (9)$$

where $\mathbf{V}$ is the node voltage vector $[V_1 e^{j\delta 1},\ldots,V_n e^{j\delta n}]$ gained from the state estimation, $\mathbf{Y_{bus}}$ the bus admittance matrix formed from the data in the NIS and $\mathbf{P_i}$ and $\mathbf{Q_i}$ are vectors containing the real and reactive powers injected to the buses. $\mathbf{P_i}$ is set point value of the generator and $\mathbf{Q_i}$ is gained from measurement at the DG unit.

2.6.4.3 Equality and inequality constraints

In power flow calculations the voltage magnitude V_i and the angle of the voltage δ_i along with the real power P_i and reactive power Q_i of every network node have to fulfil the power flow equations. In this optimization problem the primary substation low voltage side node is selected as the slack bus, where voltage magnitude and angle are constant, but real and reactive power values vary. As such, voltage magnitude and angle at this node must fulfil the following constraints:

$$V_1 - \frac{V_{orig}}{m} = 0 \quad (10)$$

$$\delta_1 = 0 \quad (11)$$

where V_{orig} is the primary substation voltage with tap ratio 1.0 and m is the OLTC tap ratio.

All the other nodes in the network are assumed to be possible points for connecting the DG and therefore operate on the reactive power control mode and not in the voltage control mode. They are all defined as PQ nodes, where the real and reactive powers are constant, but the voltage angle and magnitude vary. All PQ buses must fulfil the following equality constraints

$$P_i - P_{gen,i} + P_{load,i} = 0 \quad (12)$$

$$Q_i - Q_{gen,i} + Q_{load,i} = 0 \quad (13)$$

where P_i and Q_i are the real and reactive powers injected to the bus, $P_{gen,i}$ and $Q_{gen,i}$ are the real and reactive powers generated in the bus and $P_{load,i}$ and $Q_{load,i}$ are the real and reactive powers consumed in the bus.

There are five inequality constraints used in the optimizing algorithm and they are used to model the technical limitations of the system. The first inequality constrain is used to limit bus voltages between the allowed limits:

$$V_{\text{lower}} \leq V_{\text{i}} \leq V_{\text{upper}} \tag{14}$$

The second inequality constrain is used to limit the real powers of the controllable active resources and the third to limit the reactive powers of the controllable active resources:

$$\text{P}_{\text{active,i,min}} \leq \text{P}_{\text{active,i}} \leq \text{P}_{\text{active,i,max}} \tag{15}$$

$$\text{Q}_{\text{active,i,min}} \leq \text{Q}_{\text{active,i}} \leq \text{Q}_{\text{active,i,max}} \tag{16}$$

The fourth inequality constrain is used to limit the primary substation transformer tap ratio between its mechanical limits and fifth is used to limit the apparent power flow through the lines below maximum allowed value:

$$m_{\text{min}} \leq m \leq m_{\text{max}} \tag{17}$$

$$S_{\text{ij}} \leq S_{\text{max}} \tag{18}$$

If the model would also include any controllable capacitors, their susceptance should also be taken into consideration by adding a constraint for its value.

2.6.4.4 Matlab implementation

The optimizing algorithm is realized using the Matlab Optimization Toolbox function called fmincon. This function uses nonlinear programming, but it assumes all variables are continuous. Since there are discrete variables involved in the objective function, fmincon cannot be used by itself to find the solution. However, since in this thesis the only discrete variable is the transformer tap ratio, a three-stage procedure is used to acquire the solution. During the first phase the solution is calculated assuming that the tap ratio is also a continuous variable. After this the two integer values that are closest to the found solution are chosen and fmincon is executed using these two values as tap changer position values. Then the result with a smaller objective function value is chosen.

In this thesis the active resources whose real and reactive powers form the vector $\mathbf{u_c}$ are only the three generators. The algorithm is, however, compatible with also using controllable loads, switched compensation equipment or energy storages as active resources. Since this implementation of the optimizing algorithm does not have any limits for the minimum target function value change taken by the algorithm, real and reactive power set points given by the optimization function will be rounded. The real power set point is rounded to the accuracy of three decimals and the reactive power to the accuracy of two decimals. This done to prevent the algorithm from making very small changes to set point values, which would needlessly trigger some of the counters mentioned in the subchapter 5.3.2. It has been planned to add a limit for the minimum optimization target function value change, but this has not yet been implemented.

Function fmincon used in this thesis is set to use interior point algorithm. In this algorithm two types of iteration steps are used: a direct step using linear approximation and a conjugate gradient step using a trust region. The direct step is normally used first

and if it fails, the conjugate step is used instead. [29] In the default case the optimizing algorithm tolerations for the constraint violation and the function value are both the fmincon default value, 1E-6. The termination tolerance of x is the interior-point algorithms default value, 1E-10. These values are used in all of the test sequences except Sequence 8.

During the initial preparations for the simulations it was noticed that the iteration did not always converge and sometimes reached the default iteration limit of 1000 iterations. This could in worst cases cause large delays to the execution time of the optimizing algorithm and so the iteration limit was manually set to 100 iterations. The effect of different iteration limits was tested during Sequence 8. It should be noted that the optimizing algorithm is designed to use reactive power as a tool to reduce the network losses and there is no power factor control included in the algorithm. Large voltage spikes may also be experienced when changing the power set points, since the algorithm is not designed to prevent them.

3 REAL TIME DIGITAL SIMULATOR

Real Time Digital Simulator (RTDS) is a power system simulator developed by the RTDS Technologies Inc. for running real time simulations and testing out actual network control and protection equipment. It is a system comprising of the simulator hardware housed in cubicles and control software that can be installed on an ordinary PC. All information in this chapter is received from [30].

3.1 Cubicles and racks

RTDSs main functions are housed in modular cards that are fitted into the racks that connect them to each other and provide fast data transfer. The racks are then combined into cubicles to form the simulator system. Figure 3.1 shows different sizes of cubicles available: full-sized (max 3 racks), mid-sized (max 2 racks), mini (max 1 rack) and portable cubicle (reduced size rack).

Figure 3.1 *RTDS cubicles [30].*

RTDS cubicles house all the necessary components of the simulator system. All of the cards (except I/O cards, Sync Cards and Front Panel Interface Cards) are connected to racks and the racks together with the power supply components are mounted into cubicles. The cubicles also feature DIN rails that are used to connect the I/O cards, Sync Cards and Front Panel Interface Cards. There are multiple different size options available for the cubicles depending on the needs of the operator. If the simulator consists of more than two racks, a special Global Bus Hub is needed in the cubicle to connect the GTWIF cards that normally handle the communication between two directly

connected racks. This Hub uses fibre optics and is separate from the Ethernet connection used to connect the GTWIF and the host computer.

Card cages called racks are used to house the cards and to provide the communication between them. The racks have a backplane connecting all of the cards to each other, but direct contact between the cards using fibre optics cable is also possible. Each rack has its own power source located at the bottom of the cubicle. When multiple racks are connected to work as a one system, the backplanes work parallel and independently to reduce bottlenecks in communication.

3.2 Cards

There are multiple different cards for different functions, for example for running the simulation, for connecting the RTDS to an outside system or for connecting multiple racks into the same system. Figure 3.2 shows two different kinds of cards: GPC processor card and GT I/O card. The cards introduced here are all of Giga-Transceiver (GT) generation, but both older and newer versions also exist.

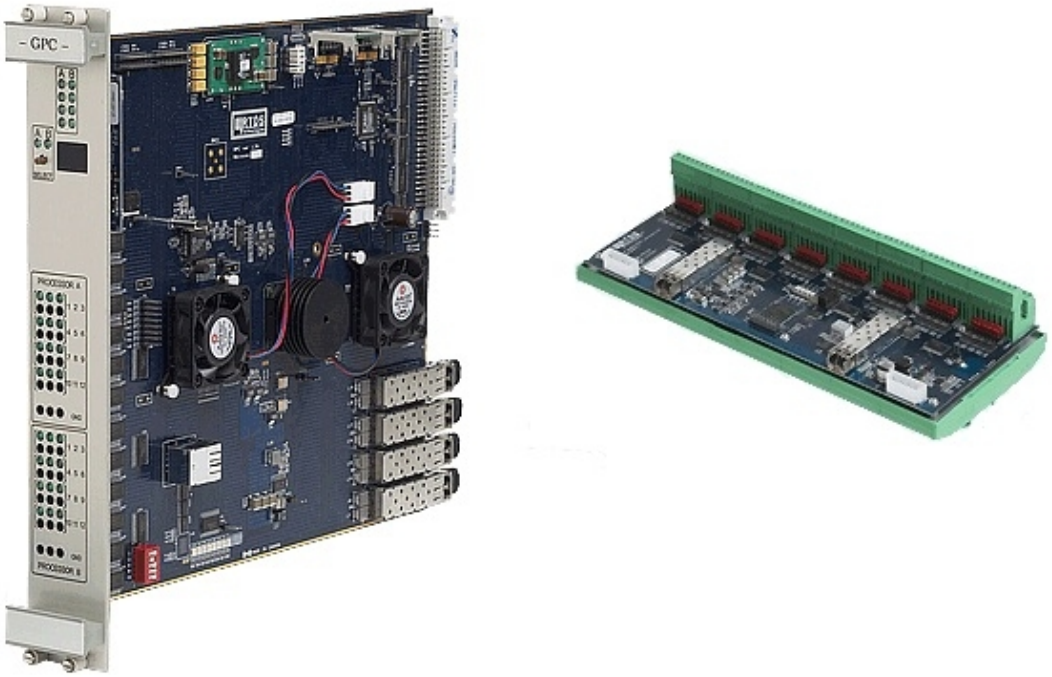

Figure 3.2 *GPC processor card (left) and GT I/O card (right) [30].*

Giga-Transceiver Workstation Interface Card (GTWIF) handles the communication between the RTDS and the host computer using Ethernet TCP/IP connection. The latest GTWIF is based on PPC405 processor and also handles the Inter-Rack Communication in simulation network comprising of six racks or less. During simulations it coordinates all of the backplane communication and the communication with the RSCAD. It also handles the rack hardware diagnostics.

The Inter-rack Communication (IRC) Switch handles the communication between multiple simulator racks up to 60 connected racks. Without it, the GTWIF could directly connect to only six racks. Using the IRC Switch also decreases the need for connections between the racks, since instead of connecting every rack to all the other racks, all racks only need to be connected to the IRC Switch.

Processor cards are the main computing units of the RTDS. PB5 cards developed 2011 feature two Freescale PowerPC MPC7448 processors operating at 1,7 GHz frequency and eight GT fibre ports. Two ports are used for connecting to I/O and rest six are used for connecting with other processor cards. The older Giga-Processor Cards (GPC) developed 2005 feature two IBM 750GX RISC 1,0 GHz processors and four GT fibre ports, two for the I/O and two for connecting with other processor cards. PB5 cards have the maximum of 72 single phase nodes per network solution and GPC cards have the maximum of 66 single phase nodes. PB5 also supports having two different network solutions per rack unlike GPC card, making it possible to have maximum of 144 single phase nodes. The older processor cards include the TPC (developed 1993, 2x12 MHz), the 3PC (developed 1997, 3x40 MHz) and the RPC (developed 2003, 2x600MHz).

Giga-Transceiver Sync cards are used to synchronize the RTDS time step with an external source and they are connected to the GTWIF card using the GT port. They are mostly located on the DIN rail but can also be located remotely.

Giga-Transceiver Input/Output (GTIO) Cards are used to connect the processor cards to the external equipment and both analogue and digital cards are available. Digital cards have 64 inputs or outputs depending on the type of the card and analogue cards have 12. Both digital and analogue cards support regular or small time step (1-2 μs). I/O cards are normally located on the DIN rail in the back of the cubicle, but can also be located remotely when connected with a longer optical cable. They can also be daisy-chained to each other or to the GT Sync card directly.

Giga-Transceiver Front Panel Interface (GTFPI) Cards are used to connect the Low Voltage and High Voltage Digital I/O Interface Panels to processor cards. Low voltage Digital Interface Panels provide 16 input and output signals at TTL voltage level and High Voltage Digital Interface Panels provide 16 solid state contacts rated for 250 Vdc. Both have 4mm safety banana jacks for connection. There is always at least one FTFPI card in every cubicle.

The Giga-Transceiver Network Communication (GTNET) card is used to connect the RTDS in real time to other applications using the Ethernet connection on 100BASE-TXRJ45, 100BASE-FX or optical fibre port. It is connected to one of the processor cards using the GT optical port at the rear of the processor card and has multiple different firmware for different connecting needs: PMU (Phasor Measurement Units), GSE (IEC 61850), SV (IEC 61850-9-2), Playback (COMTRADE files on the PC) and DNP 3.0 (Distributed Network Protocol).

3.3 Software

RTDS cubicles are controlled from a separate PC through Ethernet connection to the GTWIF card. The control software suit is called RSCAD and it comes together with Component Model Libraries.

RSCAD is the control and analysis software of the RTDS that is used to build and run power system simulations and to analyse the results of these simulations. It is modular software consisting of seven independent module programs:

- *File Manager* for handling simulation files and launching other modules.
- *Draft* for inputting parameter data and creating simulation networks using graphical interface.
- *Cable* for modelling cables by entering their physical data.
- *Tline* for modelling transmission lines by entering their physical data or positive and zero sequence impedances.
- *Runtime* for running simulations, acquiring result data and initiating control actions during the simulation.
- *Multiplot* for post simulation analysis and exporting data to other environments.
- *Component builder* for creating custom component models.

The RTDS system includes extensive libraries of power system components, control system components and protection and automation components. Power system component library includes, but is not limited to, transmission lines, cables, voltage and current sources, machines, transformers, compensators, FACTSs, SVCs and DGs. Control system component libraries include user-inputs, constants, data conversion, functions, generator controls and standard control blocks. Protection and automation libraries include protective relays, metering components, IEC 61850 functions, SCADA functions and extended file playback. These libraries are used as a source for component models in the Draft program module and they can be expanded by creating own custom component with the Component Builder program module or custom transmission line or cable models using Tline and Cable program modules respectively.

4 SOFTWARE TESTING

When software is being tested, proper planning of the testing methods and objectives of the tests must be done to achieve useful results. Inputs, outputs and functionality must all be considered during the planning. Different approaches to testing can be divided to the black-box, white-box and grey-box testing.

4.1 Box-type testing

In the black-box testing the tester does not have any information about the inner operations of the software. He might have information about the intended functionality of the software and try to confirm this functionality by giving different inputs to the software and seeing whether output is in accordance with the assumed functionality. He also might not know what the functionality of the software is, but try to confirm it by giving the software inputs and observing the outputs. These kinds of tests are functional, meaning that the general function of the software is being tested without any concern about what kind of inner mechanisms create these results. As such, black-box testing cannot detect faults in software that doesn't produce any visible errors in the output. Exhaustive testing is also very hard, if not impossible, when number of different possible input permutations is high.

In white-box testing the tester has a full access to the software code and he performs tests to confirm that the inner logic and structure of the program is valid. In this case there is no need to go through all of the possible inputs as long as logic of the program is solid and all different inputs are taken into consideration. White-box testing is structural, meaning it is conducted to confirm that inner structure of the software has no errors or unnecessary parts. It does not, however, consider whether the software does things that it was originally planned to do as long as its inner structure is solid. It also cannot detect missing parts of the code as long as all of the other parts of the code can run as intended without the missing part.

In grey-box testing the tester has some information about the inner workings of the software or can communicate with the creator of the software to confirm or deny conclusions made from the observations of the software. He might be able to limit the number of tests needed to test the functionality by understanding that same structure is being used in multiple parts of the software. Also by understanding the way the software is supposed to work, he can detect when a part of the software is missing or not working as intended. This way he can at the same time test the functionality and the structure of the software.

In this thesis testing method is the grey-box testing: the tester has information about the inner workings of the algorithms being tested, but is not going to go check whole code for errors. When performed tests give out reading that are clearly erroneous or contradict previous expectations, inner structure of the algorithm will be examined to find possible errors and tester will be communicating with the creator of the algorithms to fix the problems that have been found or to offer advice for the further development of the algorithms. [31, p. 1-3]

4.2 Software-in-the-Loop testing

Testing done in this thesis can also be classified as Software-in-the-Loop (SIL) testing. In SIL testing the actual software being developed is tested using simulator environment to evaluate its performance and to verify its functionality. Difference to the traditional testing is that the tests are not performed only to confirm the validity of the model so that the actual software could be created or after the software is finished to confirm that it works as intended, but to also test the software during the development. This is often done with simulator where operations of the lower level environments surrounding the actual software are simplified for the testing purposes. This is true for this thesis also, since the RTDS is used to model the actual distribution network and the model used is simplified version because of the limitations of the simulator hardware available. However, the aim of these simplifications is to keep the operation of the model as close to the real network as possible while alleviating the simulation load of the hardware. Same tests can be used as a part of the creation of the software and for testing of the finished software. For this purpose the revision control is important part of the SIL process to avoid already fixed problems from resurfacing in later revisions of the program.

Main advantages of the SIL testing are skipping the model validation testing before creation of the actual software and making testing faster and easier than the real life application testing, since parts of the modelling environment can be simplified and simulation speed adjusted. It is also possible to run tests that would not be possible to run in real life situation because of the limitations of the existing hardware and software or the danger to the system or bystanders. As long as the simulation parameters are properly documented, tests are also easily repeatable. The SIL testing does have a few limitations, including the scalability of the simulation and the possibility of modifications needed to the software. When testing needs to be executed in a large simulation environment without simplifying model too much, hardware costs can be quite high. Interface of the software tested might also need minor modifications in order to connect it to the simulation environment when compared to connecting to an actual system. [32]

4.3 Real time testing

Simulations in this thesis are executed in real time using the RTDS system. Compared to non-real time simulators like PSCAD there are certain distinct advantages in using a real time simulator: actual devices can be connected and tested since the simulators time domain operation is identical to the actual systems and the tests are run faster. Algorithm tests like the ones done during this thesis also benefits from real time simulations since there are questions concerning execution times and delays that need to be answered and in non-real time simulations these cannot be realistically tested. Since the non-real time simulation of one second usually takes more than one seconds time to be run, but the algorithms run in real time, difference between the systems makes the results unrealistic.

Downside of the real time simulation is the simulation hardware required: since behaviour of all system components need to be simulated in real time, specialized simulation hardware is required. The RTDS system consists of multiple processor cards which each are set to simulate specific system components. Since processing power of single processor is limited, number of processors available limits the size of the simulated system. During this thesis the simulation network model is further simplified by combining some of the load nodes and distribution lines.

5 TESTING SETUP

This chapter introduces the hardware and software used in the tests along with test model data, sequence data and specifications of the metering and data collection during the sequences. Reasons for the metering value and graph choices are also presented.

5.1 Hardware and software

The hardware used in the testing of the algorithms is partially based on the same setup that was previously used during the Adine project tests. The software includes Matlab and the RTDS control software RSCAD. PSCAD X4 was used to confirm the model equivalence during the preparation phase but it was not used during the simulations.

5.1.1 Connection setup

In this thesis the testing setup is constructed as depicted in the Figure 5.1. A single PC is running both the Matlab and the RSCAD. The data transfer between these two programs is handled with shared text files (ASCII format).

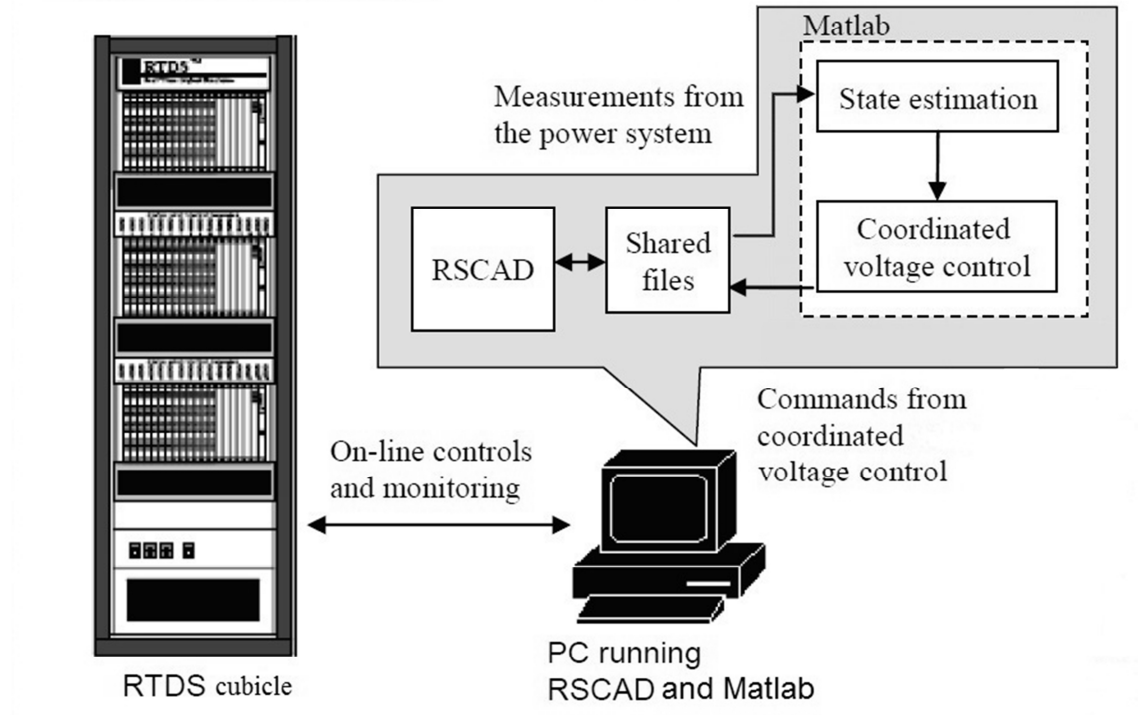

Figure 5.1 *The connection setup.*

RSCAD writes the measurement values into the first shared file five times per second and Matlab reads this information once every second for the rule based algorithm and once every 4 seconds for the optimizing algorithm. Matlab then executes the voltage control algorithm using these values and writes the received set point values into the second shared file. RSCAD reads these values once every second and makes changes to the simulation settings accordingly.

5.1.2 Simulation setup

The RTDS system installed at the Tampere University of Technology includes two cubicles with one rack installed in each. The rack used for the simulations in this thesis contains two GPC cards, one 3PC card, a Digital Optical Isolation System (DOPTO) input/output card, three GTNET cards (not used for anything during these simulations) and one GTWIF card.

The other rack includes five 3PC cards, one RPC card and one GTWIF card. Racks can be connected to acquire more processing power for the simulation, but this was not necessary during this thesis. The RSCAD software used during tests is version 2.026.1, the version of Matlab software is 7.12.0 (R0211a) and the version of PSCAD X4 is 2011-05-31.

5.2 Network model

Network used in this thesis is the same as the one used during the Adine project and it is depicted in the Figure 5.2. The network consists of one substation (Heinäaho) and two feeders (Ritari and Kihniö) and it is based on an actual rural distribution network owned by the Koillis-Satakunnan Sähkö Oy and it is located in the western Finland. In the actual network substation Heinäaho has five feeders, but because the lowest network voltage is always found on the feeder Kihniö and because feeder Ritari is used for connecting the DGs, only these two feeders have been modelled. The load data in the maximum, minimum and two separate average situations along with the distribution line, primary transformer and supply network parameters have been obtained from the DNO. [33]

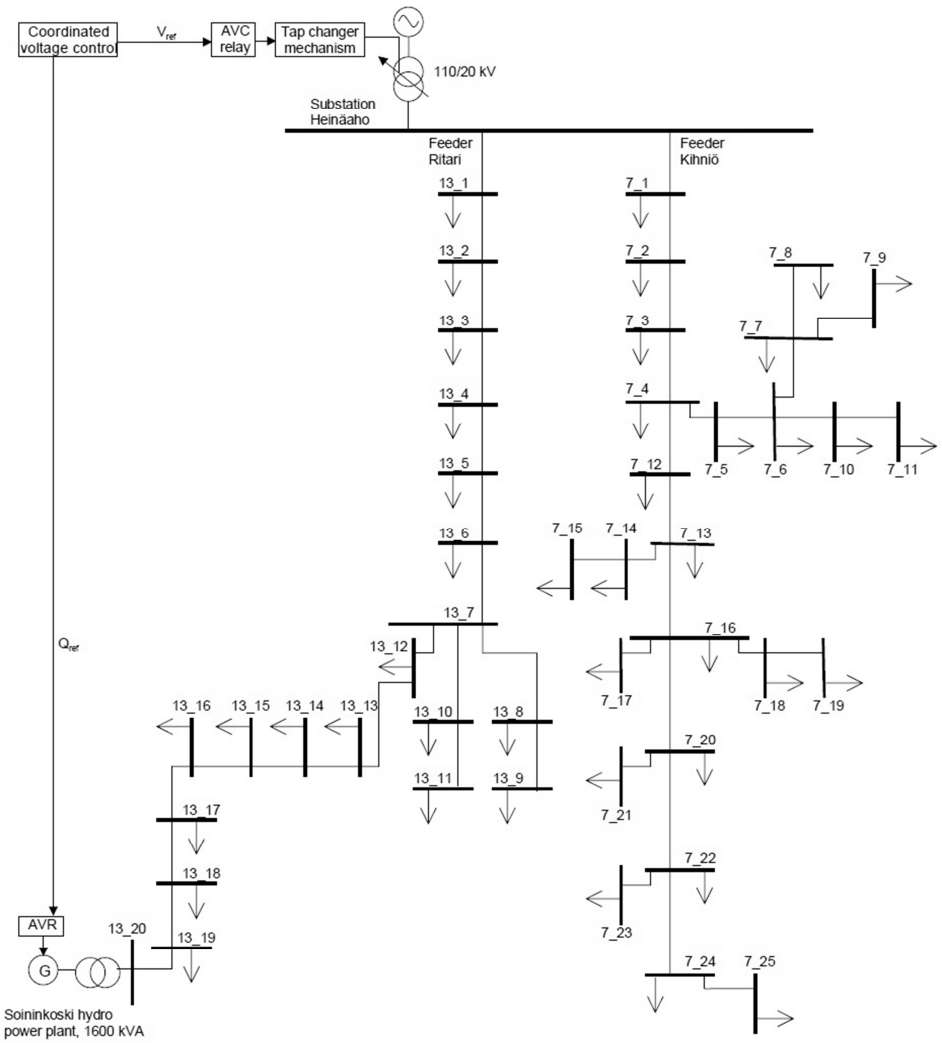

Figure 5.2 *Network model used during Adine project [33, p. 7].*

For the RTDS tests the network will be simplified because of the limitations of the simulation hardware available. Figure 5.3 depicts the simplified network model used. The loads have been combined to the remaining buses and the lines have been combined so that there is only one set of line parameters for each line.

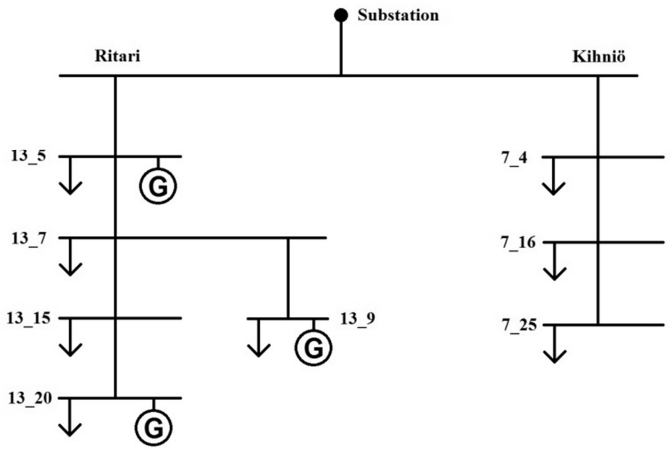

Figure 5.3 *Network model used in RTDS simulations.*

The voltage values of all the simplified network buses are compared to original network values in the Table 5.1. In this table the loading condition is Middle 1, the tap changer is permanently set to the value 1.0000 and all three generators are disconnected from the network.

Table 5.1 *Comparison between the original and simplified networks.*

Bus	V(pu), PSCAD original	V(pu), PSCAD simplified	V(pu), RSCAD simplified
Substation	1,050	1,050	1,050
13_5	1,044	1,044	1,044
13_7	1,043	1,042	1,042
13_9	1,043	1,042	1,041
13_15	1,039	1,038	1,038
13_20	1,038	1,038	1,038
7_4	1,042	1,040	1,040
7_16	1,037	1,035	1,035
7_25	1,037	1,034	1,034

As can be seen from the Table 5.1, there are some minor changes in the bus voltages between simplified and original models, but these are all 0.003 pu or smaller and therefore acceptable. Especially simplified PSCAD and RSCAD models are very close to each other, the largest difference being 0,001 pu. The Table 5.2 presents information about how the loads have been combined to the new buses.

Table 5.2 *The simplified load buses.*

New bus	The load buses combined to the new bus
13_5	13_1, 13_2, 13_3, 13_4, 13_5
13_7	13_6, 13_7, 13_10, 13_11, 13_12
13_9	13_8, 13_9
13_15	13_13, 13_14, 13_15, 13_16, 13_17
13_20	13_18, 13_19, 13_20
7_4	7_1, 7_2, 7_3, 7_4, 7_5, 7_6, 7_7, 7_8, 7_9, 7_10, 7_11
7_16	7_12, 7_13, 7_14, 7_15, 7_16, 7_17, 7_18, 7_19
7_25	7_20, 7_21, 7_22, 7_23, 7_24, 7_25

The loads in the network are modelled so that they can be set to be static constant power, constant current or constant impedance loads, but they are only used as constant power loads in all of the sequences, except Sequence 9, which uses constant impedance loads. Load data and distribution line parameter data for the simplified network model are represented in Tables 5.3 and 5.4 respectively.

Table 5.3 *The simplified model load parameters.*

Node	Maximum (Saturday 6 p.m. in January)		Minimum (Saturday 4 a.m. in July)		Middle 1 (weekday 12 p.m. in April)		Middle 2 (weekday 2 p.m. in November)	
	P [MW]	Q [MVAr]	P [MW]	Q [MVAr]	P [MW]	Q [MVAr]	P [MW]	Q [MVAr]
13_5	0,24333	0,06899	0,04017	0,01000	0,10145	0,02783	0,11775	0,03252
13_7	0,23410	0,06629	0,03621	0,00920	0,09338	0,02578	0,10431	0,02890
13_9	0,06966	0,01948	0,01073	0,00250	0,02818	0,00753	0,03153	0,00851
13_15	0,26588	0,07500	0,04046	0,01040	0,12281	0,03403	0,14439	0,04033
13_20	0,04586	0,01267	0,00729	0,00160	0,01903	0,00503	0,02165	0,00580
7_4	0,76071	0,21613	0,11684	0,03040	0,33581	0,09366	0,39007	0,10913
7_16	0,27675	0,07784	0,04739	0,01180	0,16261	0,04504	0,19847	0,05570
7_25	0,13049	0,03695	0,02141	0,00570	0,07770	0,02171	0,09697	0,02737

Table 5.4 *The simplified model distribution line parameters, positive and zero sequence, values are presented as per unit values (Sb = 100 MW, Ub = 20 kV).*

From	To	R+	X+	Cap.susc.+	R 0	X 0	Cap.susc. 0
Substation	13_5	1,500868	1,389242	0,00023797	2,104220	7,336785	0,00013912
13_5	13_7	0,660660	0,298740	0,00003719	0,776100	1,467180	0,00002383
13_7	13_9	1,352101	0,396305	0,00004604	1,499472	1,886943	0,00003043
13_7	13_15	2,783932	0,910862	0,00010831	3,127007	4,379783	0,00007080
13_15	13_20	2,231384	1,817034	0,00016737	2,677315	5,118719	0,00011903
Substation	7_4	1,489772	1,202876	0,00020950	2,008257	6,384740	0,00012207
7_4	7_16	1,899514	1,393712	0,00019164	2,489914	7,078843	0,00011657
7_16	7_25	1,173741	0,790167	0,00010680	1,526774	3,975732	0,00006606

The generators are modelled as synchronous machines in reactive power control mode (IEEE AC8B) with a nominal power of 1600 kVA and modified so that they reach the real power output of 1360 kVA with the mechanical moment value of 1,0 pu. They have the inertia constant H value of 2 MWs/MVA. The distribution lines in network are modelled using π-connection and the OLTC is controlled with an AVC-relay. The AVC relay dead band is 1,5% and it operates with ±9 of 1,67% steps (1.0 ± 9 * 0,0167 pu.). There is no line-drop compensation implemented in this model. The substation transformer and the supply network parameters are presented in Table 5.5.

Table 5.5 *The transformer and supply network parameters.*

Transformer		Supply network	
Winding connection	Y-Y	Initial voltage (L-L, RMS)(kV)	110
Rated power (MWA)	16	Initial frequency (Hz)	50
Leakage inductance (pu)	0,001	Initial phase (°)	0
No load losses (pu)	0,000	Positive seq. impedance (Ω)	48,341
Primary / secondary voltage (kV)	110 / 21	Positive seq. imp. phase angle (°)	65,821

During this thesis the rule based algorithm has the following settings: the basic substation control maximum voltage is 1,05 pu and the minimum voltage is 0,95 pu, the restoring substation control maximum voltage is 1,05 pu and the minimum voltage is 1,00 pu, the substation control margin is 0,002 pu (other voltage must be a tap step + margin away from its limit for the tap changer to operate), the hysteresis is 0,005 pu. Step used in the reactive and real power control is 0,01 MVAr or MW, which is also the control marginal. The reactive power minimum value is -0,44 MVAr and the maximum value is 0,44 MVAr, this also applies for the optimizing algorithm. The optimizing algorithm maximum network voltage value is 1,05 pu and the minimum value 0,95 pu.

Because of a software bug encountered in the RSCAD program while constructing the RSCAD network model, a capacitor with the capacitance of 10 μF has been connected to the low voltage side of the primary transformer to supress the error and allow the simulation to be run. It was also tested using PSCAD that as long as the said capacitor is not larger than 10000 μF, it has no visible effect to the voltage profile of the network and therefore 10 μF capacitor can be assumed to be small enough to not affect the simulation results in any significant way. This capacitor, however, produces some reactive power, which can be seen from the power flow graph of primary substation during simulations. Even when generators are not producing any reactive power, the flow of reactive power is up from distribution network towards the transmission network.

5.3 Metering

To ensure properly usable and comparable data can be acquired from the simulations, some care must be taken to select the variables being metered during the running of the simulations. This chapter is used to state the reasons for different variables being metered.

5.3.1 Plot graphs

The following values will be monitored by plotting the data series gained from the RSCAD and Matlab into 2d-plots with time (s) as the x-axis and the monitored value as the y-axis. The RSCAD values are used for all of the actually metered variables and the Matlab values are only used for those variables that are gained from the algorithms as output values, such as the selected tap setting and the real and reactive power set points.

The network maximum and minimum voltages are the primary reason for any actions taken by the algorithms and therefore it is important to meter these values to understand why the algorithm performed control actions when it did. Other important voltage values are the bus voltages of the DG connection points and the primary substation voltage, since these are the locations where the network maximum voltage is most probably located at. The voltage reference value of the OLTC is followed to see that the substation voltage has changed according to the set point value changes.

The real and reactive powers of all three DG units are also metered. Real power adjustments are used to incite changes in the network status and the algorithms also curtail real power production when necessary. Reactive power production or consumption is used as a control method by the algorithms when substation control is not enough to correct the situation. Power set point values are also followed to see how the set point changes have affected the actual power values. Power factors of the DG units are also calculated from the real and reactive power set points, since real life machines may have limits to their possible power factor values.

The DG connected to the network may decrease or increase the need for real and reactive power to be taken from the transmission network through the primary substation transformer. In some cases power flow through the transformer might even be reversed and the power could be flowing up to the transmission network. These cases affect the losses caused by the transfer of power. Therefore both the real and the reactive power transferred through the primary substation are also metered. The tap changer position is followed using a graph to make it easier to notice which changes in the other graphs are caused by the tap changer actions.

5.3.2 Counters

The following values are used to record the number of certain actions or outcomes related to the operation of the algorithms. The amount of occurrences is followed without recording the information about when the occurrences happened, but this information is deductible from the simulation output data if necessary.

According to results from the survey conducted by W. Dietrich in [34] and later discussed in [35, p. 8], 40% of faults in the substation transformers are caused by a failure of the OLTC. This is due to the OLTCs mechanical nature. Since the algorithms use the OLTC set point change as a control method for the voltage control, it can be assumed that they will significantly increase the amount of the OLTC actions at the primary substation and therefore increase the probability of equipment failure and/or need for OLTC maintenance.

Since the AVR can be built as a fully solid state machine without any moving parts, it is not as vulnerable to the faults as the OLTC, but since in this thesis it is the only another component which has its set point changed as part of the CVC, it provides a good comparison for the OLTC action value and should therefore be also metered. AVR receives a reactive power set point value from the algorithm, which is then used to form the voltage reference value. Besides these reactive power set points, the real power set point changes are also followed, even though these affect the mechanical moment directly and not through the AVR. Both set points are followed with separate counters that record the sum of actions from all three generators.

As stated in [28, p. 2], when using the optimizing algorithm, it is important to make sure that the optimization function always converges. This will be done by following the output value from the fmincon function that records the reason of function ter-

mination during each of the algorithms executions. This variable, called exitflag, can receive values explained in the Table 5.6.

Table 5.6 *The optimization function exitflag values [36].*

3	AVCO / TCO signal blocked optimization function execution.
2	Change in `x` was less than `options.TolX` and the maximum constraint violation was less than `options.TolCon`.
1	First-order optimality measure was less than `options.TolFun`, and the maximum constraint violation was less than `options.TolCon`.
0	Number of iterations exceeded `options.MaxIter` or number of function evaluations exceeded `options.MaxFunEvals`.
-1	The output function terminated the algorithm.
-2	No feasible point was found.
-3	Objective function at current iteration went below `options.ObjectiveLimit` and maximum constraint violation was less than `options.TolCon`.

Of these values 3, 2 and 1 mean that the algorithm is working as intended: it either has found a solution or is prevented from operating because the AVC relay or the tap changer is still operating. Values 0, -1, and -2 mean that there was a problem with the algorithm and it has not converged to an optimal solution. Value 0 means function did not converge before exceeding the maximum number of iterations, which in this thesis is set to 100. Value -1 means that the function that called the fmincon function issued order to stop the iteration, value -2 that there is no solution that fits within the limits. Value -3 means that the target function value has gone below a pre-set objective function value, but this option is not used during this thesis. [36]

In a case where the algorithm is not able to take any more control actions to correct the network voltage levels, it outputs an alert message. To test the limits of the algorithms capabilities, it is important to examine the situations where algorithm is not able to make any more control actions and therefore these alerts are also monitored.

5.3.3 Metrics

The following characteristic values will be processed from the simulation data and used to compare the effectiveness of the algorithms. All of the mentioned values, except the average algorithm execution time, will be normalized either by multiplying them with [simulation time (s) / number of data points (pcs)] or by using trapezoidal integration (curtailed production and areas outside allowed voltage limits).

The curtailed production is one of the two variables that are being minimized by the optimizing algorithm and it also directly affects the profitability of the DG owners

business. Losses caused by the transfer of power are the second variable being minimized by the optimizing algorithm. These losses are realized as financial losses for the distribution network operator and are also metered. The optimizing algorithm target function value will be calculated for both algorithms. First part of the calculation is to sum up all the power generation and consumption values in the network and the power transferred through the primary substation transformer to gain the total losses from the power transfer in the network. This value will be multiplied with the price of losses mentioned in the subchapter 2.6.4.2, 44.6 €/MWh. To this value is then summed the amount of real power curtailed in the network multiplied with price of the curtailed production 82.8 €/MWh and the received value is [€]. It should be noted that this only works when all of the load values are known. During Sequence 9 they are all metered and in all of the other sequences loads are constant power loads with known values.

The area between the maximum voltage plot and the maximum allowed voltage line is calculated using trapezoidal integration. Integration is only done for those moments when the maximum voltage is higher than the largest allowed value (1,05 pu) or the minimum voltage is lower than the lowest allowed value (0,95 pu). These areas have been highlighted with orange color in the Figure 5.4.

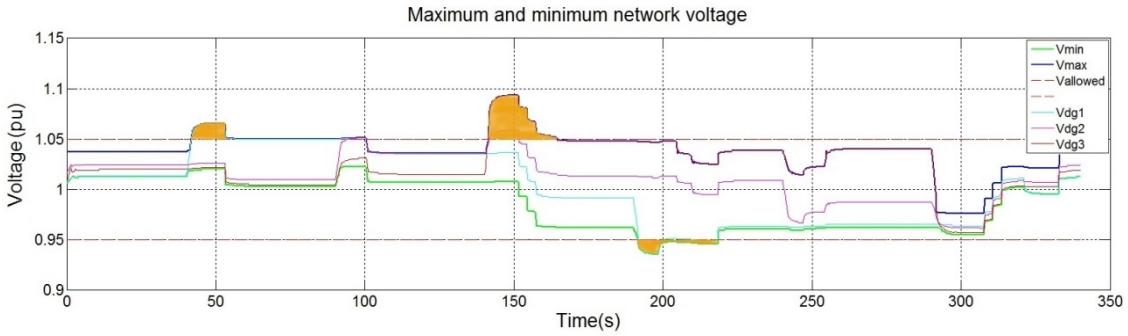

Figure 5.4 *Area outside voltage bounds.*

The gained value is [pu * s]. The duration [s] during which either the maximum or the minimum voltage or both are out of allowed limits is also calculated.

The average algorithm execution time excluding the reading and writing of the shared files is also calculated. During every execution of the algorithm, timer records the time it takes for the algorithm to arrive into a solution and these times are then summed together and divided with the number of the data points.

5.4 Test sequences

The RTDS tests are run in sequences where at the predetermined points adjustments will be made to the simulation network. The goal of these adjustments is to see how well control algorithms react to changes in the network status and whether they can keep all of the values within their allowed limits. With the optimizing algorithm it is also important to confirm that the fmincon function always converges to a solution.

All the sequences except the Sequence 9 are executed using static power loads and all the sequences are executed using all four different load conditions presented in the Table 5.3. Numbering of the generators is as follows: the DG unit at bus 13_5 is known as DG1, the DG unit at bus 13_9 is known as DG2 and the DG unit at bus 13_20 is known as DG3. This numbering holds true for all the other sequences except Sequences 4 and 5. Time delays of the rule based algorithms basic substation, reactive and real power controls are set to 4 seconds and time delays for the corresponding restoring controls are set to 6 seconds. The AVC relay delay is 3 seconds and the tap changer delay is 1 second, the optimizing algorithm is executed once every four seconds and the rule based algorithm is executed once every second. These delays are same as ones used in previous PSCAD simulations. In real situation these delays are often considerably longer, but since these test sequences are short and changes happen fast, the delays are shortened as well.

5.4.1 Sequence 1: Comparison with the PSCAD simulations

PSCAD simulations using the same algorithms and the same network data as in this thesis will be presented in a paper that will be published on a later date. To confirm similar results are gained from both the PSCAD and the RSCAD, the same simulation sequence will be used as in PSCAD simulations. This sequence is presented in Table 5.7.

Table 5.7 *Sequence 1, bolded values are changed at the particular moment.*

Time	Mechanical moment of DG1 [pu]	Mechanical moment of DG2 [pu]	Mechanical moment of DG3 [pu]
0 s	**0,1**	**0,1**	**0,1**
20 s	**1,0**	0,1	0,1
50 s	1,0	**1,0**	0,1
80 s	1,0	1,0	**1,0**
130 s	**0,1**	1,0	1,0
160 s	0,1	**0,1**	1,0
190 s	0,1	0,1	**0,1**

5.4.2 Sequence 2: Sequence 1 with longer durations between changes

When Sequence 1 was executed, it was noticed that the network status did not always have time to stabilize before next change was executed. Therefore it was decided to increase the time between each mechanical moment change by 20 seconds to ensure the algorithms can always reach a feasible network status or output the alert message before network state is changed again. This sequence is also used as the base sequence for the comparison with other sequence and it is presented in the Table 5.8.

Table 5.8 *Sequence 2.*

Time	Mechanical moment of DG1 [pu]	Mechanical moment of DG2 [pu]	Mechanical moment of DG3 [pu]
0 s	**0,1**	**0,1**	**0,1**
40 s	**1,0**	0,1	0,1
90 s	1,0	**1,0**	0,1
140 s	1,0	1,0	**1,0**
190 s	**0,1**	1,0	1,0
240 s	0,1	**0,1**	1,0
290 s	0,1	0,1	**0,1**

5.4.3 Sequence 3: Production emphasis shifting

The purpose of this sequence is to see how the algorithms react to the emphasis of production shifting from one DG bus to another. This should make the maximum network voltage location change multiple times during the sequence without the voltage limits being exceeded. The rule based algorithm should not react unless the voltage limit is exceeded at some bus, but the optimizing algorithm should always make control actions when the most ideal network state changes. Sequence 3 is introduced in the Table 5.9.

Table 5.9 *Sequence 3.*

Time	Mechanical moment of DG1 [pu]	Mechanical moment of DG2 [pu]	Mechanical moment of DG3 [pu]
0 s	**0,1**	**0,1**	**0,1**
20 s	**0,5**	0,1	0,1
40 s	**1,0**	0,1	0,1
60 s	1,0	**0,5**	0,1
80 s	1,0	**1,0**	0,1
100 s	**0,5**	1,0	0,1
120 s	**0,1**	1,0	0,1
140 s	0,1	1,0	**0,5**
160 s	0,1	1,0	**1,0**
180 s	0,1	**0,5**	1,0
200 s	0,1	**0,1**	1,0
220 s	**0,5**	0,1	1,0
240 s	**1,0**	0,1	1,0
260 s	1,0	0,1	**0,5**
280 s	1,0	0,1	**0,1**
300 s	**0,1**	0,1	0,1

5.4.4 Sequence 4: Generation at both feeders

In this sequence the DG1 located at the bus 13_5 is removed and instead placed on the feeder Kihniö's bus 7_25. This is done to see how the algorithms react to a situation with production at both of the feeders. The actual sequence used is the same as during Sequence 2.

5.4.5 Sequence 5: Exceeding limits while generation at both feeders

This sequence uses the same configuration as Sequence 4, but this time the generators are controlled so that the maximum voltage exceeds its allowed limits on both of the feeders. This is done by increasing the mechanical moment of the DG1 to the maximum value of 1,5 pu instead of 1,0 pu.

5.4.6 Sequence 6: Power generation increased in small steps

During this sequence the mechanical moment values of the generators are increased in steps of 0,25 pu to observe how the algorithms react to smaller changes than the ones used during the previous sequences. Sequence 6 is presented in the Table 5.10.

Table 5.10 *Sequence 6.*

Time	Mechanical moment of DG1 [pu]	Mechanical moment of DG2 [pu]	Mechanical moment of DG3 [pu]
0 s	**0,00**	**0,00**	**0,00**
20 s	**0,25**	0,00	0,00
40 s	0,25	**0,25**	0,00
60 s	0,25	0,25	**0,25**
80 s	**0,50**	0,25	0,25
100 s	0,50	**0,50**	0,25
120 s	0,50	0,50	**0,50**
140 s	**0,75**	0,50	0,50
160 s	0,75	**0,75**	0,50
180 s	0,75	0,75	**0,75**
200 s	**1,00**	0,75	0,75
220 s	1,00	**1,00**	0,75
240 s	1,00	1,00	**1,00**

5.4.7 Sequence 7: Algorithm limit test

In this sequence the output powers of the DG plants are increased in steps of 0,25 pu while the load multiplier of feeder Ritari is decreased in steps of 0,2 and the load multi-

plier of feeder Kihniö is increased in steps of 0,2. The purpose of this sequence is to force the algorithm at the same time near both the maximum and the minimum network voltage limits. The production curtailment parts of the algorithms have also been disabled so that the algorithm is forced into a situation where it cannot make any more correcting actions. If the real power curtailment wouldn't be disabled, the algorithms could curtail all of the production from the DGs and the feeder load multiplier changes alone are not enough to force the maximum or minimum voltage out of bounds. The actual sequence is presented in the Table 5.11.

Table 5.11 *Sequence 7.*

Time	Mechanical moment of DG1 [pu]	Mechanical moment of DG2 [pu]	Mechanical moment of DG3 [pu]	Feeder Ritari load multiplier	Feeder Kihniö load multiplier
0 s	**0,00**	**0,00**	**0,00**	**1,0**	**1,0**
20 s	**0,25**	0,00	0,00	1,0	1,0
40 s	0,25	**0,25**	0,00	1,0	1,0
60 s	0,25	0,25	**0,25**	1,0	1,0
80 s	0,25	0,25	0,25	**0,8**	**1,2**
100 s	**0,50**	0,25	0,25	0,8	1,2
120 s	0,50	**0,50**	0,25	0,8	1,2
140 s	0,50	0,50	**0,50**	0,8	1,2
160 s	0,50	0,50	0,50	**0,6**	**1,4**
180 s	**0,75**	0,50	0,50	0,6	1,4
200 s	0,75	**0,75**	0,50	0,6	1,4
220 s	0,75	0,75	**0,75**	0,6	1,4
240 s	0,75	0,75	0,75	**0,4**	**1,6**
260 s	**1,00**	0,75	0,75	0,4	1,6
280 s	1,00	**1,00**	0,75	0,4	1,6
300 s	1,00	1,00	**1,00**	0,4	1,6
320 s	1,00	1,00	1,00	**0,2**	**1,8**

5.4.8 Sequence 8: The algorithms having time delay

The algorithms will operate very fast with the simulation network used in this thesis since the network is very simple. In a real life situation the algorithms would need to process information about much larger and more detailed network and therefore they are tested using two different time delays inserted into the algorithm before the part where new set point values are written to the shared file. This is meant to emulate the time it would take for the algorithm to arrive into a solution in a real situation. The used delays are 4 and 12 seconds and the actual sequence used is the same as during Sequence 2.

5.4.9 Sequence 9: Using impedance loads

In this sequence the algorithms are tested using loads that have constant impedance values instead of constant power values, which are used in all of the other sequences. The constant power load is the hardest case for the voltage control, since voltage decreasing won't decrease the power consumed by the load. Therefore most of the simulations are executed using constant power loads, but this sequence is included to see how the algorithms react to another type of a load model. The actual sequence used is the same as during Sequence 2.

5.4.10 Sequence 10: Simulation of wind power plants

In this sequence the DGs are simulating wind power plants, meaning their mechanical moment will change according to randomly changing wind conditions. Mechanical moment data is acquired from PSCAD using MOD2 type wind turbine model, turbine controller and wind source components. Each of the three DGs has a unique mechanical moment sequence.

5.4.11 Sequence 11: Iteration limits and termination tolerance

As explained in the subchapter 2.6.4.4, the optimizing algorithm uses a three-phased method to find the optimal tap changer position. During the initial testing it was noticed, that quite often one of the two possible tap changer positions around the optimal continuous tap changer position was so far away from a feasible network state that the function did not converge even after 1000 iterations. The other position tested was almost always very easily feasible and required less than 50 iterations. The maximum number of iterations was set to 100 during previous test sequences, since going through 1000 iterations was causing considerable lag to the execution of the algorithm. During this sequence the effect of different iteration limits will be tested.

Two of the options available for the fmincon function are the termination tolerance of the function value and termination tolerance of the vector x, that includes vectors $\mathbf{u_d}$, $\mathbf{u_c}$ and $\mathbf{x}$ defined in the subchapter 2.6.4.1. By default the termination tolerance of the function value is 1E-6 and the termination tolerance of the vector x is 1E-10. There is also a third tolerance, the allowed constraint violation. By default this value is 1E-6, the same as the function value tolerance, and since it must also be met for the iteration to finish successfully, it will be always changed the same way as the function value termination limit.

In this sequence the optimizing algorithm will be tested using different maximum amounts of iterations and different termination tolerances to see how this affects the effectiveness of the algorithm. The actual sequence used in these tests is the same as during Sequence 2 and the different test parameters are presented in the Figure 5.5.

Iterations: 50 **Function value termination limit: 1E-4** **x termination limit: 1E-8**	**Iterations: 500** **Function value termination limit: 1E-4** **x termination limit: 1E-8**
Iterations: 50 **Function value termination limit: 1E-8** **x termination limit: 1E-12**	**Iterations: 500** **Function value termination limit: 1E-8** **x termination limit: 1E-12**

Figure 5.5 *Sequence 11 parameters.*

5.4.12 Sequence 12: Effect of the supply network strength

In this sequence the strength of the transmission network supplying the primary substation will be changed to see how this affects the execution of the voltage control algorithms. The supply network impedance will be first set to 50% and then to 200% of the original value of 48,341 Ω while executing the same changes as during Sequence 2. This simulation emulates a situation where the primary substation is supplied by two or more feeders (for example, as part of a ring topology) and one of them experiences a fault, which causes the supply network impedance seen from the distribution network to change.

6 SIMULATION RESULTS

In this chapter the results gained from the RTDS simulations are presented and interesting parts are highlighted and discussed. Key metrics and counter values are presented for every sequence using tables similar to the Table 6.1 below, where Middle 1, Middle 2, Maximum and Minimum are the different load cases discussed in the subchapter 5.2.

Table 6.1 *Example result table.*

	Middle 1	Middle 2	Maximum	Minimum
Curtailed production (kWh)				
Network losses (kWh)				
Target function value (€)				
Over-voltage area (pu * s)				
Under-voltage area (pu * s)				
Duration the voltage is out of bounds (s)				
Average algorithm execution time (s)				
Errors (pcs)				
OLTC steps taken (pcs)				
P set point changes (pcs)				
Q set point changes (pcs)				

Curtailed production, network losses and target function value, over-voltage area and under-voltage area are calculated as presented in the subchapter 5.3.3. The duration voltage is out of bounds and the average algorithm execution times are also explained in the same subchapter. Errors, OLTC steps and power set point changes are followed with counters introduced in the subchapter 5.3.2 and it should be noted, that the real power counter only records how many times the algorithm changes the set point and the real power changes that are part of the sequences are not included in this value.

Tables like the Table 6.1 will be presented for all of the sequences, separate ones for both the optimizing algorithm and the rule based algorithm. All different plot graphs are introduced for Sequence 1 Middle 1 case, but after that will only be included when they are needed to explain the results presented in the tables. Data for all of the graphs and metrics along with the Matlab code used to process it can be found at [37].

6.1 Sequence 1

Sequence 1 is used as a comparison case for the PSCAD simulation results and all of the plot graphs for the optimizing algorithm Middle 1 case are presented. The first figure

includes the primary graphs: network maximum and minimum voltages together with voltages of the buses connecting the DGs; substation voltage together with OLTC voltage reference value and deadband; measured real powers of the DGs and real power set point values; measured reactive powers of the DGs and reactive power set point values. The secondary graphs include: tap changer position; real and reactive powers transferred through the primary substation; DG power factor values; optimizing algorithm exitflag values. Tap changer positions are reverse: position 19 has the lowest tap ratio of 0,85 and position 1 has the highest tap ratio of 1,15, whereas position 10 has a ratio of 1,00. This is caused by the tap changer being located on the high voltage side of the primary transformer.

6.1.1 Optimizing algorithm

Primary graphs for the optimizing algorithm are presented in the Figure 6.1 below.

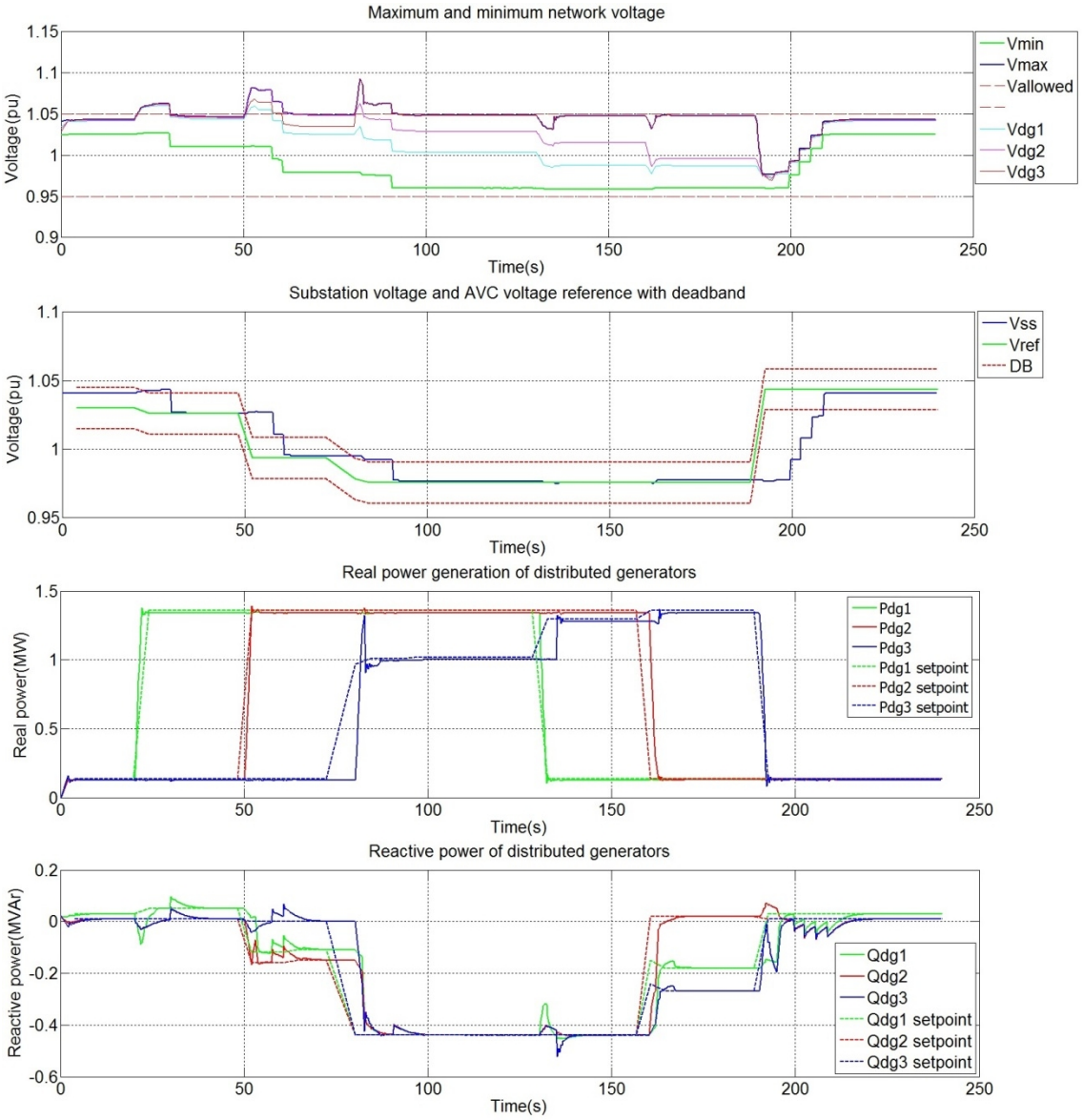

Figure 6.1 *Primary graphs, optimizing algorithm, Middle 1.*

It can be seen from the Figure 6.1 that the network maximum voltage goes over the allowed level (1,05 pu) every time one of the DGs has its real power generation increased. During the first increment the algorithm manages to lower the voltage to the allowed limits by using only the tap changer and during the second increment it also starts to consume reactive power with the DG1 and DG2. Moments when the tap changer operates are easily identified from steps down in all of the voltages in the first graph: one step around time 30s and two steps between 60 s and 70 s. These changes can also be identified from the second graph, which shows the substation voltage, its reference value and deadband. When the substation voltage ends up outside the deadband, the tap changer operates to bring it near the reference value again.

When DG3s real power is increased at 80 s, the tap changer can only be used once since the minimum voltage is already close to the allowed minimum voltage value (0,95 pu) and therefore the algorithm controls all of the DGs to consume the maximum amount of reactive power (0,44 MVAr) to lower the maximum voltage. All three DGs have their reactive power consumption set to maximum value of 0,44 pu at 80 seconds as seen from the fourth graph, but since this won't lower the maximum voltage enough, the real power generation of the DG3 is also curtailed as shown in the graph three. DG3 is chosen for curtailment since the network maximum voltage is located at its connecting bus and therefore it has the highest voltage sensitivity value of the three DGs in the network. The production curtailment and the reactive power consumption are applied instantly, but the tap changer operates only at 90 s, since it has built in delay. After these operations the network maximum voltage is restored between allowed limits.

When the real power generation of the DG1 is lowered at 130 s, part of the real power curtailment of the DG3 is removed. When DG2s generation is also lowered at 160 s, the curtailment is completely removed and the DG3 reaches its nominal real power generation. At this time amount of the reactive power consumption of the DGs is also lowered: DG2s reactive power returns to positive value near 0, but DG1s and DG3s reactive powers still stay negative. These two reactive powers finally return to positive values after the real power generation of the DG3 is lowered at 180 s. After this the tap changer also operates four times to bring the network voltages near the original level.

In graph 4 it can be seen that the algorithm had been changing the reactive power generation of the DG1 even before the generators were used to consume reactive power after 50 s point. Between 0 s and 50 s the DG1 was generating reactive power to keep the network voltages as high as possible to minimize the transfer losses while still staying within the allowed voltage limits. Figure 6.2 presents the secondary graphs for the optimizing algorithm in the Middle 1 case.

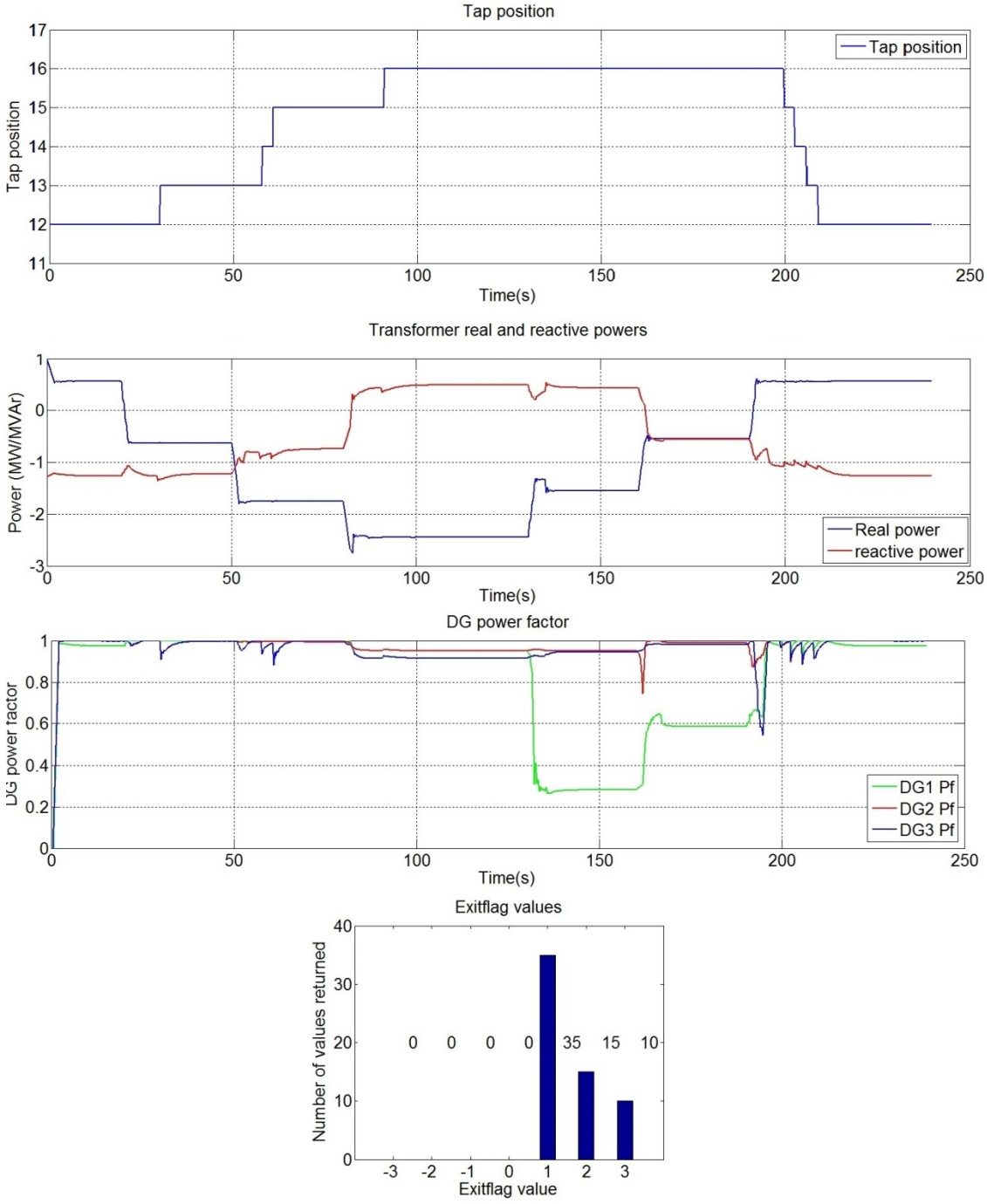

Figure 6.2 *Secondary graphs, optimizing algorithm, Middle 1.*

Transformer real and reactive powers are presented with positive flow being from the transmission network to the distribution network. The real power transfer through the primary transformer lowers in clear steps as changes are implemented to the mechanical moments of the DGs since all of the loads are modelled as static constant power loads. The reactive power fluctuates during the real power changes, but mostly stays at a constant level. A large increment and a change in the direction of the reactive power flow can be seen around 80 seconds when the DGs start to consume reactive power to lower the voltage as ordered by the algorithm. The reactive power flow reverses again and

returns to its previous value around 170 seconds when the algorithm reacts to the real power generation reduction that is part of the sequence.

In Figure 6.2 graph two the reactive power flowing through the primary substation transformer has a negative value when the generators are not consuming reactive power (before 80 s and after 160 s). In a case like this any capacitors installed at the substation need to be disconnected, since more reactive power is generated than consumed in the simulation network. Transmission network owners also generally try to prevent the reactive power flow in the transmission network by collecting a fee when reactive power flows to or from the transmission network is considerable compared to real power flow. Especially flow from the distribution network to the transmission network is considered harmful. In this case the flow is caused by the 10 μF capacitor which cannot be disconnected since it is used to suppress the software bug discussed in subchapter 5.2.

The power factor values of the DG units are calculated from the actual measured values and since the algorithms do not have any power factor control included, these fluctuate strongly when the real power generation is reduced and the reactive power consumption is used at the same time. In these simulations the power factor sometimes reaches very low values as seen from the Figure 6.2 graph three. Some of these values might not be within the possible operational zone of a real world generator, but this is not considered during this thesis. The exitflag values show that the algorithm has finished execution with feasible solution during every cycle; in cases of the values 1 and 2 by converging to a solution and in case of the value 3 by being blocked by the AVCO/TCO signal.

6.1.2 Rule based algorithm

Figures 6.3 and 6.4 include the rule based algorithms graphs corresponding to the optimizing algorithms graphs in the Figures 6.1 and 6.2. When comparing the real power graphs, it should be noted that the set point values are presented differently for the rule based algorithm and the optimizing algorithm. This is a consequence of the different output value types of the algorithms: the rule based algorithm outputs a change value ΔPdg that is summed to the existing real power set point value to receive the new value whereas the optimizing algorithm outputs a new set point value Pdg.

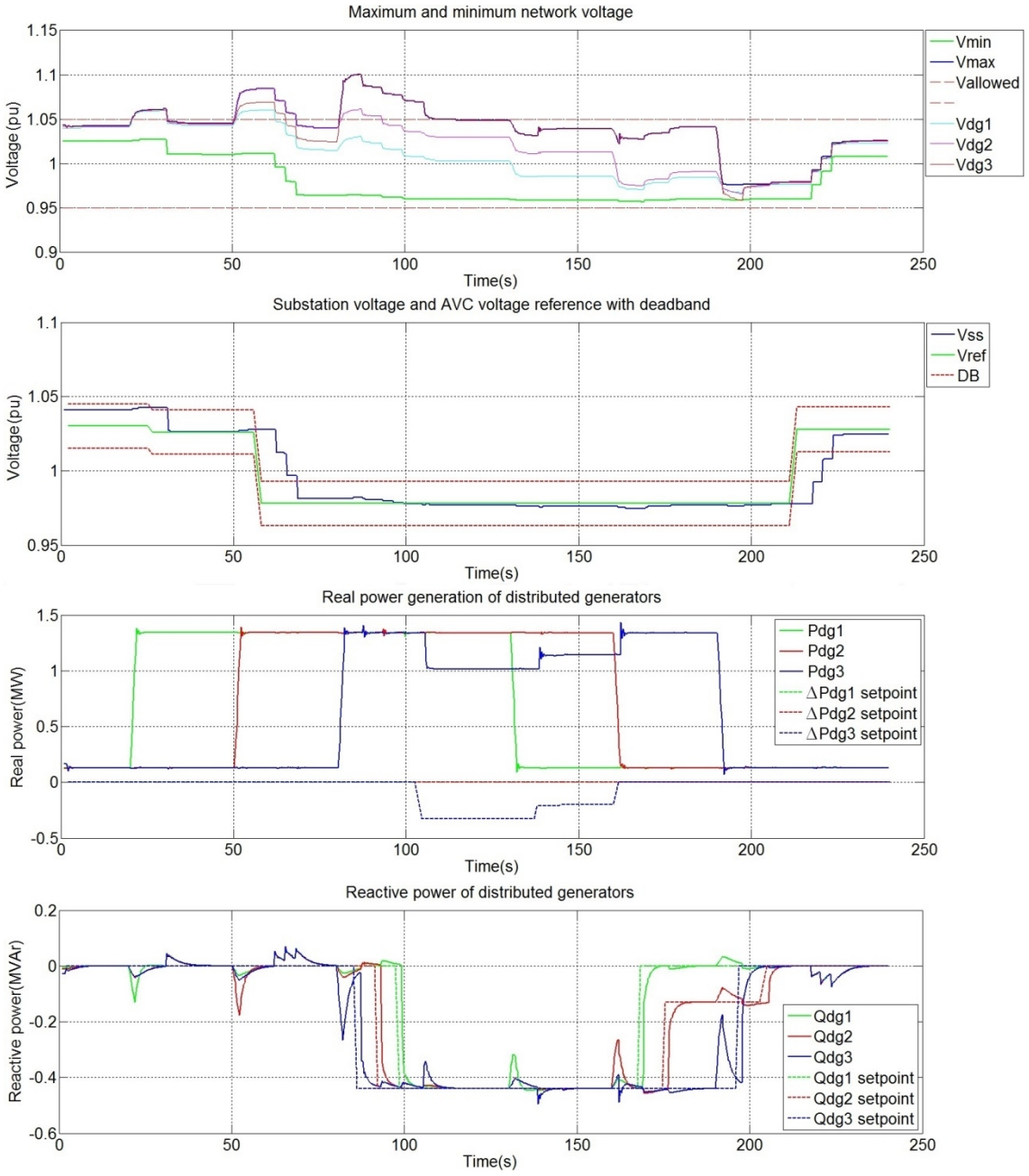

Figure 6.3 *Primary graphs, rule based algorithm, Middle 1.*

Since the rule based algorithm does not have exitflag values, the Figure 6.4 only includes three graphs: Tap changer position, transformer real and reactive power and DGs power factors.

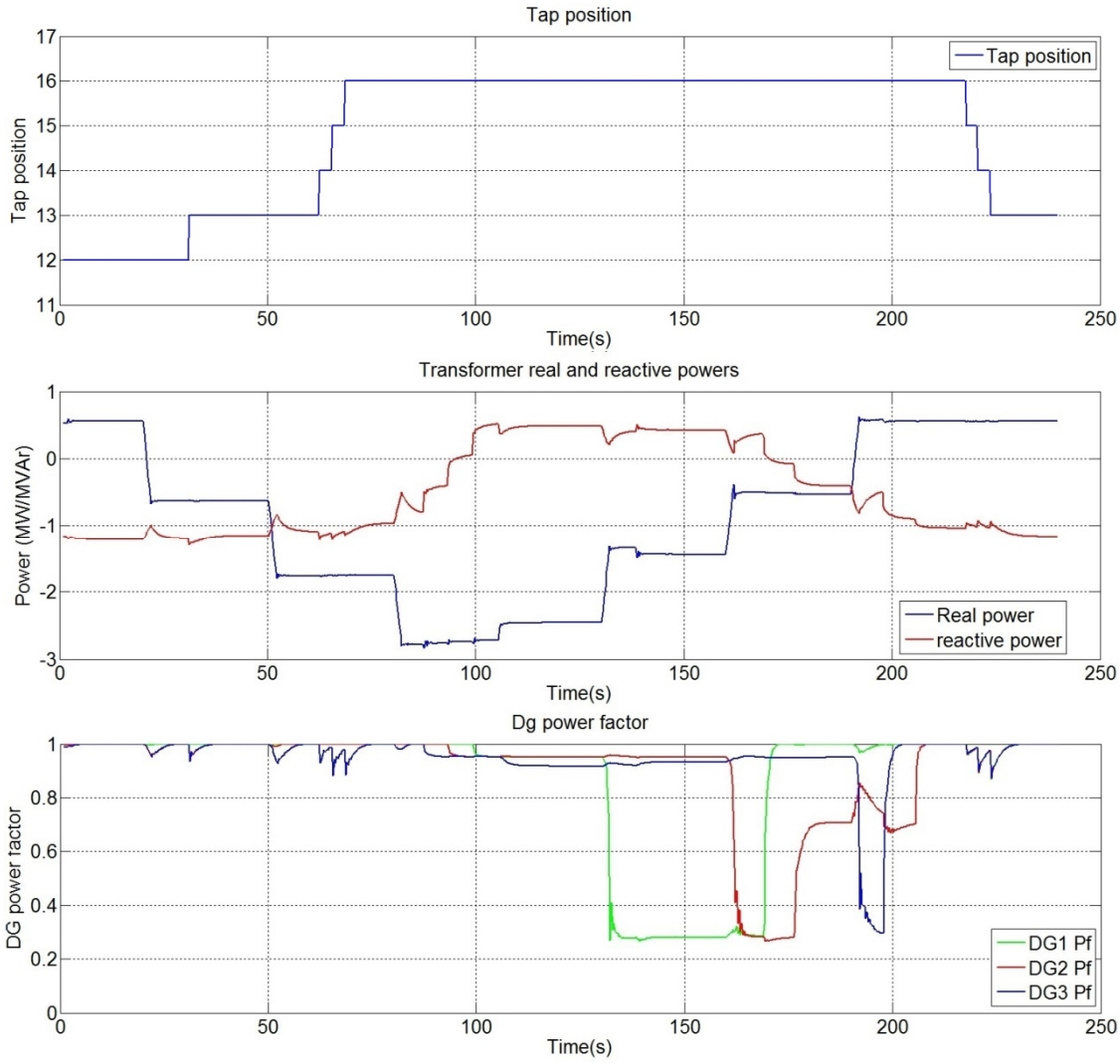

Figure 6.4 *Secondary graphs, rule based algorithm, Middle 1.*

The reactions of the rule based algorithm are very similar to those of the optimizing algorithm, but there are certain differences, which will be discussed in the next chapter.

6.1.3 Comparison of the algorithms

The rule based algorithm reacts to the voltage limit violations in a similar manner as the optimizing algorithm, first with tap changer action, then with reactive power consumption and lastly with real power curtailment. The most notable difference is that the rule based algorithm only operates a single active resource at a time. The reactive power of the DG3 is set to the negative maximum value at around 90 s, DG2s at around 95 s, DG1s at around 100 s and around 105 s the real power curtailment is implemented to the DG3. With the optimizing algorithm all of these operations were executed simultaneously around 80 s, allowing for a much faster response.

There was a difference between algorithms reactions during the DG2 real power increment at 50 s: the optimizing algorithm only stepped down two tap steps and handled the remaining over-voltage by consuming reactive power with the DG1 and DG2.

The rule based algorithm uses three tap steps and does not changed the reactive power set points. Another difference is evident when the algorithms restored the voltage levels after the real power generation had decreased: the optimizing algorithm strived to keep the network maximum voltage as high as possible while still staying within the voltage limits. The rule based algorithm used the restoring control to remove the changes it had previously made to the power set points and the OLTC reference value, but it won't allow the network maximum voltage to get closer than 0,01 pu below the allowed limit. Because of this the network maximum voltage stays at 1,04 pu around 150 second point and 180 second point. Tables 6.2 and 6.3 show metric values used to compare effectiveness of the algorithms.

Table 6.2 *Optimizing algorithm results, Sequence 1.*

	Middle 1	Middle 2	Maximum	Minimum
Curtailed production (kWh)	5,8	4,7	3,7	3,7
Network losses (kWh)	8,5	8,6	8,5	9,5
Target function value (€)	0,8504	0,7722	0,6889	0,7297
Over-voltage area (pu * s)	0,4996	0,5229	0,5153	0,4561
Under-voltage area (pu * s)	0,0000	0,0000	0,0000	0,0000
Duration the voltage is out of bounds (s)	33,2239	29,5708	17,9456	37,9242
Average algorithm execution time (s)	1,2557	1,4019	1,2539	0,9246
Alerts (pcs)	0	0	0	0
OLTC steps taken (pcs)	8	8	6	9
P set point changes (pcs)	4	4	3	4
Q set point changes (pcs)	20	20	19	19

Table 6.3 *Rule based algorithm results, Sequence 1.*

	Middle 1	Middle 2	Maximum	Minimum
Curtailed production (kWh)	4,4	4,2	3,7	2,6
Network losses (kWh)	8,8	8,8	8,9	9,6
Target function value (€)	0,7541	0,7367	0,6985	0,6462
Over-voltage area (pu * s)	1,3440	1,1070	1,0064	1,6455
Under-voltage area (pu * s)	0,0000	0,0000	0,0000	0,0000
Duration the voltage is out of bounds (s)	56,3418	60,8581	40,5596	73,0318
Average algorithm execution time (s)	0,0127	0,0138	0,0121	0,0131
Alerts (pcs)	0	0	0	0
OLTC steps taken (pcs)	7	7	6	8
P set point changes (pcs)	4	4	4	3
Q set point changes (pcs)	7	6	7	6

The differences in curtailed production and network losses are quite small between the two algorithms since the sequence is quite short. Generally the optimizing algorithm tends to curtail more production during the sequence than the rule based algorithm, since it makes all the necessary changes simultaneously and therefore the dura-

tion of the curtailment is longer. This also leads to having a larger target function value, since the curtailed real power is priced almost twice as high as the network losses power. On the other hand the optimizing algorithm also operates to minimize the network losses whereas the rule based only reacts to the voltage limit violations. This leads to the network losses being smaller with the optimizing algorithm, which partially compensates for having larger amount of curtailed production. The main difference in the effectiveness of the algorithms can be seen from the under- and over-voltage areas and the duration voltage is out of bounds. The voltage is out of bounds 1,55 – 2,25 times longer and the over-voltage area is 1,40 – 3,65 times larger with the rule based algorithm than with the optimizing algorithm. Since voltage safety is the highest priority, the optimizing algorithm can be deemed to work clearly better during this sequence.

The average algorithm execution time of the rule based algorithm is about 100 times faster than the optimizing algorithms. This is caused by the iteration process of the fmincon function and is as expected. As an average the optimizing algorithm takes one more tap changer step than the rule based algorithm when returning the voltages after 200 s. This is caused by the optimizing algorithms effort to minimize the network losses, whereas the rule based algorithm only strives to return the OLTC reference to the original value. Since there is a deadband around the reference value, having the same reference value does not always equal having the same tap value.

Real power set point changes are generally quite similar between the algorithms. However, the optimizing algorithm does sometimes make small changes to the set point value, causing few extra changes. There are many more reactive power set point changes when using the optimizing algorithm than with the rule based algorithm since the reactive power is used to minimize the network losses by raising the voltage levels.

During the construction of the test network model in the RSCAD it was noticed that the optimizing algorithm sometimes overreacts when changing the real and reactive power set points of the DGs. This error was never isolated and therefore in these sequences there can be seen points where the optimizing algorithm makes multiple changes after each other, like the ones at 80 s in the Figure 6.1 real power graph or at 160 s in the Figure 6.1 reactive power graph. Almost always the set point value is fast corrected and causes no problems with the coordinated voltage control. The same algorithm and network data was tested using PSCAD simulations and this error did not occur at all. Therefore it is concluded to be caused by the RSCAD test model and not being a fault in the algorithm design. It might be caused be by the 10 μF capacitor connected to the primary transformer low voltage side to suppress the error discussed in subchapter 5.2.

6.1.4 Comparison with the PSCAD simulations

Results from previously conducted PSCAD simulations are presented in Figures 6.5 and 6.6. These figures present the optimizing algorithm and the rule based algorithm respectively in the Middle 1 load case. These simulations have been conducted by the staff of

TUT Department of Electrical Engineering before work on this thesis began and the results of these simulations will be published as an article on a later date.

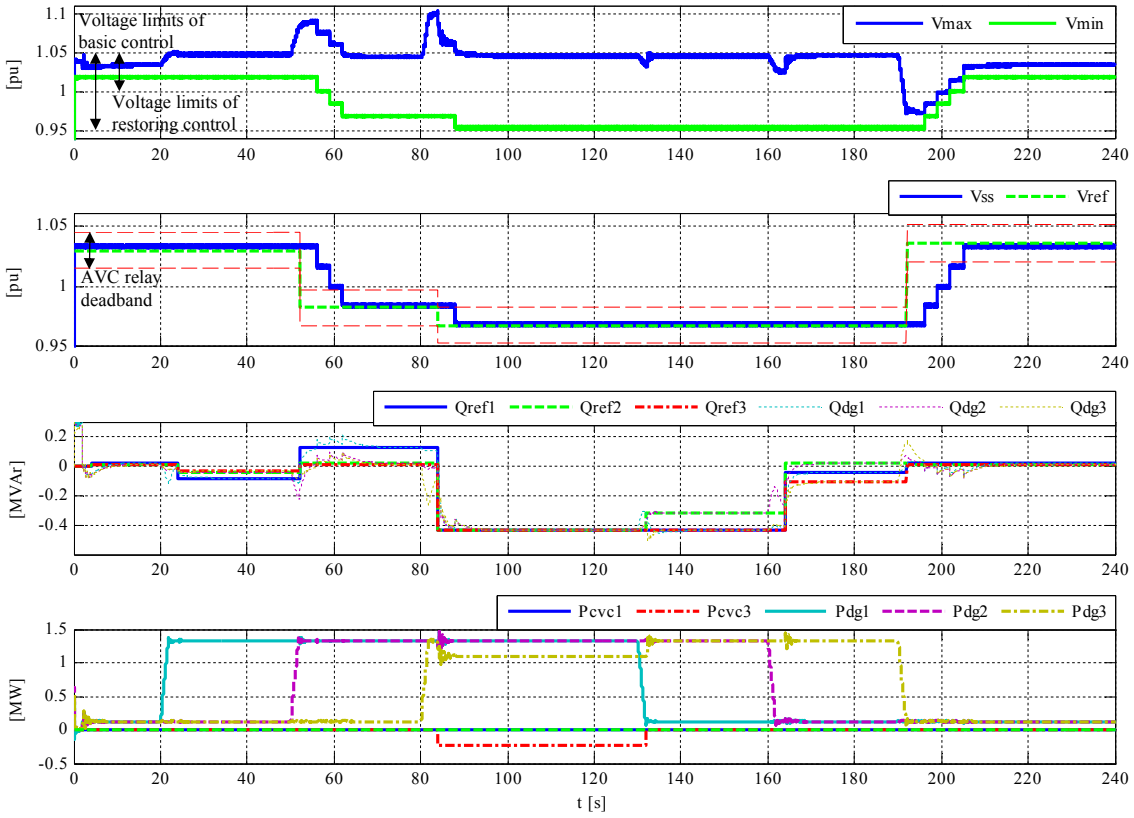

Figure 6.5 *Optimizing algorithm, Middle 1, PSCAD.*

When Figure 6.5 is compared to the Figure 6.1, certain differences can be pointed out. The first real power increment at 20 s doesn't make the network maximum voltage increase out of bounds in PSCAD, but in RSCAD it does. Therefore the tap changer operates once around 20 s and only twice at 50 s, whereas in PSCAD it operates three times at 50 s. After the tap steps around 50 s the substation voltage reference is 0,98 pu in PSCAD, but 1,00 pu in RSCAD, which also causes the reactive power to behave differently. In PSCAD some reactive power is generated to keep the network maximum voltage near its maximum value, but in RSCAD reactive power is being consumed. The response to the real power increment at 80 s is similar in both simulations: one tap step, maximum reactive power consumption and approximately 0,25 MW of production curtailment at the DG3. When DG1s real power generation is decreased at 130 s, the PSCAD version of the algorithm is able to remove all of the real power curtailment and to decrease the reactive power consumption of the DG2 approximately 0,1 MVAr. At the same situation the RSCAD version of the algorithm is able to reduce the real power curtailment, but not completely remove it. After the real power generation is reduced at 160 s and 190 s, both algorithms reduce reactive power consumption and around 200 s the tap changer steps up four times. Even though many actions are executed differently in the two simulators, the logic behind the changes is the same and the order in which

the changes are made is the same. Real power curtailment is started from the DG3 and reactive powers of the generators are restored in same order: first the DG2, then the DG1 and the DG3 as last.

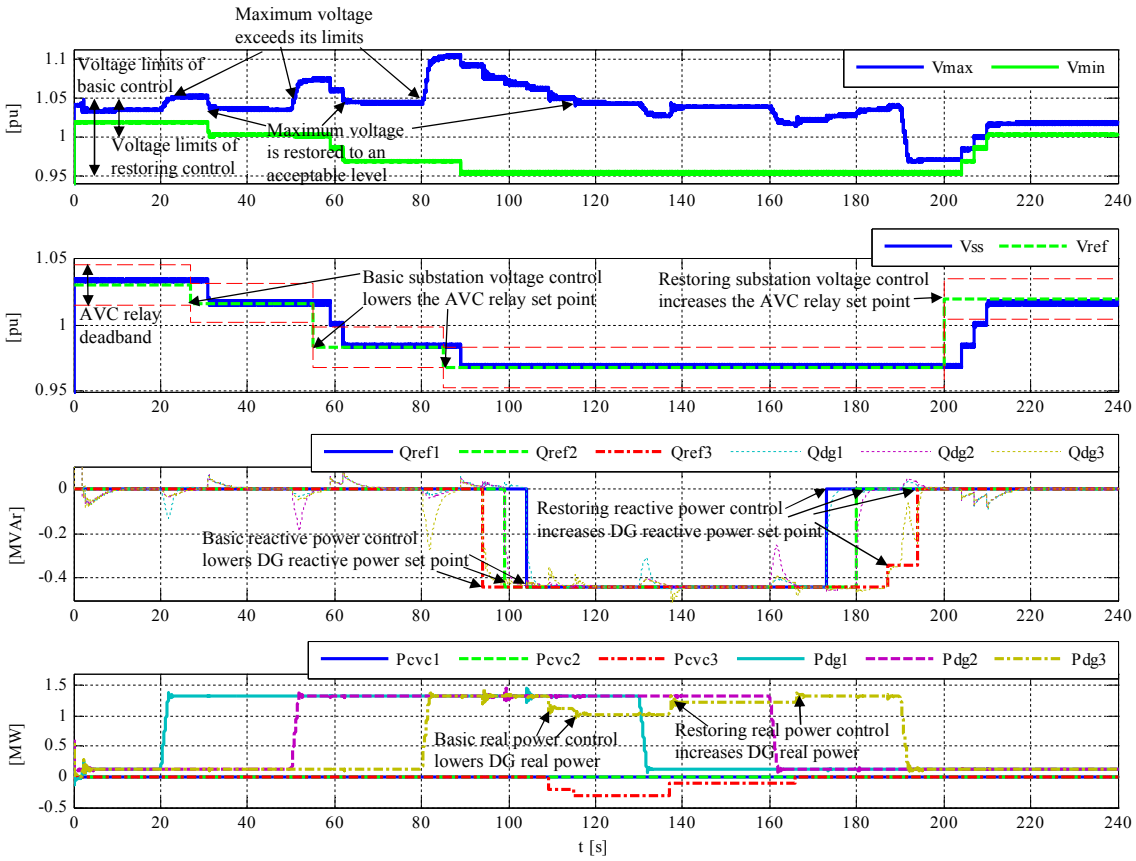

Figure 6.6 *Rule based algorithm, Middle 1, PSCAD.*

As was the case with the optimizing algorithm, the rule based algorithm results also differ between the two simulators. In The PSCAD simulation it is enough take two tap steps after 50 s, but in RSCAD three steps are needed. After 90 s the PSCAD algorithm takes one more tap step, sets reactive power consumption to the maximum value at all three generators and curtails the real power generation of the DG3. In RSCAD the same actions are executed except the tap step, since one more tap step was taken previously. When real power generation is decreased later during the sequence, in both simulations the actions the algorithms are similar, but the amounts of changes vary again. PSCAD version of the algorithm is able to decrease the reactive power consumption faster, but both algorithms are able to only remove it completely after 190 s. In both simulations the tap changer steps up three times around 200 s, one less step than with the optimizing algorithm.

Even though neither of the two algorithms functioned exactly the same way in both of the simulators, the logic behind the control actions and the order in which the resources were used were the same. There might have been some minor differences with the setup of the network state at the start of the sequence which caused the differences

between the simulators, but the results show that algorithms are working as intended in the real time simulator environment as well as in a non-real time environment. Later results also show that there are probably some small differences between simulator models, but these differences were never isolated. They might be caused by the 10 µF capacitor as discussed before.

6.2 Sequence 2

Sequence 2 is almost the same as Sequence 1, except this time there are 20 seconds more time between the changes of the mechanical moment. This sequence is also used as base for most of the later sequences and therefore it is used as this thesis's base case. Tables 6.4 and 6.5 include metrics for the comparison of the algorithms.

Table 6.4 *Optimizing algorithm results, Sequence 2.*

	Middle 1	Middle 2	Maximum	Minimum
Curtailed production (kWh)	5,9	4,8	3,7	3,8
Network losses (kWh)	11,4	11,5	11,5	12,7
Target function value (€)	0,9946	0,9087	0,8182	0,8774
Over-voltage area (pu * s)	0,5106	0,5545	0,5555	0,5025
Under-voltage area (pu * s)	0,0000	0,0000	0,0000	0,0000
Duration the voltage is out of bounds (s)	23,7783	31,0186	19,4347	37,2431
Average algorithm execution time (s)	1,1887	1,2570	1,2309	0,9967
Alerts (pcs)	0	0	0	0
OLTC steps taken (pcs)	8	8	6	9
P set point changes (pcs)	4	4	3	4
Q set point changes (pcs)	17	20	18	19

Table 6.5 *Rule based algorithm results, Sequence 2.*

	Middle 1	Middle 2	Maximum	Minimum
Curtailed production (kWh)	5,9	4,9	4,1	3,4
Network losses (kWh)	11,6	11,7	11,7	12,8
Target function value (€)	1,0004	0,9232	0,8580	0,8470
Over-voltage area (pu * s)	1,2198	1,2266	1,1271	1,6569
Under-voltage area (pu * s)	0,0000	0,0000	0,0000	0,0000
Duration the voltage is out of bounds (s)	52,3881	64,3521	42,9839	73,5271
Average algorithm execution time (s)	0,0101	0,0107	0,0096	0,0100
Alerts (pcs)	0	0	0	0
OLTC steps taken (pcs)	7	7	6	8
P set point changes (pcs)	4	4	4	3
Q set point changes (pcs)	7	6	7	6

Same as during the Sequence 1, the optimizing algorithm works faster to bring the voltage within the allowed limits and has smaller network losses. The duration voltage is out of bounds is roughly two times longer with the rule based algorithm than with

the optimizing algorithm. However, with longer times between the changes than during the Sequence 1, the difference in curtailed production is changed. Figure 6.7 explains why the optimizing algorithm is able to curtail less production in Maximum and Middle 2 cases.

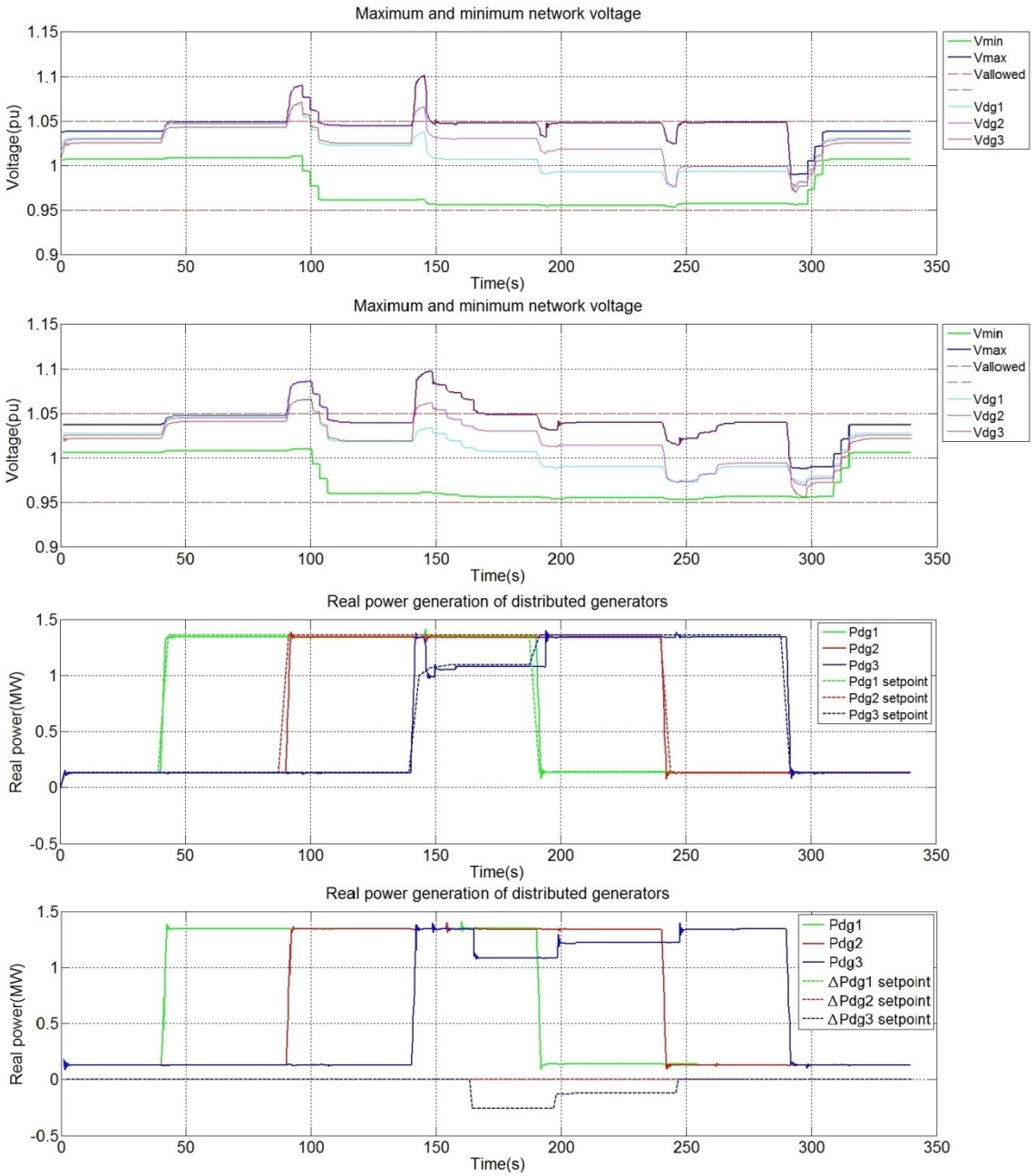

Figure 6.7 *Network voltages and reactive powers, Maximum case, optimizing algorithm graph on the top and rule based algorithm graph on the bottom.*

When real power production of the DG1 is lowered at 190 s, optimizing algorithm is able to remove all of the real power curtailment from the DG3 and keep the network maximum voltage below 1,05 pu. The rule based algorithm also removes part of the curtailment, but because the restoring part of the rule based algorithm has a 0,01 pu

safety marginal when increasing the voltage, it won't allow the network voltage above the value of 1,04 pu. Rest of the curtailment is only removed when the DG2 decreases the real power generation at 240 s. When times between mechanical moment changes of the sequence are longer, the time between real power generation subtractions of the DG1 and DG2 is also longer. This means that there is a longer duration the rule based algorithm is curtailing production while the optimizing algorithm is not curtailing production than during the Sequence 1. Optimizing algorithm is only able to curtail less production in Maximum and Middle 2 cases because in these cases the loads have the highest values. When loads are smaller, there is more need for the real power curtailment and the reduction in curtailment caused by the delay in rule based algorithm is larger.

Figure 6.8 shows the amount of curtailment that could be implemented to correct the situation, but which is not implemented because of the delay with the rule based algorithm, highlighted with orange color. This delay is caused by the rule based algorithm only operating one active resource at the time. Because of this it only curtails production after all the other changes have been implemented. If it reacted like the optimizing algorithm, Pdg3 would be set to around 1,1 pu before 150 s point instead of at around 160 s point.

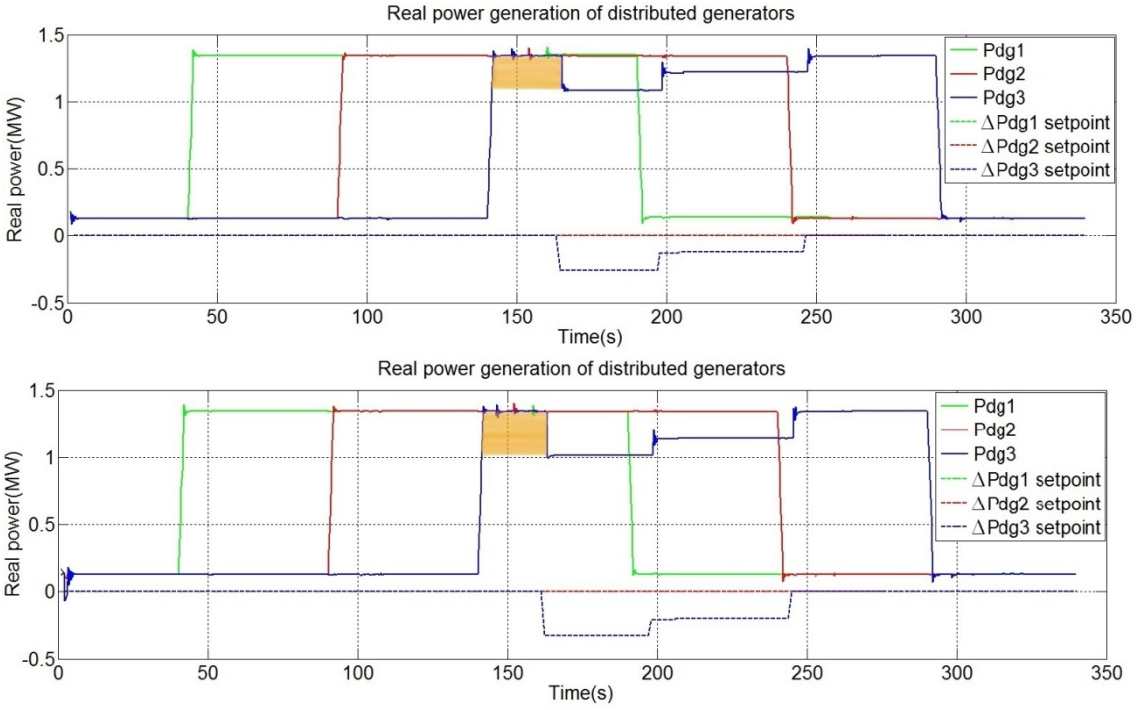

Figure 6.8 *Real power generation, rule based algorithm, Maximum case graph on the top and Middle 1 case graph on the bottom.*

Points where the algorithm changes reactive power set points of the generators can be identified from the small spikes in the particular generators real power graph. Since the amount of curtailment that could be implemented, but is not implemented is only affected by the loading situation, but the extra curtailment caused by the time between mo-

ment changes is directly dependent of the time between changes, if times between the changes were further increased, the optimizing algorithm would eventually have a smaller amount of curtailment in all of the cases.

6.3 Sequence 3

In Sequence 3 the production emphasis is shifting without the network voltage violating its limits. This causes the optimizing algorithm to operate multiple times while the rule based algorithm does not activate. Tables 6.6 and 6.7 include metrics for the comparison of the algorithms.

Table 6.6 *Optimizing algorithm results, Sequence 3.*

	Middle 1	Middle 2	Maximum	Minimum
Curtailed production (kWh)	0,5	0,3	0,1	0,1
Network losses (kWh)	8,2	8,1	7,9	8,7
Target function value (€)	0,4019	0,3867	0,3606	0,3947
Over-voltage area (pu * s)	0,6246	0,6213	0,4899	0,6209
Under-voltage area (pu * s)	0,0000	0,0000	0,0000	0,0000
Duration the voltage is out of bounds (s)	52,6236	50,0031	44,4991	67,4021
Average algorithm execution time (s)	0,9811	1,0533	1,1304	0,7679
Alerts (pcs)	0	0	0	0
OLTC steps taken (pcs)	12	10	8	11
P set point changes (pcs)	3	2	1	1
Q set point changes (pcs)	48	58	53	48

Table 6.7 *Rule based algorithm results, Sequence 3.*

	Middle 1	Middle 2	Maximum	Minimum
Curtailed production (kWh)	0,0	0,0	0,0	0,0
Network losses (kWh)	8,5	8,5	8,3	9,1
Target function value (€)	0,3806	0,3790	0,3690	0,4047
Over-voltage area (pu * s)	0,7637	0,7431	0,6442	0,8269
Under-voltage area (pu * s)	0,0000	0,0000	0,0000	0,0000
Duration the voltage is out of bounds (s)	71,3675	76,2469	60,6057	86,7772
Average algorithm execution time (s)	0,0112	0,0104	0,0104	0,0095
Alerts (pcs)	0	0	0	0
OLTC steps taken (pcs)	9	9	8	10
P set point changes (pcs)	0	0	0	0
Q set point changes (pcs)	11	11	10	9

The network losses are smaller with the optimizing algorithm, which is to be expected since the rule based algorithm does not consider the network losses at all. Target function value is, however, smaller for the rule based algorithm in the Middle 1 and Middle 2 cases. This is once again caused by the optimizing algorithm reacting faster by implementing all of the correcting actions at the same time whereas the rule based algo-

rithm controls active resources one by one. This is presented in the Figure 6.9, which shows the network voltage and the real power generation graphs for the Middle 1 case of both the rule based algorithm and the optimizing algorithm.

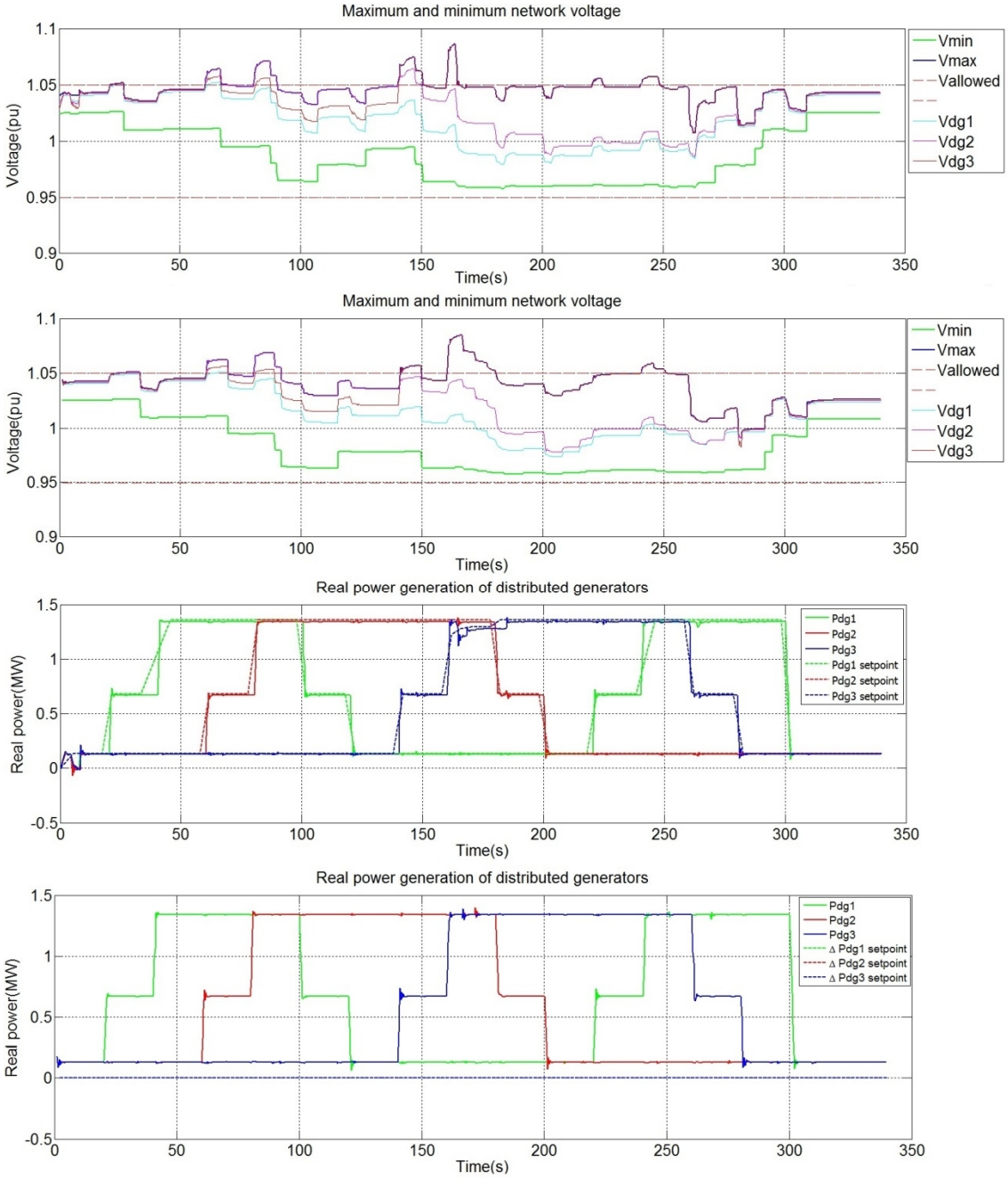

Figure 6.9 *Network voltages and real power generation, optimizing algorithm graph on the top and rule based algorithm graph on the bottom.*

The optimizing algorithm always aiming for the optimal network situation can have both good and bad results: at 125 s the optimizing algorithm initiates a tap changer step to get the network maximum voltage near the allowed maximum value. At 140 s the real power generation of the DG3 is increased and the network maximum voltage exceeds the allowed limit. The limit is also exceeded with the rule based algorithm at this point,

but both the maximum voltage violation and the over-voltage area are larger with the optimizing algorithm since it had initiated a tap changer step up earlier and the rule based algorithm had not.

At 160 s the real power generation of the DG3 is increased again and the optimizing algorithm reacts immediately: it increases the reactive power consumption and curtails the real power generation of the DG3. These measures are able to return the network maximum voltage to the allowed level in less than 10 seconds. The rule based algorithm also reacts to this over-voltage, but it uses the active resources one by one, increasing the reactive power consumption as seen from the Figure 6.10.

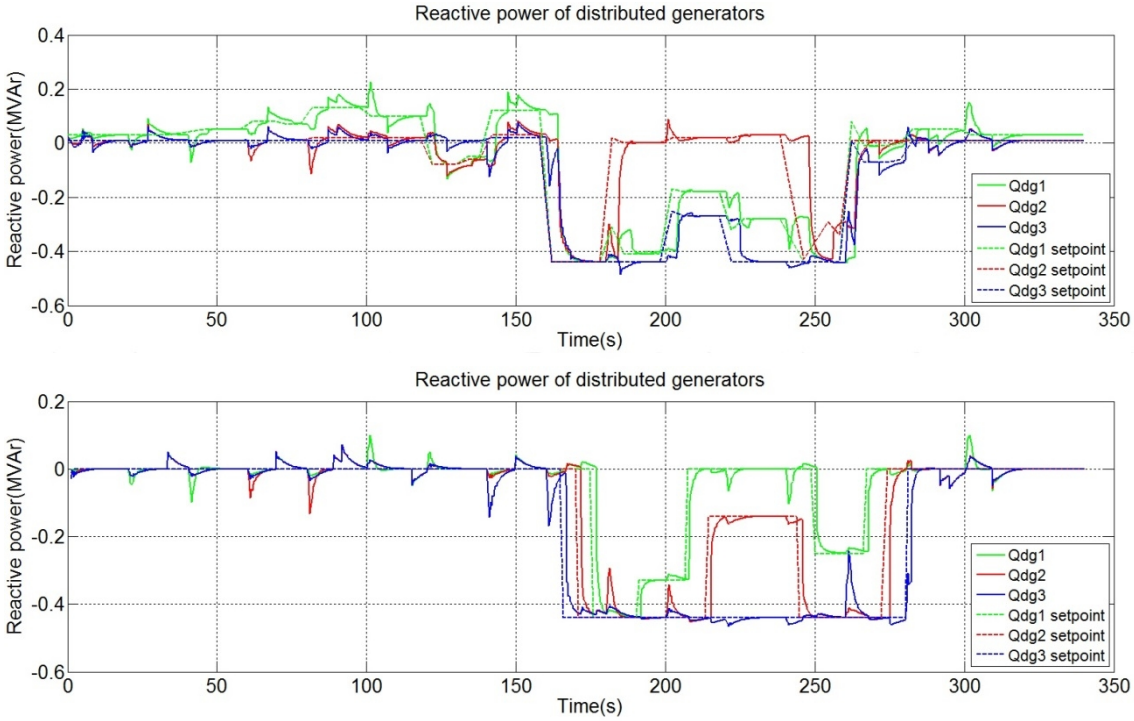

Figure 6.10 *Reactive powers of the DGs, optimizing algorithm graph on top and rule based algorithm graph on the bottom.*

However, since it takes 20 s for the rule based algorithm to change the set points of all three generators, there is no need for the production curtailment. The DG2s real power generation is decreased as a part of the sequence at 180 s and the network maximum voltage lowers.

When a situation like the one detailed above occurs, the target function value is lower with the rule based algorithm, but the optimizing algorithm is still working better, since it is able to return the network maximum voltage to the allowed level much faster. Number of the reactive power set point changes is much higher for the optimizing algorithm during this sequence. As can be seen from the Figure 6.10, the optimizing algorithm is changing set points during the whole sequence, but the rule based algorithm only between 160 s and 280 s. There are a lot of overreacting changes with the optimizing algorithm caused by the error discussed during the Sequence 1. If we consider there

being one faulty change per every correct change, we can half the number of changes to gain an approximation of the actual changes, but this number is still more than two times larger than the number of changes initiated by the rule based algorithm. Having more set point changes is not harmful as long as data transfer capacity is not exceeded, but it is good to notice this difference between the algorithms.

Since the algorithms have different priorities when they are calculating the set point values, they sometimes end up using different active resources in the same situation. This is visible on the Figure 6.10 around 180 s, when both algorithms start restoring the reactive power consumption of the DGs to the original level of 0 MVAr. The optimizing algorithm chooses the DG2 to be restored first and the DG1 second, but the rule based chooses the DG1 first and the DG2 second. The optimizing algorithm also adjusts the reactive power of the DG3 at the same time as the DG1s whereas rule based algorithm only adjusts one at time in order of the voltage sensitivity.

6.4 Sequence 4

During Sequence 4 the DG1 is moved to the Kihniö feeder so that there is generation on both of the feeders. The mechanical moment changes are the same as during the Sequence 2. Tables 6.8 and 6.9 include metrics for the comparison of the algorithms.

Since production is more equally divided between the feeders during this sequence, both algorithms can keep the voltages in control without any production curtailment. Because of this the target function value is only controlled by the network losses and the optimizing algorithm reaches a lower target function value in all of the cases except the Minimum case. During the Minimum case the optimizing algorithm is behaving irregularly: twice during the sequence it initiates a tap step only to reverse this action as soon as it is realized. There is also some irregularity with the reactive power set points, but this will be discussed in detail later in this chapter.

Table 6.8 *Optimizing algorithm results, Sequence 4.*

	Middle 1	Middle 2	Maximum	Minimum
Curtailed production (kWh)	0,0	0,0	0,0	0,0
Network losses (kWh)	10,4	9,9	8,2	12,6
Target function value (€)	0,4642	0,4425	0,3635	0,5603
Over-voltage area (pu * s)	0,5982	0,7565	0,5436	0,5202
Under-voltage area (pu * s)	0,0669	0,0902	0,1820	0,0070
Duration the voltage is out of bounds (s)	37,5031	37,8738	38,7608	37,5006
Average algorithm execution time (s)	1,0528	0,9809	0,9048	0,7117
Alerts (pcs)	0	0	0	0
OLTC steps taken (pcs)	12	12	12	15
P set point changes (pcs)	0	0	0	0
Q set point changes (pcs)	21	53	22	43

Table 6.9 *Rule based algorithm results, Sequence 4.*

	Middle 1	Middle 2	Maximum	Minimum
Curtailed production (kWh)	0,0	0,0	0,0	0,0
Network losses (kWh)	11,0	10,4	9,1	12,5
Target function value (€)	0,4928	0,4635	0,4073	0,5559
Over-voltage area (pu * s)	1,0383	1,1161	0,7503	1,2866
Under-voltage area (pu * s)	0,0000	0,0095	0,1509	0,0081
Duration the voltage is out of bounds (s)	46,9023	44,4642	74,0023	65,4900
Average algorithm execution time (s)	0,0077	0,0076	0,0091	0,0063
Alerts (pcs)	0	0	0	0
OLTC steps taken (pcs)	9	9	10	10
P set point changes (pcs)	0	0	0	0
Q set point changes (pcs)	5	7	8	3

Both of these irregularities are probably caused by the error discussed during the Sequence 1 results. The over-voltage area is smaller with the optimizing algorithm than with the rule based algorithm in all of the cases. In the Maximum case the over-voltage area of the rule based algorithm is greatly diminished compared to the other cases since a tap changer step is taken at 100 s, as seen from the Figure 6.11. This causes the voltage spike at 140 s to have a lower peak value than with the optimizing algorithm, but it also causes the network losses to be clearly larger with the rule based algorithm, since the maximum network voltage is more than 0,01 pu lower than the allowed maximum voltage between 100 and 140 s.

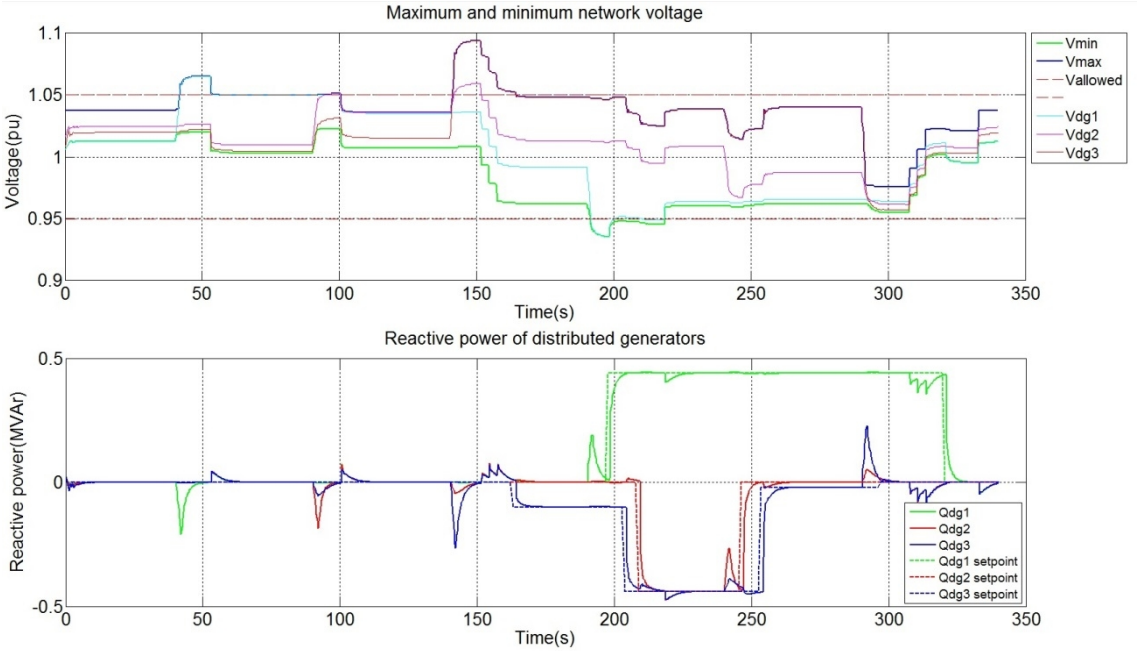

Figure 6.11 *Network voltages and reactive powers of the DGs, Maximum case, rule based algorithm.*

Figure 6.11 also explains why the voltage is out of bounds so long during the Maximum case when the rule based algorithm is used. When the minimum voltage drops at 190 s, the rule based algorithm increases the reactive power generation of the DG1 to the maximum, but this is not enough to bring the voltage within the allowed limits. Next the algorithm increases the reactive power consumption of the DG2 and DG3 to the maximum value to lower the maximum network voltage and to allow a tap changer step up to be taken. During all of these operations, which are executed one by one, the minimum network voltage is lower than the lowest allowed value.

The under-voltage area is clearly larger with the optimizing algorithm in all of the cases except the Minimum. During this sequence the optimizing algorithm is able to move the OLTC to the position 18 by compensating the drop in network minimum voltage with an increased reactive power generation at the DG1 and DG2. The rule based algorithm is only able to move to the position 17 and therefore the network minimum voltage is not as close to its limit as it is with the optimizing algorithm. When the real power generation of the DG1 is lowered at 190 s, the network minimum voltage drops below the minimum allowed limit, but this drop is larger with the optimizing algorithm, since it was operating closer to the limit already before the drop. This is presented using the Middle 2 case in the Figure 6.12.

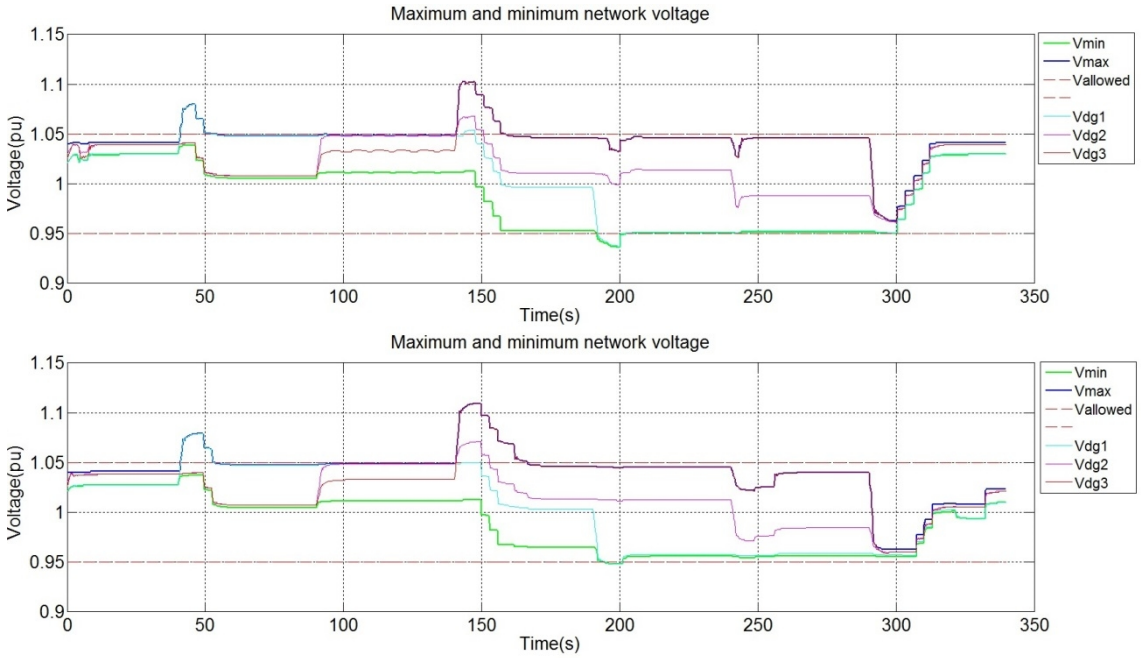

Figure 6.12 *Network voltages, optimizing algorithm graph on the top and rule based algorithm graph on the bottom.*

During the Sequence 4 there were irregularities with the optimizing algorithm in the Middle 2 and Minimum cases: there were a lot more reactive power set point changes than during the Middle 1 and Maximum cases, these have been marked red in the Table 6.8. More detailed analysis of these changes is illustrated in the Figure 6.13.

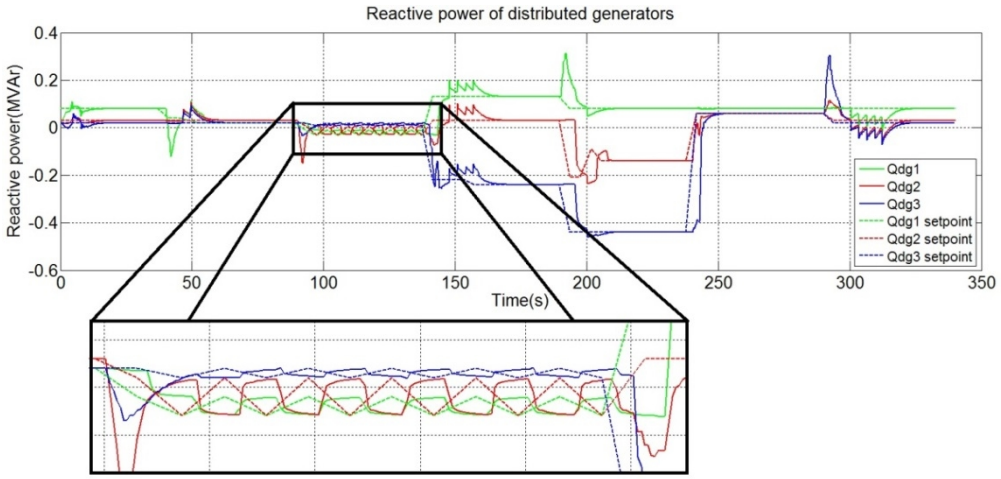

Figure 6.13 *Reactive powers of the DGs, optimizing algorithm, Middle 2 case.*

Between 90 s and 140 s the reactive power set point values of the DGs change multiple times between two discrete values. When the actual reactive power reaches the set point value, the algorithm concludes that the other position would be more optimal and again changes the set point value. This alternating behaviour continues until the real power generation increases at 140 s and the algorithm resumes action normally. It seems possible that this behaviour is caused by the same error in simulation network model that was discussed during Sequence 1 results, which causes the algorithm to inaccurately predict how much effect changing the real and reactive power set points has to the voltage levels. Since this behaviour is also observed during Sequences 9, 11 and 12, it is improbable that it is caused by having generation on both of the feeders.

Figure 6.14 shows the network voltages and the reactive powers during the Minimum case.

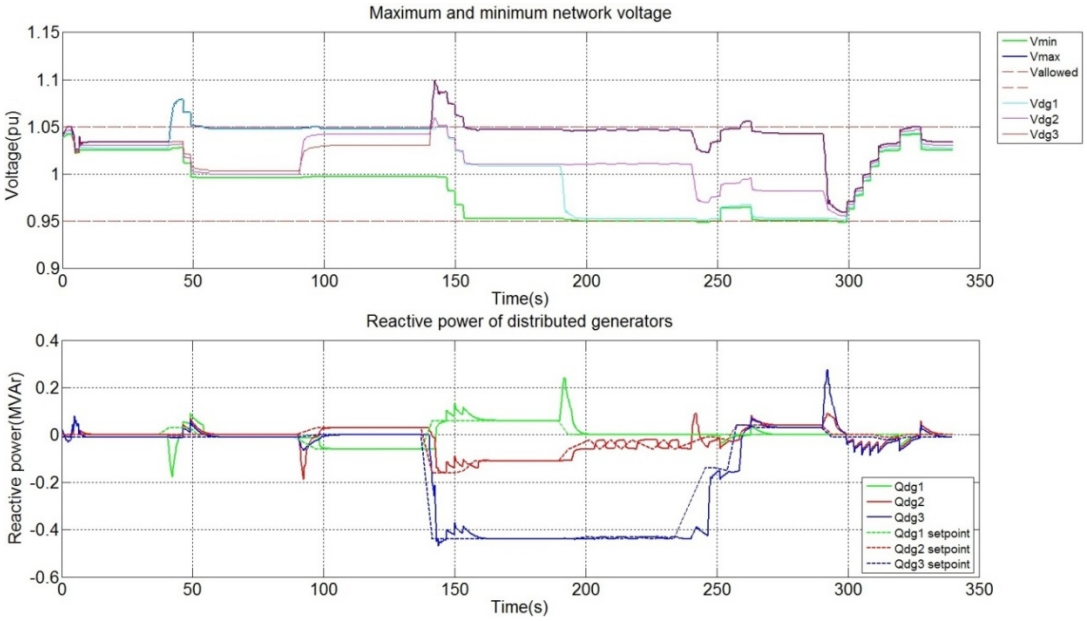

Figure 6.14 *Network voltages and reactive powers, Minimum case, optimizing algorithm.*

There were also more OLTC steps taken during the optimizing algorithm Minimum case than in the other cases. At first this seems like an error from the inaccuracy like the ones discussed before, but when results are more closely examined, it can be concluded that the optimizing algorithm is working just as intended. At 240 s when the DG2 real power production is decreased, the network minimum voltage drops barely below the allowed minimum value. This causes the algorithm to initiate a tap step and to decrease the reactive power consumption of the DG3 to increase the minimum voltage. After the voltage returns to normal levels, the algorithm concludes it can undo the tap step if it also stops the reactive power consumption with the DG3 and instead produces 0,5 MVAr. When it implements these changes, the maximum voltage temporarily increases higher than the maximum allowed limit, but returns to normal after the tap changer delay is over and a tap step is taken at 265 s. Here the optimizing algorithm causes small over-voltage due to the fact that it executes all of the control actions simultaneously, but the tap changer has a delay and the power set point change has no delay. There is also one extra tap step at the end of the sequence: algorithm initiates one more tap step after five previous ones, but is forced to undo it when the maximum network voltage reaches its limit. When data of the Figure 6.14 is observed, it appears that the maximum voltage had not yet stabilized when the optimizing algorithm initiated a tap step at 320 s, which caused it to make the false assumption that one more tap step could be taken.

6.5 Sequence 5

Sequence 5 is the same as the Sequence 4, except now the DG1 located on the Kihniö feeder is set to operate at 1,5 times the nominal real power generation to ensure the maximum network voltage is over the allowed limit on both of the feeders. Tables 6.10 and 6.11 include metrics for the comparison of the algorithms.

Table 6.10 *Optimizing algorithm results, Sequence 5.*

	Middle 1	Middle 2	Maximum	Minimum
Curtailed production (kWh)	0,0	0,0	0,0	0,0
Network losses (kWh)	13,6	12,9	10,8	16,1
Target function value (€)	0,6076	0,5755	0,4796	0,7177
Over-voltage area (pu * s)	0,7731	0,6737	0,6007	0,5411
Under-voltage area (pu * s)	0,0402	0,0732	0,1581	0,0015
Duration the voltage is out of bounds (s)	34,4477	35,8309	40,2616	24,8240
Average algorithm execution time (s)	1,0059	1,0152	0,9190	0,7405
Alerts (pcs)	0	0	0	0
OLTC steps taken (pcs)	12	12	12	13
P set point changes (pcs)	0	0	0	0
Q set point changes (pcs)	30	21	35	43

Table 6.11 *Rule based algorithm results, Sequence 5.*

	Middle 1	Middle 2	Maximum	Minimum
Curtailed production (kWh)	0,0	0,0	0,0	0,0
Network losses (kWh)	14,3	13,5	11,7	16,4
Target function value (€)	0,6363	0,6025	0,5226	0,7306
Over-voltage area (pu * s)	1,2872	1,1375	0,7618	1,1092
Under-voltage area (pu * s)	0,0000	0,0102	0,1489	0,0054
Duration the voltage is out of bounds (s)	43,6434	46,9848	62,0094	58,7501
Average algorithm execution time (s)	0,0076	0,0076	0,0091	0,0068
Alerts (pcs)	0	0	0	0
OLTC steps taken (pcs)	9	9	10	10
P set point changes (pcs)	0	0	0	0
Q set point changes (pcs)	5	7	8	5

Same as during the Sequence 4, neither of the algorithms needs to curtail any production. This time the optimizing algorithm also reaches smaller network losses and therefore smaller target function value in all of the cases despite the same error that was observed during the Sequence 4 causing extra reactive power set point changes in all of the cases except Middle 2. The over-voltage area is clearly smaller with the optimizing algorithm, but the under-voltage area is larger because the optimizing algorithm operates closer to the minimum allowed network voltage thanks to being able to take one more tap changer step than the rule based algorithm, same as during the Sequence 4. Figure 6.15 shows network voltages in the Middle 1 case of the Sequence 5.

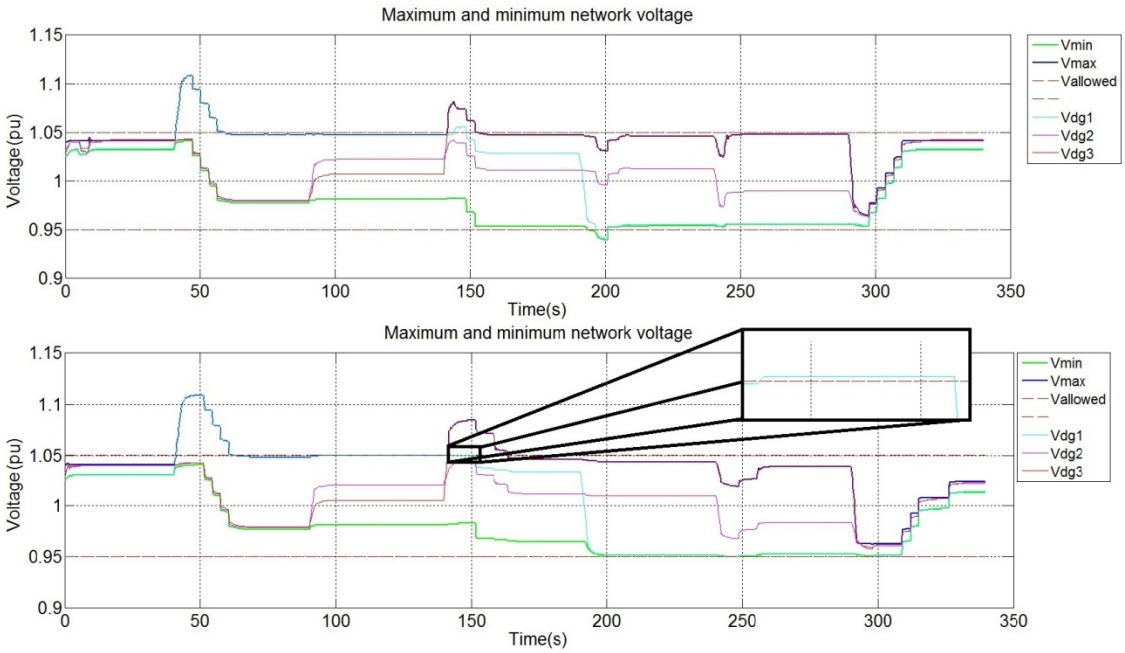

Figure 6.15 *Network voltages, Middle 1, Optimizing algorithm graph on the top and rule based algorithm graph on the bottom.*

As can be seen from Figure 6.15, both the DG1s and DG3s voltages are out of allowed limits after 140 s and since the DG1 is located on the feeder Kihniö, both feeders have over-voltage at the same time. Voltage on feeder Kihniö with rule based algorithm is only barely over the limit, but it would be enough to cause the algorithm to operate even if there were no over-voltage on the other feeder. The under-voltage limit is also violated in optimizing function case because the algorithm is operating closer to the limit than the rule based algorithm when DG1 decreases its real power production.

6.6 Sequence 6

During the Sequence 6 the mechanical moments of the DGs are raised from 0 to 1,00 pu using steps of 0,25 pu. The idea is to see how the algorithms react to smaller changes than the ones used during the previous sequences and to have a base case that can be compared to the Sequence 7 results. Tables 6.12 and 6.13 include metrics for the comparison of the algorithms.

Table 6.12 *Optimizing algorithm results, Sequence 6.*

	Middle 1	Middle 2	Maximum	Minimum
Curtailed production (kWh)	3,7	3,4	2,9	3,0
Network losses (kWh)	9,3	9,3	8,6	10,2
Target function value (€)	0,7165	0,6912	0,6234	0,7011
Over-voltage area (pu * s)	0,3560	0,4367	0,3298	0,4768
Under-voltage area (pu * s)	0,0000	0,0000	0,0000	0,0000
Duration the voltage is out of bounds (s)	55,1531	60,9960	43,5648	59,7697
Average algorithm execution time (s)	1,2169	1,1026	1,5258	0,8584
Alerts (pcs)	0	0	0	0
OLTC steps taken (pcs)	4	4	3	5
P set point changes (pcs)	2	1	2	2
Q set point changes (pcs)	30	36	37	30

Table 6.13 *Rule based algorithm results, Sequence 6.*

	Middle 1	Middle 2	Maximum	Minimum
Curtailed production (kWh)	2,6	2,5	2,2	2,3
Network losses (kWh)	9,6	9,5	9,0	10,5
Target function value (€)	0,6457	0,6276	0,5812	0,6559
Over-voltage area (pu * s)	0,6576	0,4974	0,5255	0,5332
Under-voltage area (pu * s)	0,0000	0,0000	0,0000	0,0000
Duration the voltage is out of bounds (s)	89,6704	86,3614	68,4751	90,0208
Average algorithm execution time (s)	0,0081	0,0081	0,0084	0,0083
Alerts (pcs)	0	0	0	0
OLTC steps taken (pcs)	4	4	3	5
P set point changes (pcs)	2	2	1	2
Q set point changes (pcs)	6	7	5	6

During this sequence the optimizing algorithm once again has smaller network losses, smaller over-voltage area and shorter time the network voltage is out of bounds in all of the cases. It also curtails more production thanks to the changes to the OLTC set point and the DG real and reactive power set points being implemented at the same moment, which in turn causes it to have a higher target function value. Difference between the algorithms in duration voltage is out of bounds is so large that the optimizing algorithm can be judged to perform better overall. Figures 6.16 and 6.17 are used to analyse the algorithms actions more closely.

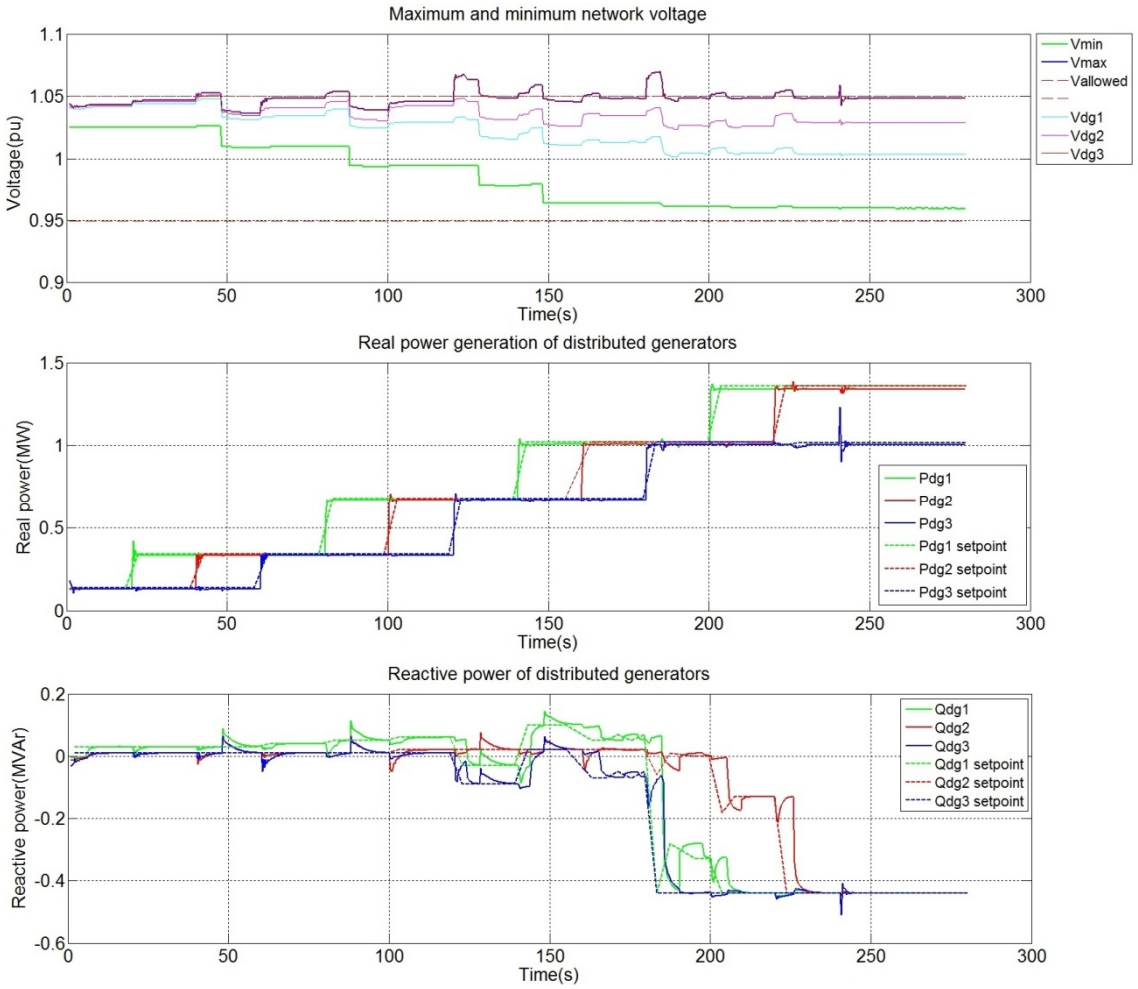

Figure 6.16 *Network voltages, real and reactive power generation, optimizing algorithm, Middle 1 case.*

In Figure 6.16 after the 120 s point the over-voltage is corrected with one tap step and by consuming reactive power with the DG2 and DG3. At 140 s when real power generation of the DG1 is increased, one tap step is again used but this time reactive power set points are all returned to positive values. After the tap step reactive power generation is needed to bring the network maximum voltage as high as possible to minimize the network losses. Therefore these cases where the reactive power set point values alternate

between positive and negative values while the real power production increases are part of optimizing algorithms operation and are not errors.

Around 180 s the optimizing algorithm decreases the reactive power set points of the DG1 and DG3. The same error that has been discussed during earlier sequences causes inaccuracy with the set point change, but this time with the DG1 the error is quite large: value first drops to -0,44 MVAR, but is soon corrected and sets around -0,34 MVAr. This causes small dip in maximum network voltage around 180s, but overall effect is still quite small.

Figure 6.17 presents the same graphs for the rule based algorithm.

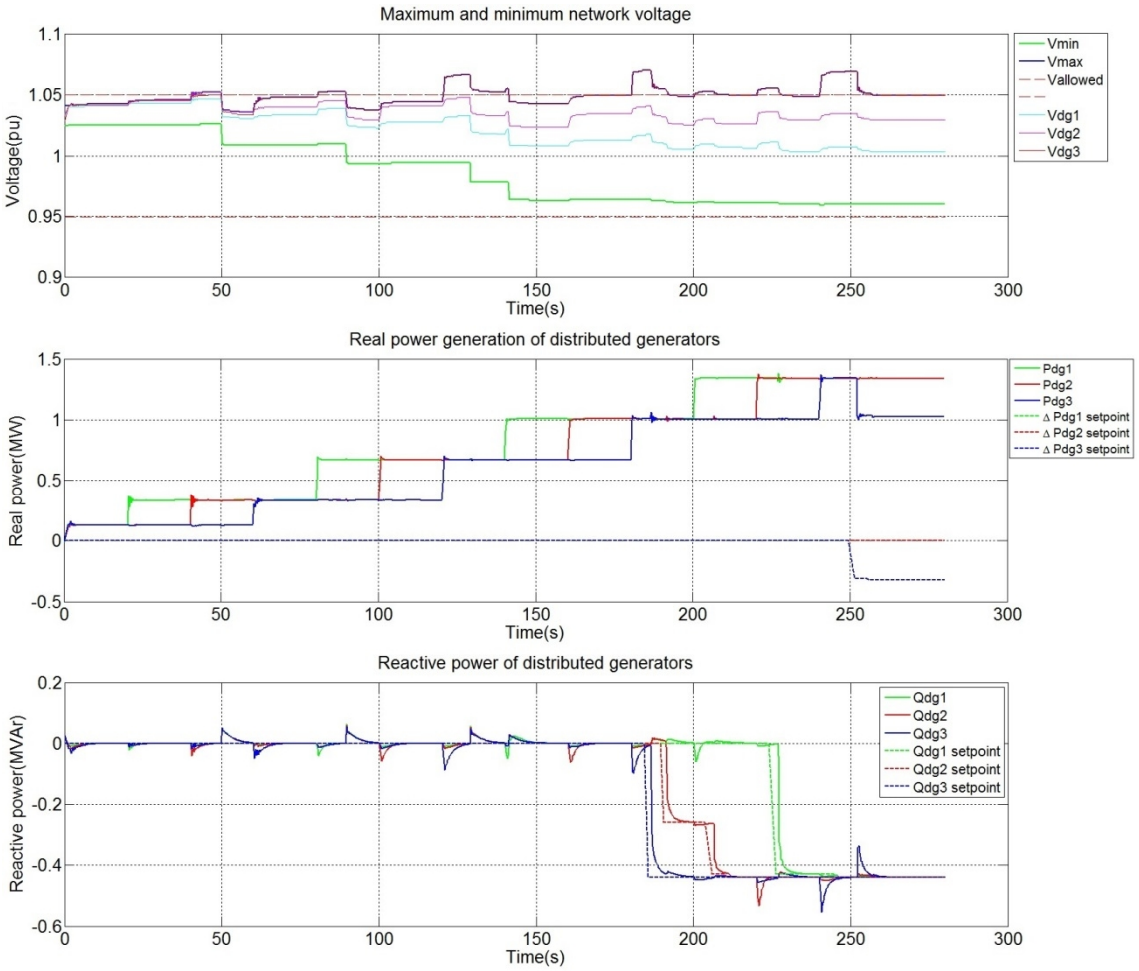

Figure 6.17 *Network voltages, real and reactive power generation, rule based algorithm, Middle 1 case.*

The rule based algorithm functions as expected, but there are two points worth mentioning: after 120 s when the DG3 real power output is increased, the algorithm initiates two tap steps. However, these are not both executed together but as two separate actions as can be seen from Figure 6.18.

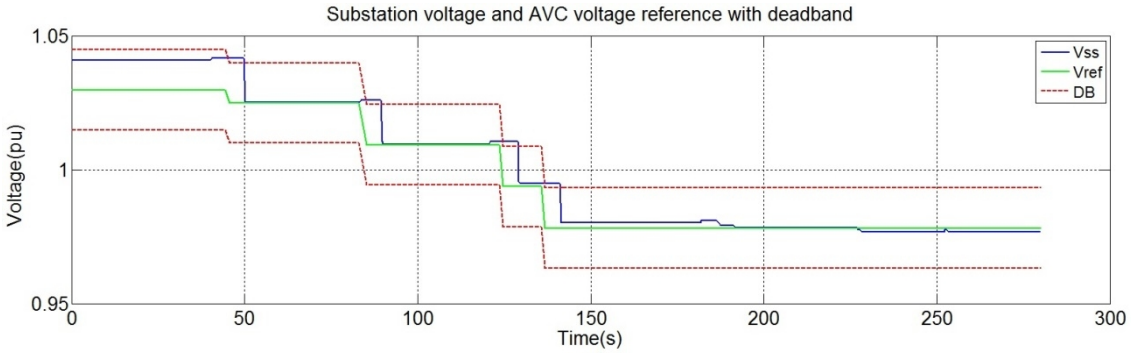

Figure 6.18 *Substation voltage reference and deadband.*

It is probable that the algorithm first concluded that one tap step would be enough to return the maximum voltage within the allowed limits. However, substation voltage does not reach exactly the value of voltage reference, but is instead a bit higher while still within the deadband after one tap step. When the algorithm is next executed, it initiates a second tap step. This inaccuracy could also be part of the problem discussed during the previous sequences, but this is the first time it affects the rule based algorithm. When the algorithm operates like this, the time while voltage is out of the allowed limits is increased since the two steps are executed as separate operations with separate delays.

Another point worth mentioning is the difference in time when the algorithms curtail real power production. The optimizing algorithm curtails production immediately at 240 s, but for the rule based algorithm this takes more than 10 seconds and during this time the maximum voltage is over the allowed limit. Since reactive power set point value of the DG1 was not at the maximum at 240 s, algorithm first moves it to the maximum value and only at next algorithm run after this change it starts the real power curtailment. Both of these actions have delays built in, causing the total reaction time to be much longer than with the optimizing algorithm.

6.7 Sequence 7

Sequence 7 has the same changes to the mechanical moments of the DGs as Sequence 6, but the load multipliers of the two feeders are also changed. Purpose of this sequence is to have the algorithms reach situation where they cannot anymore make any changes to improve network status while the network voltage is outside of its allowed limits. For this reason the real power curtailing has been disabled. Tables 6.14 and 6.15 include metrics for the comparison of the algorithms.

Table 6.14 *Optimizing algorithm results, Sequence 7.*

	Middle 1	Middle 2	Maximum	Minimum
Curtailed production (kWh)	0,0	0,0	0,0	0,0
Network losses (kWh)	22,9	24,4	17,3	17,2
Target function value (€)	1,0231	1,0878	0,7724	0,7680
Over-voltage area (pu * s)	2,8160	5,5695	6,0703	1,4180
Under-voltage area (pu * s)	0,1714	0,0000	0,0402	0,0000
Duration the voltage is out of bounds (s)	164,5278	181,6767	184,9019	107,6650
Average algorithm execution time (s)	1,2942	1,5246	1,5035	1,0902
Alerts (pcs)	31	36	36	16
OLTC steps taken (pcs)	4	3	4	5
P set point changes (pcs)	0	0	0	0
Q set point changes (pcs)	26	22	34	35

Table 6.15 *Rule based algorithm results, Sequence 7.*

	Middle 1	Middle 2	Maximum	Minimum
Curtailed production (kWh)	0,0	0,0	0,0	0,0
Network losses (kWh)	23,5	25,8	18,5	17,3
Target function value (€)	1,0491	1,1502	0,8260	0,7719
Over-voltage area (pu * s)	2,2114	3,6726	4,6211	1,5129
Under-voltage area (pu * s)	0,3229	0,0207	0,0000	0,0000
Duration the voltage is out of bounds (s)	179,6712	200,9605	192,0552	139,5783
Average algorithm execution time (s)	0,0072	0,0070	0,0072	0,0068
Alerts (pcs)	109	129	129	55
OLTC steps taken (pcs)	4	5	2	5
P set point changes (pcs)	0	0	0	0
Q set point changes (pcs)	7	4	7	6

Since the production curtailment has been disabled, target function value is formed only from the network losses. This allows the optimizing algorithm to reach a lower target function value in all of the cases. The duration voltage is out of bounds is again smaller with the optimizing algorithm, since it reacts faster to the over- and under-voltages, and both algorithms are unable to correct situation after the same moment. Unlike in most sequences this far, the over-voltage areas are larger when using the optimizing algorithm. This is caused by how the algorithms react when they encounter the limits of their capabilities. As can been seen from the Figure 6.19, in the Maximum case both algorithms encounter their limits at the same time, when the DG3 real power generation is increased at 220 s.

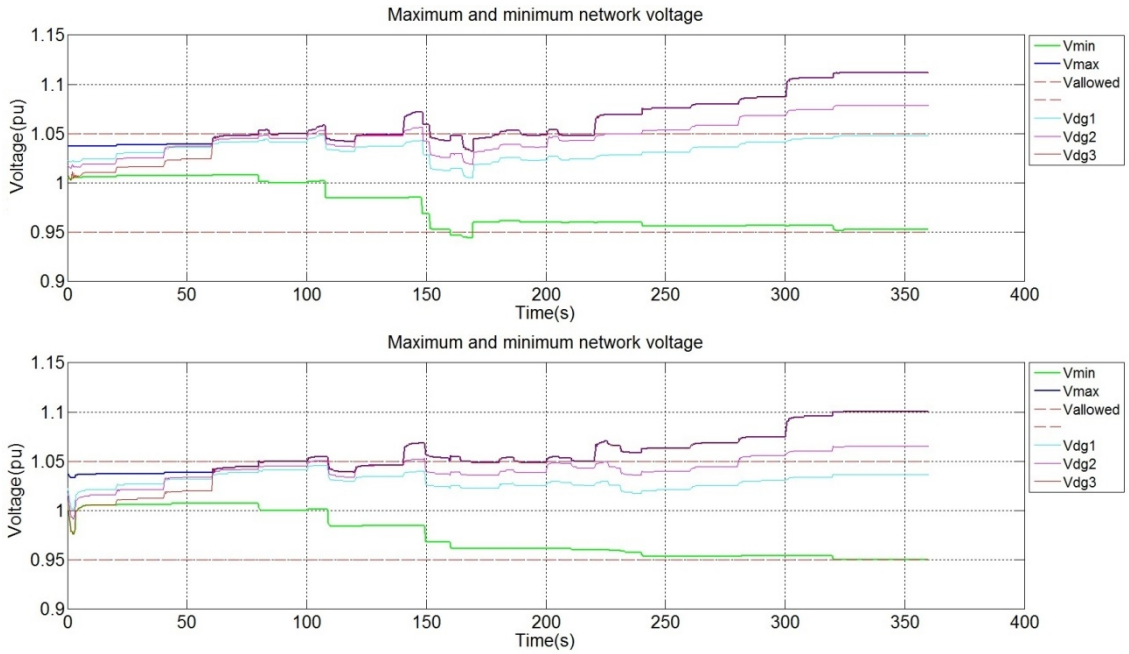

Figure 6.19 *Network voltages, Maximum case, optimizing algorithm graph on top and rule based algorithm graph on the bottom.*

Figure 6.20 shows reactive power graphs for the Maximum case and the difference in reaction between the algorithms when they cannot correct the over-voltage.

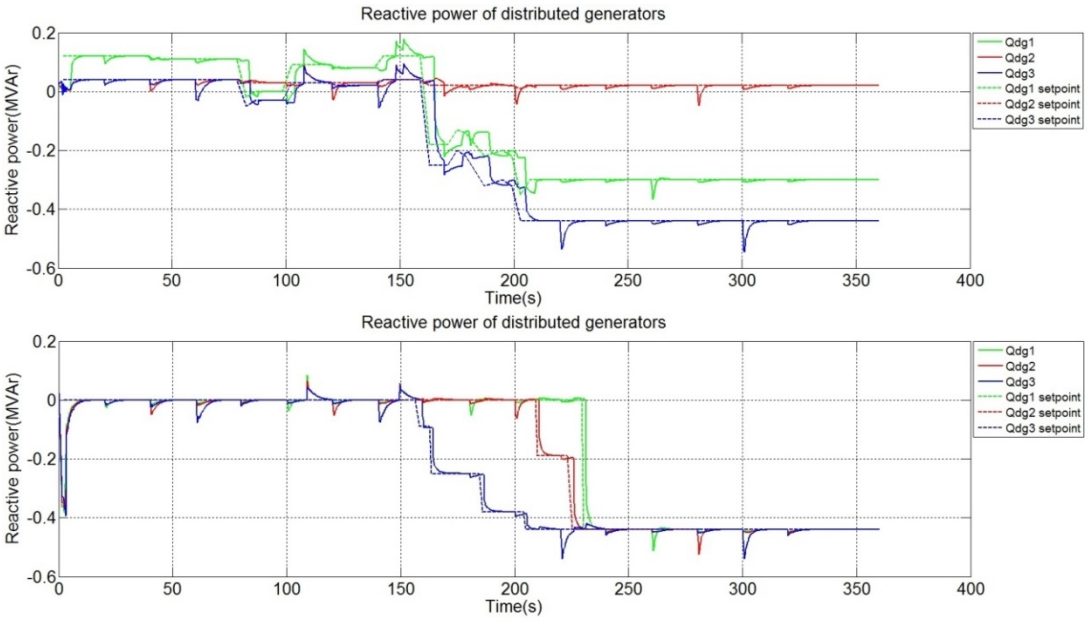

Figure 6.20 *Reactive powers, Maximum case, optimizing algorithm graph on top and rule based algorithm graph on the bottom.*

At this point the optimizing algorithm concludes that no solution can be found and outputs an alert message without executing any more control actions. The rule based algorithm keeps on initiating control actions until all of the three DGs have their reactive power consumption at the maximum value. Even though this won't return the maximum

voltage within the allowed limits, it reduces the violation enough to make a difference in the over-voltage area metric.

Both of the algorithms are built to not use the tap changer to lower the maximum network voltage if it would result in the minimum network voltage lowering below the allowed value. From voltage safety point of view it could be more beneficial to lower the voltage even if minimum voltage would drop too low. Therefore it might be beneficial to include a priority list for cases like these so that the algorithms would rather allow the minimum voltage limit to be violated than the maximum voltage limit.

6.8 Sequence 8

During the Sequence 8 a time delay has been implemented between the coordinated control part of the algorithm and the part that writes new reference values into the file. This is meant to emulate the algorithm handling a simulation of a much more complex network. Tables 6.16 - 6.19 include metrics for the comparison of the algorithms.

Table 6.16 *Optimizing algorithm results, Sequence 8, delay 4 seconds.*

	Middle 1	Middle 2	Maximum	Minimum
Curtailed production (kWh)	5,2	4,7	3,8	3,6
Network losses (kWh)	11,5	11,4	11,4	12,6
Target function value (€)	0,9426	0,8960	0,8180	0,8562
Over-voltage area (pu * s)	1,0620	1,2810	0,9164	0,9063
Under-voltage area (pu * s)	0,0000	0,0000	0,0000	0,0000
Duration the voltage is out of bounds (s)	48,0684	60,4793	38,2163	62,5718
Average algorithm execution time (s)	5,3372	5,3092	5,2017	4,8844
Alerts (pcs)	0	0	0	0
OLTC steps taken (pcs)	8	8	6	9
P set point changes (pcs)	7	4	4	3
Q set point changes (pcs)	21	25	21	24

Table 6.17 *Optimizing algorithm results, Sequence 8, delay 12 seconds.*

	Middle 1	Middle 2	Maximum	Minimum
Curtailed production (kWh)	4,2	5,3	4,7	2,2
Network losses (kWh)	11,4	11,5	11,2	12,8
Target function value (€)	0,8532	0,9499	0,8889	0,7568
Over-voltage area (pu * s)	2,4204	2,5778	2,3060	2,5313
Under-voltage area (pu * s)	0,0000	0,0000	0,0000	0,1289
Duration the voltage is out of bounds (s)	98,9510	116,0744	94,7776	147,7923
Average algorithm execution time (s)	13,2710	13,5073	13,3650	12,9343
Alerts (pcs)	0	0	0	0
OLTC steps taken (pcs)	8	8	6	11
P set point changes (pcs)	5	3	3	2
Q set point changes (pcs)	17	20	21	21

Table 6.18 *Rule based algorithm results, Sequence 8, delay 4 seconds.*

	Middle 1	Middle 2	Maximum	Minimum
Curtailed production (kWh)	4,5	4,0	3,1	0,0
Network losses (kWh)	11,9	12,0	12,0	13,2
Target function value (€)	0,9026	0,8654	0,7882	0,5880
Over-voltage area (pu * s)	2,1863	2,2414	2,1675	2,7921
Under-voltage area (pu * s)	0,0000	0,0000	0,0000	0,0000
Duration the voltage is out of bounds (s)	86,0201	106,3730	73,8170	99,4035
Average algorithm execution time (s)	4,0348	4,0358	4,0340	4,0325
Alerts (pcs)	0	0	0	0
OLTC steps taken (pcs)	7	6	6	8
P set point changes (pcs)	4	4	4	0
Q set point changes (pcs)	7	7	7	6

Table 6.19 *Rule based algorithm results, Sequence 8, delay 12 seconds.*

	Middle 1	Middle 2	Maximum	Minimum
Curtailed production (kWh)	0,3	0,0	0,0	0,0
Network losses (kWh)	12,4	11,9	11,8	12,3
Target function value (€)	0,5751	0,5320	0,5259	0,5506
Over-voltage area (pu * s)	4,1274	4,5434	3,5998	4,874
Under-voltage area (pu * s)	0,0000	0,0000	0,0000	0,0000
Duration the voltage is out of bounds (s)	179,2152	183,0786	123,4485	181,1141
Average algorithm execution time (s)	12,0818	12,0835	12,0789	12,0601
Alerts (pcs)	0	0	0	0
OLTC steps taken (pcs)	4	4	6	8
P set point changes (pcs)	2	0	0	0
Q set point changes (pcs)	5	6	6	4

The effects of the delay are presented for the rule based algorithm in the Figure 6.21 and for the optimizing algorithm in the Figure 6.22.

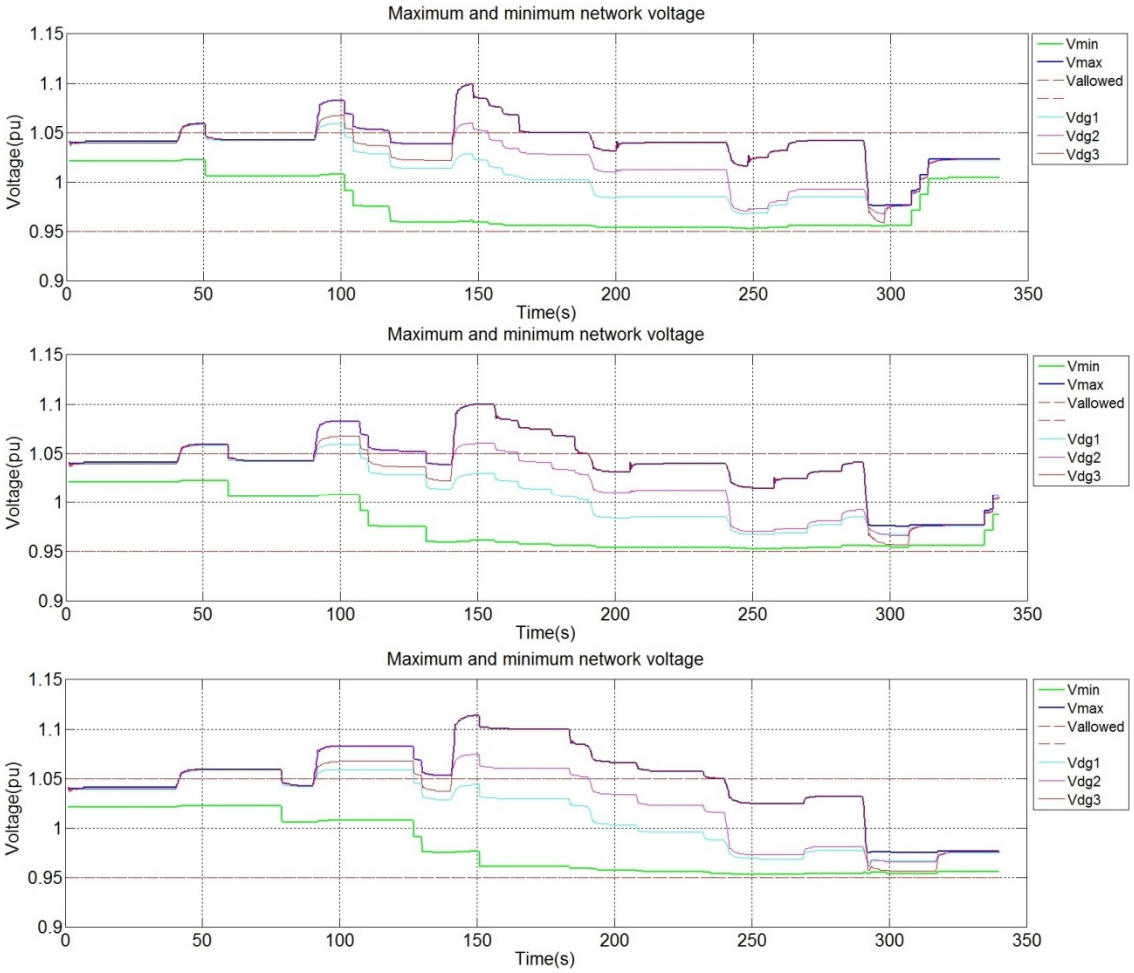

Figure 6.21 *Rule based algorithm, Middle 2 case; Sequence 2 on top, Sequence 8 with 4s delay in middle and Sequence 8 with 12 s delay on bottom.*

As expected, extra delay causes more harm to the rule based algorithm, since it uses the controllable resources one at time and because it already has a built in delay as part of the algorithm. This causes the duration voltage is out of bounds to be much longer and the over-voltage area to be much larger for the rule based algorithm. However, both algorithms having the same amount of delay is an unrealistic scenario. During the earlier sequences the average algorithm execution time of the rule based algorithm has been roughly hundred times faster than the average algorithm execution time of the optimizing algorithm. It is probable that the execution time of the optimizing algorithm also increases much faster when the network size is increased, since the optimization operation becomes much more complex while there are only as many new voltage sensitivity values added for the rule based algorithm as new connections are added to the network. Voltage sensitivities also only need to be calculated once per each unique connection setup of the network whereas optimization is run from the start every time.

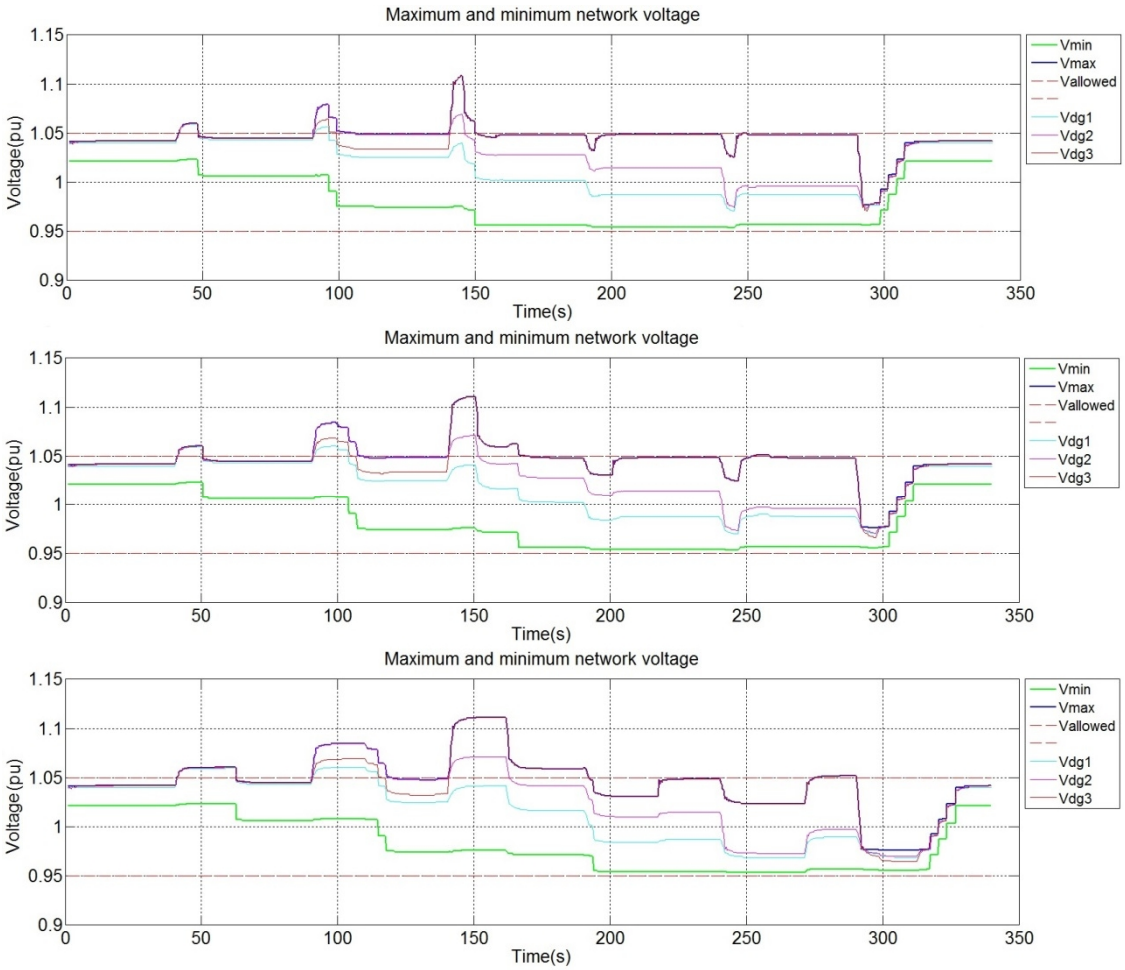

Figure 6.22 *Optimizing algorithm, Middle 2 case; Sequence 2 on top, Sequence 8 with 4s delay in middle and Sequence 8 with 12 s delay on bottom.*

The target function value actually decreases with the delay, but this is because the algorithms react slower to the over-voltages and therefore curtail less production during the sequence. Optimizing algorithm network losses are also smaller with larger delay in some of the cases, because the algorithm reacts slower to the over-voltages and network losses are inversely dependent of the network voltage. The same applies to the situations where network maximum voltage lowers and stays on lower value for the duration of the delay before the optimizing algorithm operates to increase the maximum network voltage. This in turn increases the network losses. The total effect of the delay on the network losses-metric depends on the balance between the cases where the voltage is either above or below the optimal value. Even though the delay doesn't affect the target function negatively most of time, it has a very bad effect on the over-voltage protection.

6.9 Sequence 9

Sequence 9 is the same as Sequence 2, but this time all of the loads in the network are modelled as static impedance loads instead of static power loads used in all the other sequences. This should be a lighter case for the algorithms, since the power consump-

tion of the load lowers as the voltage in bus connecting it lowers and increases when the voltage increases. Tables 6.20 and 6.21 include metrics for the comparison of the algorithms.

Table 6.20 *Optimizing algorithm results, Sequence 9.*

	Middle 1	Middle 2	Maximum	Minimum
Curtailed production (kWh)	5,4	4,7	3,9	3,1
Network losses (kWh)	11,4	11,4	11,0	12,8
Target function value (€)	0,9524	0,8985	0,8128	0,8246
Over-voltage area (pu * s)	0,5746	0,6033	0,5089	0,6752
Under-voltage area (pu * s)	0,0000	0,0000	0,0000	0,0509
Duration the voltage is out of bounds (s)	33,3497	36,0772	49,6953	53,2603
Average algorithm execution time (s)	1,2250	1,2981	1,2703	0,8997
Alerts (pcs)	0	0	0	0
OLTC steps taken (pcs)	8	8	6	11
P set point changes (pcs)	5	5	5	3
Q set point changes (pcs)	21	22	33	16

Table 6.21 *Rule based algorithm results, Sequence 9.*

	Middle 1	Middle 2	Maximum	Minimum
Curtailed production (kWh)	6,1	5,2	4,5	3,4
Network losses (kWh)	11,4	11,5	11,3	12,8
Target function value (€)	1,0117	0,9395	0,8731	0,8555
Over-voltage area (pu * s)	1,3158	1,2407	0,9939	1,6468
Under-voltage area (pu * s)	0,0000	0,0000	0,0000	0,0000
Duration the voltage is out of bounds (s)	63,5166	67,5364	42,3910	71,7030
Average algorithm execution time (s)	0,0108	0,0109	0,0098	0,0101
Alerts (pcs)	0	0	0	0
OLTC steps taken (pcs)	7	7	6	8
P set point changes (pcs)	4	4	4	4
Q set point changes (pcs)	7	7	6	6

When the metrics of the Sequences 9 and 2 are compared, it can be concluded that the load type does not affect the operation of the algorithms much. Network losses are a bit smaller during the Sequence 9 with the rule based algorithm, but there is almost no difference in the optimizing algorithm Middle cases. In Minimum and Maximum cases the differences are mostly caused by errors that will be discussed later in this chapter. It can be concluded that the load type affects rule based algorithm losses since the algorithm does not try to affect them. The optimizing algorithm already tries to control the network losses and therefore they already are at an optimal level. The state estimation model of the algorithms uses constant power load values instead of measurements during the sequence even though the loads are not constant power loads. In a real life application of the algorithm, it would most probably use load curve data improved with real

time measurements from AMR and other measuring equipment to create the state estimate.

Target function values of the rule based algorithm are higher during the Sequence 9, since the algorithm curtails more production than during the Sequence 2. This does not seem to improve the over-voltage area-metric or duration the voltage is out of bounds-metric, which are either higher or about the same as during the Sequence 2. With the optimizing algorithm differences are even smaller, with a little more curtailed production, but larger area- and duration-metric values during the Sequence 9.

Few irregularities were observed during the Sequence 9 optimization algorithm Middle 1 case: when the real power generation of the DG3 is increased at 90 s, the network maximum voltage increases above its allowed maximum value and the algorithm initiates two tap steps and orders the DG1 and DG2 to start consuming reactive power as seen in the Figure 6.23. At 105 s these changes have been implemented, but the maximum voltage is still barely over the allowed limit. At this point the algorithm orders one more tap step and removes the reactive power consumption from the DG1 and DG2. Since there is delay involved in the tap changer action, but the reactive power set point is changed immediately, the network maximum voltage rises near the value 1,06 pu for about five seconds before the tap changer operates and returns the voltage within the allowed limits.

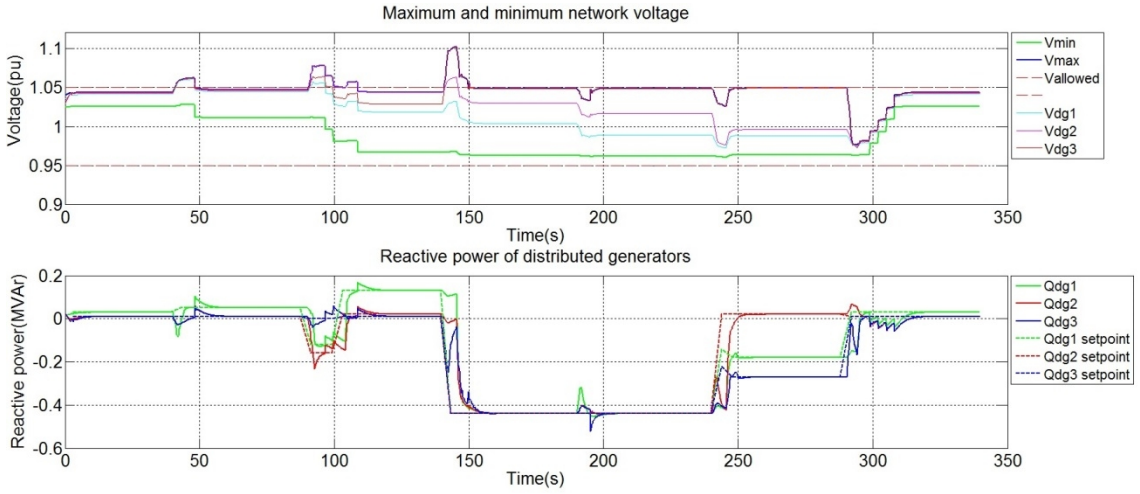

Figure 6.23 *Network voltages and reactive power generation, Middle 1 case, optimizing algorithm.*

This behaviour is probably caused by the same inaccuracy as discussed before: the algorithm assumed its actions before 100 s would be enough to return the voltage within the allowed limits. After 100 s it is forced to operate again and since the tap change has some delay, this action increases the voltage limit violation until the tap changer has operated.

During the optimizing algorithm Maximum case there were particularly many reactive power set point changes with the DG2 and DG3. This was caused by an alter-

nating behaviour between two set points similar to that observed during the Sequences 4 and 5. During the optimizing algorithm Minimum case there were more tap steps taken than during the other cases or during the rule based algorithm Minimum case. This also caused the under-voltage area metric to have a nonzero value as can be seen from Figure 6.24.

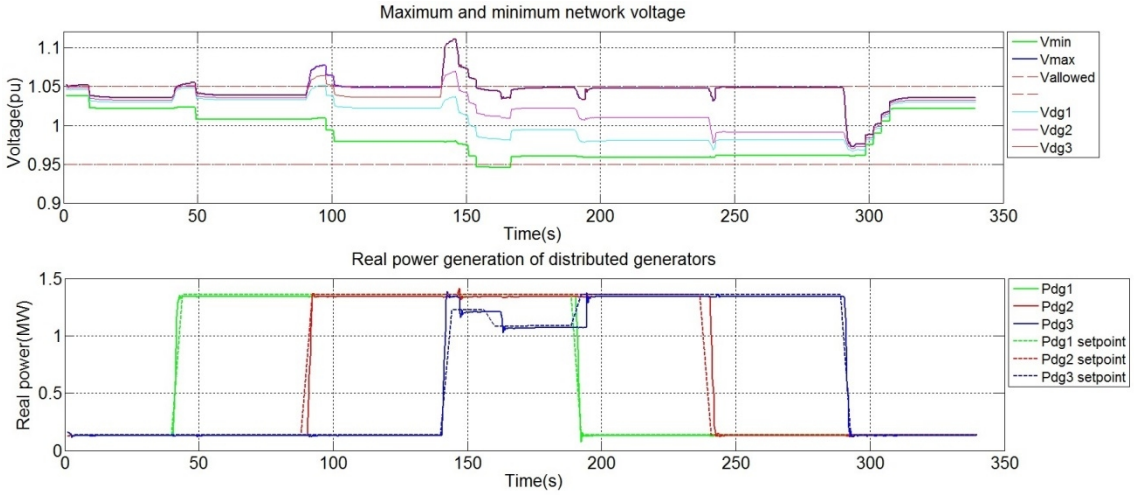

Figure 6.24 *Network voltages and real powers, Minimum case, optimizing algorithm.*

The algorithm initiated two tap steps and curtailed the DG3 real power production around 150 s to return the network maximum voltage within allowed limits. This however caused the network minimum voltage to decrease out of its allowed limits and the algorithm was forced to curtail more real power production to allow one tap step up. This returned the voltages within the allowed values, but the optimizing algorithm should have been able to find this optimal point immediately. Same as during earlier sequences, the small differences between the models are the probable cause for this behaviour.

6.10 Sequence 10

During Sequence 10 the three DGs were used to simulate wind power plants. This was achieved by exporting mechanical moment data from a PSCAD simulation and using it as an input for the generator models. Each of the DGs has its own set of data, which is different from two others, but same data sets are used for every case and both algorithms. The mechanical moment data is fluctuating quite much since the generators are simulating directly fed induction generators. Tables 6.22 and 6.23 include data from the simulations.

Table 6.22 *Optimizing algorithm results, Sequence 10.*

	Middle 1	Middle 2	Maximum	Minimum
Curtailed production (kWh)	15,6	14,1	17,7	16,3
Network losses (kWh)	3,7	3,3	3,1	4,1
Target function value (€)	1,4517	1,3059	1,5930	1,5279
Over-voltage area (pu * s)	0,4577	0,3283	0,1822	0,5490
Under-voltage area (pu * s)	0,0000	0,0000	0,0000	0,0000
Duration the voltage is out of bounds (s)	32,3143	25,6597	21,2211	48,6418
Average algorithm execution time (s)	0,3685	0,4811	0,4447	0,3678
Alerts (pcs)	0	0	0	0
OLTC steps taken (pcs)	24	20	21	26
P set point changes (pcs)	72	78	75	70
Q set point changes (pcs)	57	50	62	54

Table 6.23 *Rule based algorithm results, Sequence 10.*

	Middle 1	Middle 2	Maximum	Minimum
Curtailed production (kWh)	0,0	0,0	0,0	0,0
Network losses (kWh)	5,6	5,4	5,0	6,5
Target function value (€)	0,2477	0,2405	0,2222	0,2905
Over-voltage area (pu * s)	1,2079	1,6202	0,8302	1,4855
Under-voltage area (pu * s)	0,0000	0,0000	0,0000	0,0000
Duration the voltage is out of bounds (s)	87,0807	115,1525	67,3332	93,7910
Average algorithm execution time (s)	0,0039	0,0042	0,0037	0,0041
Alerts (pcs)	0	0	0	0
OLTC steps taken (pcs)	4	4	3	6
P set point changes (pcs)	0	0	0	0
Q set point changes (pcs)	0	0	0	0

During this sequence most of the metrics show that the optimizing algorithm is operating considerably better than the rule based algorithm: network losses, over-voltage areas and duration voltage is out of bounds are all considerably smaller with the optimizing algorithm. This is offset by the amount of curtailed production and control actions initiated by the algorithm: optimizing algorithm initiates approximately six times more tap changes, which means that during a sequence where voltages are fluctuating a lot, tap changer is continuously operating up and down between two or three values, as seen from the Figure 6.25. Target function value is also much larger with the optimizing algorithm, since it curtails production at multiple points.

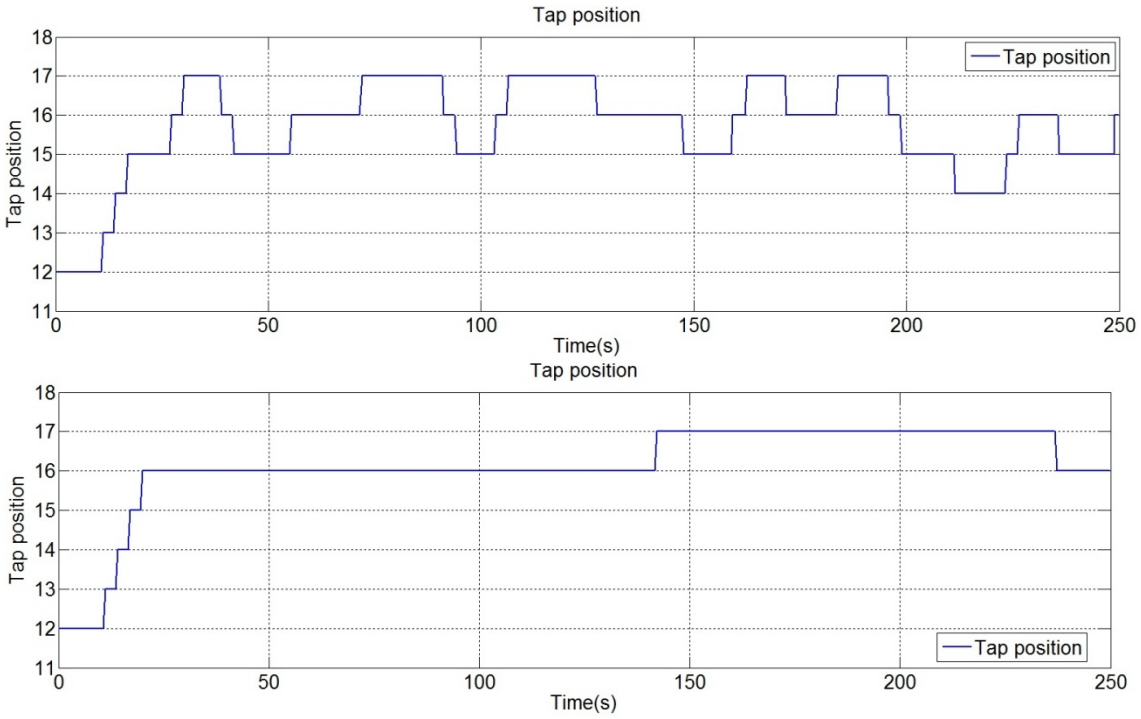

Figure 6.25 *Tap positions, Minimum case, optimizing algorithm graph on the top and rule based algorithm graph on the bottom.*

Reason for these tap changes the optimizing algorithm initiates can be seen in the Figure 6.26, which shows network voltages for both of the algorithm in the Figure.6.25's case.

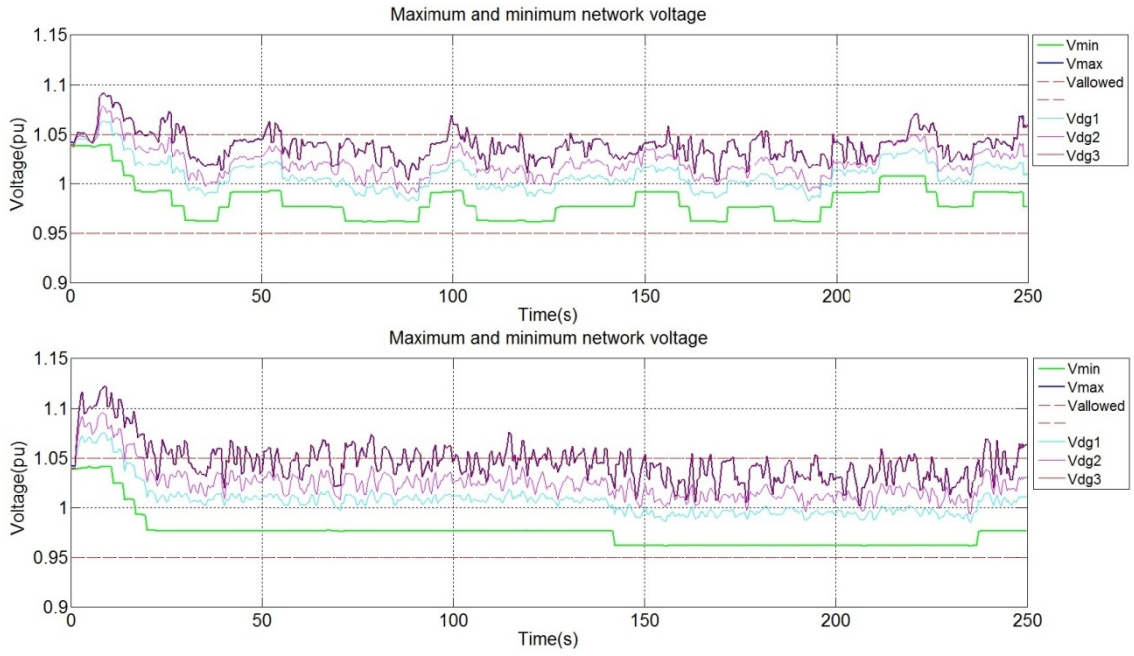

Figure 6.26 *Network voltages, Minimum case, optimizing algorithm graph on the top and rule based algorithm graph on the bottom.*

Every tap step is initiated according to the optimizing algorithm design principle: either to lower the voltage in case of the over-voltage or to increase it when the network maximum voltage drops more than a tap step away from its allowed maximum value. Therefore the algorithm is working exactly as intended when it is initiating tap steps. However, effects of the real and reactive power set point changes are not as easy to deduct. The Figure 6.27 shows real and reactive power graphs of the DG3 for the optimizing algorithm. The rule based algorithm did not initiate any changes to the real or reactive power, so these graphs are omitted.

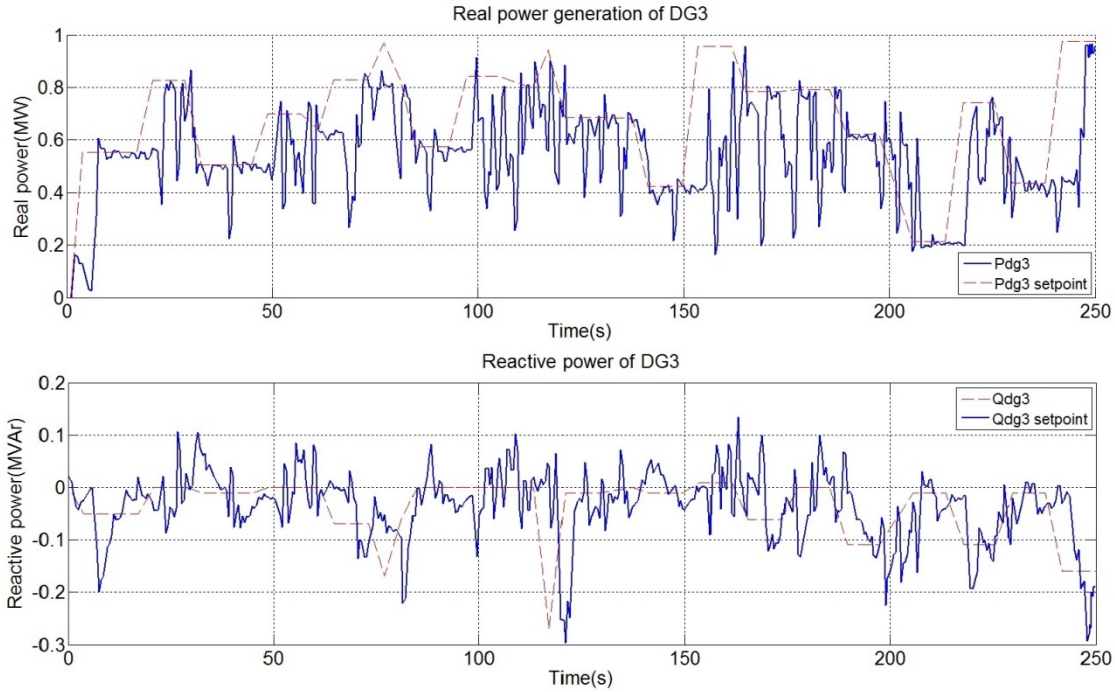

Figure 6.27 *Real and reactive power of the DG3, Minimum case, optimizing algorithm.*

The optimizing algorithm real power curtailment was executed a bit differently during this sequence compared to the other sequences: instead of reacting to the over- or under-voltages by liming the real power generation, real power changes that are part of the sequence were only executed if they kept the real power value under the value set by the algorithm. If a change would have set the real power value above the set point value given by the algorithm, the set point value was used instead. The algorithm did, however, receive information about the maximum moment available from the generator, which means it could also increase the set point value if network state allowed it. This way the algorithm itself prevents some of the fluctuations from happening during the sequence, but there was no way to execute this sequence the same way as the other sequences, since the mechanical moment is changing every second and it would always overwrite the real power curtailment if not executed this way. This also means that if a change sets the real power generation below the set point value given by the algorithm, this change is executed, since it presents a situation where the wind velocity is not enough to

produce most optimal amount of real power and the optimizing algorithm only calculates new optimal point once every 4 seconds.

From Figure 6.26 it can be seen that the four largest voltage violations during the sequence for the optimizing algorithm (excluding large violation right at the start of the sequence) are located at 25 s, 55 s, 100 s and 225 s. Right before each of these violations the optimizing algorithm has increased the real power set point value of the DG3 as seen from the Figure 6.27. The network maximum voltage is also located at the DG3 connection bus during the whole sequence, so changes to the DG3 affect the network maximum voltage directly.

The way the optimizing algorithm control is executed during this sequence means that at these four points mentioned earlier, the algorithm has either falsely concluded that it is advantageous to the network status to allow the larger real power generation or that the situation has considerably changed right after the change was executed. The result at every point is that the maximum voltage increases above the allowed maximum value and a tap changer action is executed by the algorithm to get the voltage within the allowed limits, resulting in the alternating behaviour of the tap changer observed in the Figure 6.25. It should also be noted that when the algorithm increases allowed real power generation of the DGs, it does not always immediately lead to the maximum voltage going out of the bounds.

With the rule based algorithm the network maximum voltage continuously rises above the allowed maximum limit between 20 s and 140s, but the algorithm only reacts to this after 140 s. Because the algorithm is designed to ignore fast transients, it only reacts when the network maximum voltage stays above allowed limit for a set duration and in situation like during this sequence it causes problems for the voltage safety. During a short moment when the network maximum voltage lowers at around 230 s, the restoring control undoes the earlier tap step, returning voltage to a level where there are constantly short limit violations.

6.11 Sequence 11

During Sequence 11 the optimizing algorithms iteration termination limits and iteration limits were changed to observe how this affects the operation of the algorithm. Tables 6.24 - 6.27 include metrics for the comparison of different limits.

Table 6.24 *Optimizing algorithm results, Sequence 11, E-4, 50 iterations.*

	Middle 1	Middle 2	Maximum	Minimum
Curtailed production (kWh)	5,6	4,8	4,0	4,0
Network losses (kWh)	11,2	11,5	11,5	12,7
Target function value (€)	0,9609	0,9116	0,8387	0,8960
Over-voltage area (pu * s)	0,5251	0,5382	0,5062	0,4492
Under-voltage area (pu * s)	0,0000	0,0000	0,0000	0,0000
Duration the voltage is out of bounds (s)	24,6924	31,3130	19,2140	34,0142
Average algorithm execution time (s)	0,6529	0,6375	0,6892	0,4806
Alerts (pcs)	0	0	0	0
OLTC steps taken (pcs)	8	8	6	9
P set point changes (pcs)	5	4	3	3
Q set point changes (pcs)	17	23	21	22

Table 6.25 *Optimizing algorithm results, Sequence 11, E-4, 500 iterations.*

	Middle 1	Middle 2	Maximum	Minimum
Curtailed production (kWh)	6,1	4,5	4,0	3,6
Network losses (kWh)	11,4	11,6	11,6	12,6
Target function value (€)	1,0123	0,8916	0,8437	0,8596
Over-voltage area (pu * s)	0,5138	0,5607	0,5031	0,5046
Under-voltage area (pu * s)	0,0000	0,0000	0,0000	0,0000
Duration the voltage is out of bounds (s)	33,7830	33,7162	19,1841	40,8387
Average algorithm execution time (s)	2,1119	1,6406	1,9311	0,7855
Alerts (pcs)	0	0	0	0
OLTC steps taken (pcs)	8	8	6	9
P set point changes (pcs)	4	5	3	4
Q set point changes (pcs)	20	21	19	21

Table 6.26 *Optimizing algorithm results, Sequence 11, E-8, 50 iterations.*

	Middle 1	Middle 2	Maximum	Minimum
Curtailed production (kWh)	10,5	4,8	3,6	3,9
Network losses (kWh)	11,5	11,6	11,5	12,8
Target function value (€)	1,3776	0,9144	0,8107	0,8911
Over-voltage area (pu * s)	1,4253	0,6762	0,7893	0,7872
Under-voltage area (pu * s)	0,0000	0,0000	0,0000	0,0000
Duration the voltage is out of bounds (s)	49,0568	40,5051	26,9333	57,8349
Average algorithm execution time (s)	1,068	1,1371	1,1612	0,9275
Alerts (pcs)	0	0	0	0
OLTC steps taken (pcs)	12	10	8	15
P set point changes (pcs)	4	5	4	3
Q set point changes (pcs)	26	26	25	32

Table 6.27 *Optimizing algorithm results, Sequence 11, E-8, 500 iterations.*

	Middle 1	Middle 2	Maximum	Minimum
Curtailed production (kWh)	5,6	4,6	3,8	3,0
Network losses (kWh)	11,4	11,5	11,4	12,8
Target function value (€)	0,9729	0,8924	0,8201	0,8219
Over-voltage area (pu * s)	1,0118	1,0165	0,9095	0,8310
Under-voltage area (pu * s)	0,0000	0,0000	0,0000	0,0925
Duration the voltage is out of bounds (s)	35,6870	46,6789	31,2911	60,6067
Average algorithm execution time (s)	3,4404	3,1270	3,0302	1,8338
Alerts (pcs)	0	0	0	0
OLTC steps taken (pcs)	8	8	6	11
P set point changes (pcs)	5	4	4	4
Q set point changes (pcs)	20	22	19	21

During Sequence 11 there was one irregularity observed: the production curtailed during the Middle 1 case with the iteration limit of 50 and the termination tolerance of E-8 is considerable larger than it should be. This is because the AVCO signal is blocking the algorithm from operating at the moment when the real power set point of the DG is changed as a part of the sequence. Since the algorithm is not running iteration to find a new optimal set point, an old set point value is instead used even though the production status has changed in the network. As can be seen from the Figure 6.28, this does not actually curtail any production since during this simulation the real power set point of the DG is only changed when the algorithm calculates a set point value that is different from the previous one or as part of the sequence. Moments when the AVCO signal blocks algorithm from changing the set points are at 90 s and 140 s, causing a noticeable difference between the real power of the DG and the set point value, as the set point is changed almost 10 s after the change of the real power value.

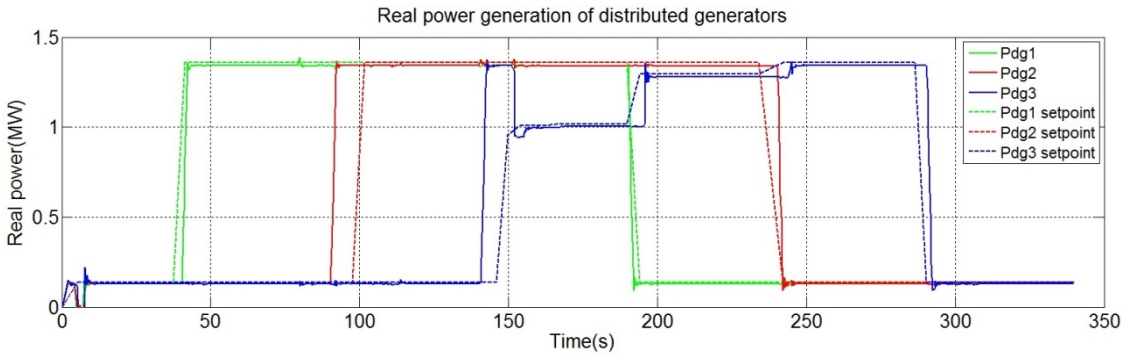

Figure 6.28 *Real power generation, Sequence 11, E-8, 50 iterations, Middle 1 case.*

Even though this does not directly affect how much production is actually curtailed, it does affect the curtailed production-metric, since this is calculated from the difference between the set point given by the algorithm and the real power value of the sequence. At 140 s it actually decreases the amount of the curtailment, since the DG3 stays at the nominal real power generation for about 10 s while the algorithm is blocked. This is the

only case during this thesis where AVCO signal is blocking the algorithm at the exact moment of the mechanical moment change and therefore the method for calculating curtailed production is not changed. This one case is considered non-comparable with other cases metrics wise, but it highlight important observation about how AVCO signal can harm the operation of the algorithm.

Increasing the maximum number of iterations from 50 to 500 increases the average algorithm execution time to 2-3 times the original value. Similarly changing the termination tolerance from E-4 to E-8 increases the average algorithm execution time to 1,5-2 times the original value. When data used to calculate the average algorithm execution time was closely examined, it was noticed that even though the average value stays below the execution cycle length of 4s, there are considerable differences between the individual execution times. When the iteration limit was 500 and the termination tolerance E-8, the longest execution time was around 8 s, but with 50 iterations and the same termination tolerance the longest time was around 2 s. This means that when the iteration limit is set to 50, the algorithm is always executed once every 4 seconds, but when the limit is set to 500, the algorithm is at some points executed only once every 8 s. This can strongly and negatively affects the duration voltage is out of bounds-metric and the over-voltage area-metric, as can be seen when results of 500 iteration and 50 iteration tables are compared.

On the other hand, when the iteration limit was set to 50 and the termination tolerance set to E-8, 3-7 times per sequence the algorithm stopped the iteration without reaching the most optimized solution because the iteration limit was exceeded, as can be seen from Figure 6.29.

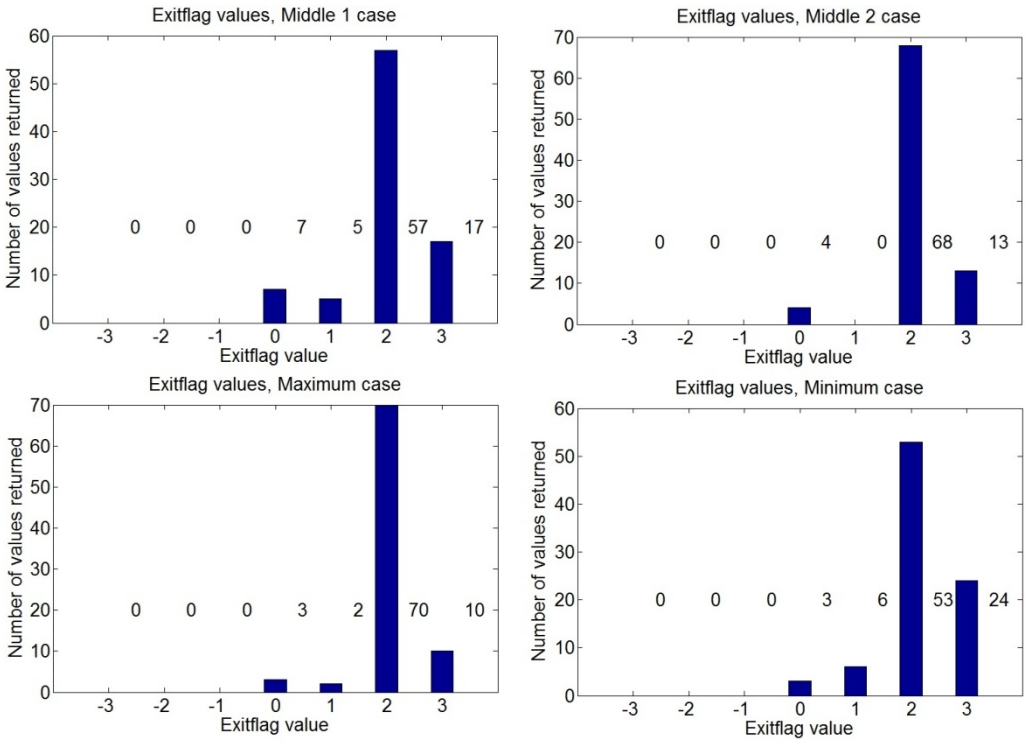

Figure 6.29 *Exitflag values, E-8, 50 iterations.*

Still, in all of these cases except the Maximum case (which is the irregular case discussed before), algorithm has a shorter time out of bounds-metric value and a smaller over-voltage area-metric value, but the target function value is larger. If the iteration is not completed successfully, the target function value is not the most optimized possible value, but from the over-voltage protection point of view, using this result can be even more preferable. The difference in the target function value is only about 1-2% in the Middle 2 and Maximum cases, but 8% in the Minimum case. In cases where the value being optimized is within allowed limits when the iteration limit is reached, the algorithm uses the end value from the optimization that was stopped before finding the most optimal value and does not output any alert message. Therefore these cases are not visible from the alert-metric in the metrics table, but only from the exitflag graphs.

Using a more strict termination tolerance has the same effect as having a larger iteration limit: it increases the average algorithm execution time which in turn increases the over-voltage areas and the duration the voltage is out of bounds. It can have positive effect on the target function value, but this is mostly caused by the algorithm curtailing less production because the optimization operation takes a longer time. Therefore the benefit gained from this is lost because of the negative effect to voltage safety.

Sequence 11 with the iteration limit of 50 and the termination tolerance of E-8 is different from the other three combinations: there are more OLTC steps taken, especially during the Minimum case. Figure 6.30 is used to elaborate this further.

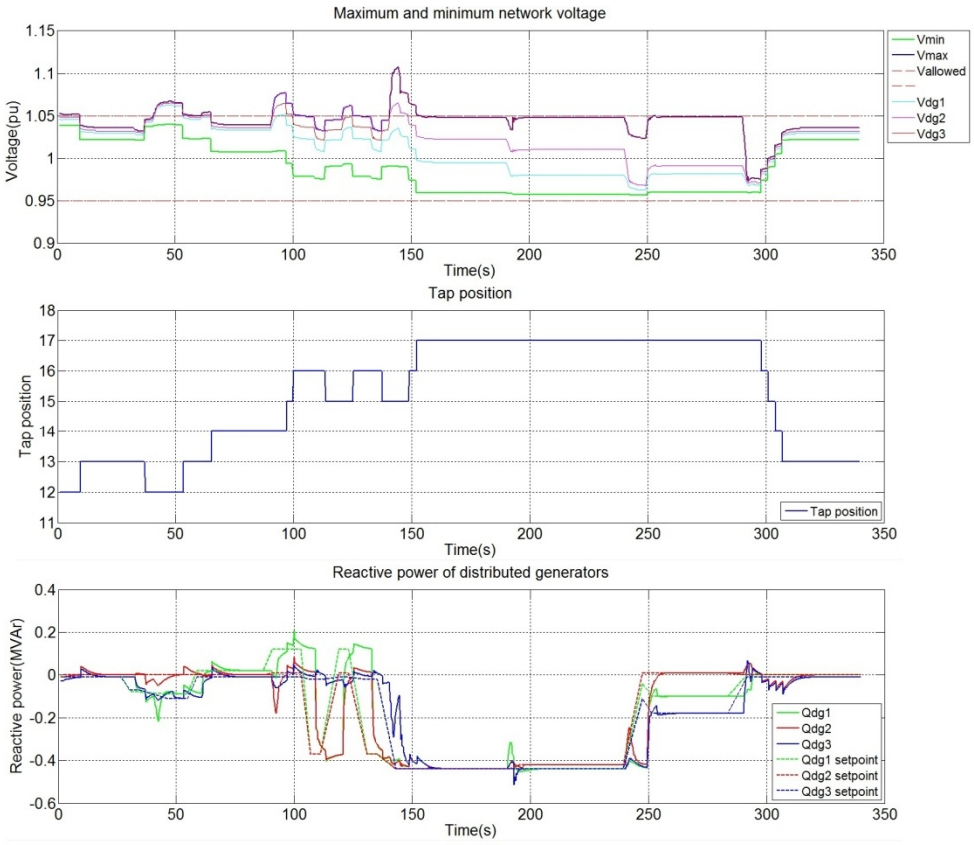

Figure 6.30 *Sequence 11, 50 iterations, E-8, network voltages, tap value and reactive powers, Minimum case.*

After getting the network maximum voltage within the allowed limits around 100 s by using the tap changer, the algorithm suddenly decides to start consuming reactive power with the DG1 and DG2 to allow the tap changer to return to the position 15. When these changes are implemented, it once again decides to move the tap changer to position 16 and to remove the reactive power consumption only to reverse these changes once more. This changing between two positions is very similar to the behaviour observed during the Sequence 4 and 5, and could be explained by the same accuracy error as discussed during the earlier sequences.

6.12 Sequence 12

During Sequence 12 the supply network strength is changed to see how this affects the algorithms. The supply network impedance is set to 50% and 200% of the original value of 48,341 Ω. Tables 6.28 - 6.31 include metrics for the comparison of the results.

Table 6.28 *Optimizing algorithm results, Sequence 12, 50%.*

	Middle 1	Middle 2	Maximum	Minimum
Curtailed production (kWh)	6,3	5,3	4,8	4,0
Network losses (kWh)	11,2	11,3	11,3	12,7
Target function value (€)	1,0225	0,9394	0,9017	0,8995
Over-voltage area (pu * s)	0,5665	0,6580	0,4988	0,5172
Under-voltage area (pu * s)	0,0000	0,0000	0,0000	0,0000
Duration the voltage is out of bounds (s)	30,6531	33,6195	19,9516	32,0958
Average algorithm execution time (s)	1,3856	1,3586	1,4182	0,9177
Alerts (pcs)	0	0	0	0
OLTC steps taken (pcs)	8	8	6	9
P set point changes (pcs)	4	4	3	3
Q set point changes (pcs)	20	19	29	15

Table 6.29 *Optimizing algorithm results, Sequence 12, 200%.*

	Middle 1	Middle 2	Maximum	Minimum
Curtailed production (kWh)	3,9	3,9	4,6	3,0
Network losses (kWh)	11,6	11,6	11,3	12,7
Target function value (€)	0,8397	0,8324	0,8784	0,8176
Over-voltage area (pu * s)	0,6433	0,6208	0,6634	0,6447
Under-voltage area (pu * s)	0,0000	0,0035	0,0242	0,0000
Duration the voltage is out of bounds (s)	37,2275	37,4846	42,0675	45,6746
Average algorithm execution time (s)	1,3003	1,2731	1,4042	0,8857
Alerts (pcs)	0	0	0	0
OLTC steps taken (pcs)	8	8	8	9
P set point changes (pcs)	5	3	6	3
Q set point changes (pcs)	22	33	19	34

Changing the supply network impedance does not have a strong effect on the network losses, they are smaller in 50% Middle 1 and Middle 2 cases, but of the same value in Minimum and Maximum cases. The impedance clearly affects the amount of curtailed production: in 200% case the amount of curtailment is lower than during 50% case in all of the cases. Increasing the supply network impedance also increases the over-voltage area-metric and duration the voltage is out of bounds-metric, but decreases the target function value since there is less production curtailment. The results of this sequence imply that smaller supply network impedance is more advantageous to the voltage safety, but as have been noticed during earlier sequences too, target function value is superior in the situation which is less favourable to the voltage safety, since less real power curtailment is used.

There were few irregularities with the optimizing algorithm during this sequence: same kind of an alternating behaviour as during some of the earlier sequences was detected during the 200% Middle 2 and Minimum cases and during the 50% Maximum case. During the 200% Maximum case voltage was out of bounds longer and there was more production curtailment than usually. This is depicted in Figure 6.31.

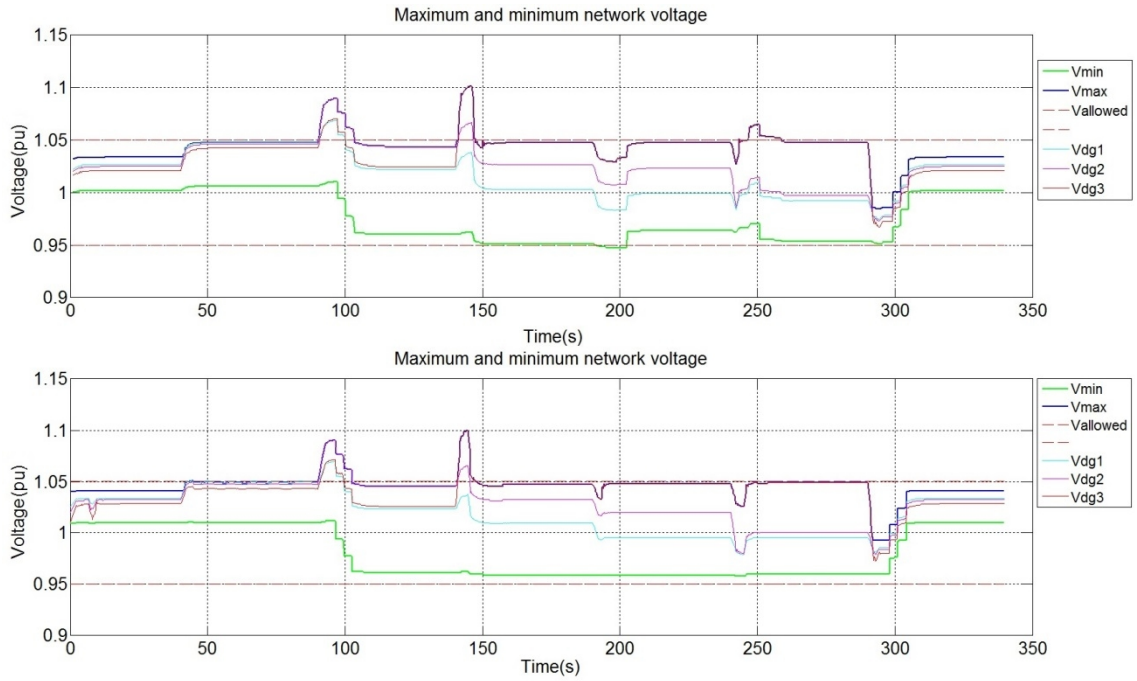

Figure 6.31 *Network voltages, Optimizing algorithm, Maximum case, 200% graph in the top and 50% graph on the bottom.*

As can be seen from the Figure 6.31, increasing the supply network impedance leads to lower network voltage values with the same initial parameters. In Maximum case this also leads the algorithm to operate closer to both of the voltage limits, which increases the duration the voltage is out of bounds, since the minimum voltage drops below the allowed value at 190 s when the DG1 output is decreased. Algorithm corrects this with a tap step, which it then undoes at 250 s. At this point it also decreases the reactive power

consumption to increase the voltage after the DG2 real power generation has been decreased. Because of the tap changer delay and inaccuracy with the reactive power set point, the maximum voltage limit is violated at this point until the tap changer has operated. This in turn affects the duration the voltage is out of bounds-metric and the over-voltage area-metric in the Maximum case.

Table 6.30 *Rule based algorithm results, Sequence 12, 50%.*

	Middle 1	Middle 2	Maximum	Minimum
Curtailed production (kWh)	6,4	5,5	5,1	3,7
Network losses (kWh)	11,5	11,6	11,5	12,6
Target function value (€)	1,0358	0,9728	0,9284	0,8648
Over-voltage area (pu * s)	1,2523	1,2855	1,0648	1,6008
Under-voltage area (pu * s)	0,0000	0,0000	0,0000	0,0000
Duration the voltage is out of bounds (s)	62,9461	65,1408	40,6558	73,6870
Average algorithm execution time (s)	0,0111	0,0105	0,0099	0,0106
Alerts (pcs)	0	0	0	0
OLTC steps taken (pcs)	7	7	6	8
P set point changes (pcs)	4	5	3	4
Q set point changes (pcs)	7	7	7	6

Table 6.31 *Rule based algorithm results, Sequence 12, 200%.*

	Middle 1	Middle 2	Maximum	Minimum
Curtailed production (kWh)	4,8	4,1	4,2	2,6
Network losses (kWh)	11,8	12,1	11,9	12,9
Target function value (€)	0,9190	0,8749	0,8787	0,7904
Over-voltage area (pu * s)	1,1569	1,1842	1,0188	1,7972
Under-voltage area (pu * s)	0,0000	0,0234	0,0302	0,0000
Duration the voltage is out of bounds (s)	51,5902	71,1705	63,7506	76,6039
Average algorithm execution time (s)	0,0103	0,0096	0,0096	0,0098
Alerts (pcs)	0	0	0	0
OLTC steps taken (pcs)	7	7	6	8
P set point changes (pcs)	4	4	2	3
Q set point changes (pcs)	6	6	7	7

The rule based algorithm results are similar to the optimizing algorithm results: increasing supply network impedance leads to smaller amount of curtailed production, larger network losses, smaller target function value and longer duration voltage is out of bounds. However, over-voltage areas are also smaller with 200% impedance in all cases except the Minimum case. At Middle 1 case duration the voltage is out of bounds is smaller in 200% case because only in this case the tap changer action at 90 s is accurately executed with three steps. In all of the other cases the algorithm first initiates two steps and the third one is executed separately when the algorithm notices that the two steps are not enough to correct the over-voltage.

The choice between the 200% and 50% impedance with the rule based algorithm is not as clear as it is with the optimizing algorithm. The duration the voltage is out of bounds is important metric for the voltage safety and for this the 50% impedance is the better case, but since in this case the over-voltage area metric is larger, the voltage violations are more severe. Target function value is always smaller in 200% case, but there are nonzero under-voltage metric values in 200% Middle 2 and Maximum cases.

7 DISCUSSION

This chapter is used to further explain the results presented in the Chapter 6 and to discuss their importance while ideas for the future development of the algorithms are presented. From the results of the simulations certain conclusions can be made: in all of the tested cases the actions of both of the algorithms were generally beneficial to the voltage, even though some small differences between the RSCAD network model and algorithms network model sometimes caused some extra actions; in none of the cases were algorithms unable to detect the over- or under-voltages or to react according to their design principles. There was some inaccuracy in the construction of the RSCAD model which caused the model to slightly differ from the model used by the Matlab algorithms. This caused the optimizing algorithm to often overreact when it enacted reactive power set point changes and sometimes when it curtailed the real power production. In reality knowing the precise electrical parameters of all the network components is also practically impossible and because of this, it is actually advantageous to observe how this inaccuracy affects the algorithms.

7.1 Algorithm comparison

Considering all the different metrics from the sequences, the optimizing algorithm was generally more efficient: in almost all of the cases it reacted faster, effectively having smaller over- and under-voltage areas and a shorter duration the voltage was out of the bounds. In most cases it also had smaller network losses, but its better efficiency also caused larger amount of real power generation being curtailed and therefore in many cases it had a larger target function value than the rule based algorithm. However this cannot be seen as a fault, since the primary function of the algorithm is to ensure the voltage safety in the network and the optimization of the costs included in the target function is a secondary objective.

The optimizing algorithm does have a one disadvantage compared to the rule based algorithm: since it aims to minimize the network losses, it keeps the network maximum voltage closer to its allowed limit than the rule based algorithm most of the time. This means that when the voltage rises fast, the resulting over-voltage spike has higher maximum value compared to the rule based algorithm. This could be taken into consideration by setting the maximum voltage value for the optimization below the maximum voltage value of the network, similarly as with the restoring part of the rule based algorithm, which returns the voltage to 1,04 pu or below while the maximum voltage limit is 1,05 pu. This would increase the network losses, but might be necessary to ensure the voltage safety in certain cases.

The optimizing algorithm tends to cause 10-30% more OLTC steps than the rule based algorithm. There are two primary reasons for this during the sequences: sometimes the optimizing algorithm initiates tap steps to get the network maximum voltage higher as a part of the optimization even though the voltage limits have not been violated. Also when recovering from a decrease of generation in the network, the optimizing algorithm tends to take more steps up than the rule based algorithm, which only aims to undo the changes it had initiated before while also keeping a safety marginal of 0,01 pu to the maximum network voltage limit as discussed before. This is evident during the end of the Sequence 2 and the other sequences that are based on it.

The loading of the network seems to have a distinct effect on the average algorithm execution time of the optimizing algorithm: in the Minimum load case the optimizing algorithm operates approximately 20-50% faster than during the other three cases in every sequence. For the rule based algorithm such differences are not observed.

The supply network strength affects the algorithm quite clearly as seen from the Sequence 12. During this sequence smaller supply network impedance seems more favourable for the algorithms, especially for the optimizing algorithm. However, this is not a parameter that can be affected much in a real life adaptation of the algorithm since it is governed by the transmission network structure.

7.2 Future development

There are still few functionalities missing from the optimizing algorithm that was tested during this thesis that have already been designed but not implemented. One of them is a limiter for the changes suggested by the algorithm. Since the optimizing algorithm always calculates the most advantageous solution for the network, sometimes the changes it suggests have a very small effect to the objective function value. To avoid the algorithm continuously making very small changes when the benefit from them is minimal, a minimum value is introduced for the change in the objective function value using a limiter presented in the Figure 7.1

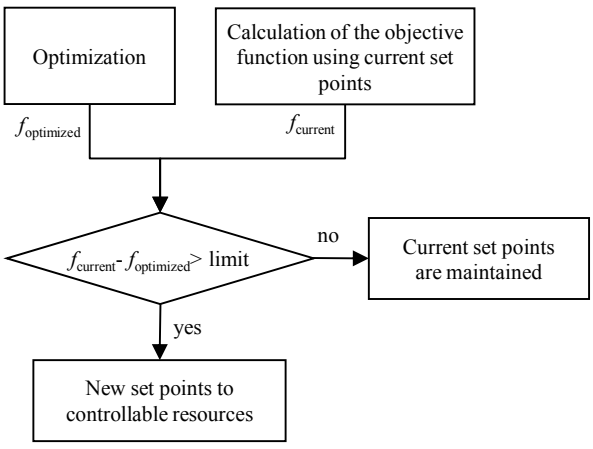

Figure 7.1 *The planned algorithm set point change limiter [28, p. 16].*

This algorithm part calculates the objective functions value using the current set points and the suggested new set points and only executes a set point change if the change in the objective function value is larger than a set limit. Since this part had not yet been implemented, the reactive power set point values suggested by the algorithm were rounded to the precision of two decimals and the real power values to the precision of three decimals. Had the limiter been implemented, it might have prevented some or all of the alternating behaviour observed during the Sequences 4, 5, 9, 11 and 12.

Another functionality missing from the optimizing algorithm is the ability to react when the optimization concludes that there is no way to bring voltages within the allowed limits. This was observed during Sequence 7: when the voltage could no longer be returned within the allowed limits, the algorithm did not initiate any changes to the controllable resources even though these changes could have reduced the severity of the voltage limit violation. Since the rule based algorithm is designed differently, it kept making changes until all of its controllable resources were used. This flaw in the optimizing algorithm could be fixed by implementing a part that would first recognize the situation from the alert message outputted by the optimization part, then figure out which limit is being violated (maximum voltage, minimum voltage or both) and then manually set all the controllable resources to their maximum value in the direction that helps to reduce the violation. Another possibility could be to run the algorithm with less strict voltage limits after it has outputted the alert message. The maximum voltage limit value could be increased and the minimum voltage limit could be decreased until the algorithm is able to converge into a solution. This solution would not bring the voltages within allowed limits, but it would use the resources optimally to bring the voltage violation to a lower level.

In the current implementations of the algorithms if the maximum voltage limit is violated, the algorithms are not able to use the tap changer to lower the network maximum voltage if this would bring the network minimum voltage to below the allowed value. When no point can be found where both network voltages are within the limits, it might be beneficial to allow lowering of the network maximum voltage with tap changer even when this brings the network minimum voltage below its allowed value, since over-voltage is a more severe voltage safety problem than under-voltage.

Other possibility of improvement for the optimizing algorithm could be to use soft limits by changing the optimization so that there are no absolute limit values between which the solution must be found but to incorporate the limits into the optimization target function. When calculating the optimal operation point, to the function value a component would be added which would increase the target function value when operating outside of the previously used hard limits. This would allow the algorithm to operate outside the hard limits when the situation requires it and by weighing the over-voltage situation with higher coefficient than the under-voltage situation, problems observed during Sequence 7 could also be mitigated and voltage safety improved. These limits could also be adjusted to fit each separate case so that it could be possible to di-

rect the algorithm to operate further from previous hard limits in cases where there are lots of fast transient or to rather allow the minimum voltage limit to be violated than the maximum limit when it is impossible to keep both of the values within the limits.

The effect of the termination tolerance and the maximum number of iterations allowed is considerable for the optimizing algorithm. Too large number of iterations leads to situations where the computational time of the algorithm exceeds the interval during which the algorithm is normally executed. On the other hand, a too small number of iterations allowed can lead to situations where no optimal solution is found. Even in these cases the optimizing algorithm usually makes changes that are still beneficial to the situation using the end value of the iteration that was stopped. The termination tolerance can also increase the computational time considerably or even prevent the algorithm from finding an optimal solution if it is set to be too strict and the differences between different solutions could be less than the variations resulting from the inaccuracy of the simulation model. Having a less strict termination tolerance decreases the computational time and the effects on the target function value are also quite small. Therefore it might be reasonable to keep the tolerance quite lenient.

In [28] it was explained that the optimizing algorithm could be used to replace the restoring part of the rule based algorithm and that it could only be implemented separately if the convergence of the iteration can be always guaranteed and the computational time remains reasonable. According to results received from this thesis's simulations, these requirements can be met at least in simple networks, but the termination tolerance of the iteration and the maximum number of iteration allowed should be adjusted in each case according to the situation. Another possibility for the implementation of the optimizing algorithm is to have both algorithms running parallel to each other and to pick the solution which is better for the situation. For this to be implemented, logic and priorities for the comparison of the suggested results needs to be developed.

The optimizing algorithm always executes the optimization with the presumption that the network situation is stable. It receives the real power set point values as inputs instead of the measured real power values, but the voltage value inputs are actual measured values. Because the network voltages do not instantly react to the production changes and because there is inertia involved when changing the power set points, at some points during the test sequences it was noticed that the optimizing algorithm initiated new control actions before the network state had stabled after previous actions or changes that were part of the sequence. In these cases the algorithm can create or enlarge the existing voltage limit violations or it can make unnecessary control actions, which it undoes soon after. However, the algorithm always corrects them when the network status becomes stable.

The biggest disadvantage of the rule based algorithm is its slowness when executing control actions. When there is a large change in the network state that requires actions from more than one active resource, the rule based algorithm reacts slowly, since it operates only one resource at the time. Use of the load flow part of the algorithm could be extended and the algorithm further developed so that it would implement all of

the needed changes at the same moment. The load flow could be calculated for the network state after the suggested change and if the results show that one change is not enough, more changes could be suggested until a feasible network status is confirmed by the load flow calculations. Only then would all of the changes be implemented at the same time. This would increase the execution time of the algorithm, but overall result could still be faster than making all the changes one at a time since there are delays included when making changes. Also during this thesis the rule based algorithm execution was already very fast, about 0,1 s in most cases, which is more than 10 times faster than the optimizing algorithm. Therefore even if execution time multiplies, it would probably still be easily acceptable.

The rule based algorithm also had multiple short over-voltages during the Sequence 10 that did not initiate any control actions. In a case where the real power generation is alternating as much as during the Sequence 10 it might be necessary to set the allowed maximum voltage value of the basic control parts of the algorithm to a lower value than the actual maximum to have a safety margin similar to the one that has been built into the restoring part of the algorithm. This would prevent short over-voltages mentioned before, but would also increase the network losses, since the voltage would be limited to a lower value. On the other hand algorithm not reacting to fast and small over-voltages can be seen as good thing since as can be seen from the optimizing algorithm results, this can lead to tap changer continuously stepping up and down, which leads to a need for more OLTC maintenance and increases the possibility of equipment failure.

7.3 Test planning evaluation

Most of the sequences were run as intended and the results are useful in planning of the algorithms further development, but the design of the Sequence 9 could have been improved in light of the gained results: during Sequence 9 constant impedance loads were used, but the state estimation of the algorithms was still executed with constant power load data. During all the other sequences this was no issue since the loads were modelled as constant power loads. It would not have been impossible to give the state estimator some meter readings from the RTDS and this would have been more realistic case considering the actual implementation of the algorithm, but this does not mean that the gained results are of no use. In current real life distribution networks loads are modelled using load curves and these are practically constant during short durations such as this thesis's sequences. Therefore the results emulate a situation where coordinated voltage control is implemented into a today's network without improved metering equipment, since there are no implementations of the AMR enhanced state estimation yet in use.

The simulation network model was mostly constructed as intended, but the unfortunate software bug in the RSCAD program forced the addition of a 10 μF capacitor to the lower voltage side of the primary transformer, which probably caused some small inaccuracy in the operation of the optimizing algorithm. However this can be seen as a

case where network parameters gained from the NIS are not 100% the same as the actual network parameters and is useful for observing how the algorithms react to this. Still, it would have been better at this point of testing of the algorithms to have a test network which is 100% the same as the model used in the algorithms.

While results from the metrics are at times contradictory, this reflects the nature of the algorithms. Voltage safety and minimization of the monetary losses are at times located at the opposite ends of the spectrum of possible control actions. In light of the results author does not have any improvements to suggest for the metric formulation.

8 CONCLUSIONS

During this thesis two coordinated voltage control algorithms were tested using the Real Time Digital Simulator. A test network model was constructed from data received from a real DNO using both PSCAD and RSCAD. The testing was conducted as a grey box testing and it was part of the algorithms development, the so called software-in-the-loop testing in a real time environment provided by the RTDS. The actual testing was carried out using 12 sequences, with the effect of changing different variables and settings being tested in each. The results were presented as graphs of the key values and as tables of metric values derived from the simulation data. The results were analysed and implications of the results were further discussed to form suggestions about the further development.

Both algorithms functioned as intended and never failed to recognize the voltage limit violations, but the optimizing algorithm is still missing some of the functions that are planned to be part of it. Because of this, the optimizing algorithm should be properly tested again after these functionalities have been implemented. The rule based algorithm is more complete, but even in this testing phase, the optimizing algorithm performed better than the rule based algorithm in most cases.

The major advantage of the optimizing algorithm is the fact that it executes all of the necessary control actions immediately whereas the rule based algorithm controls only one active resource at the time. This leads to much shorter duration the voltage is out of its limits, but also increases the amount of production curtailment used. However, since the voltage safety is the first priority, this cannot be seen as a fault. The execution time of the rule based algorithm was much faster than that of the optimizing algorithm. In any future application of the optimizing algorithm the termination tolerance and the iteration limit should be chosen to fit the situation, since they greatly affect the effectiveness of the algorithm.

The rule based algorithm could be developed further by increasing the use of the load flow functionality to decide all of the needed control actions and to execute them simultaneously. Other options include replacing the restoring control part of the rule based algorithm with the optimizing algorithm or using both algorithms at the same time and choosing the better result. This way the rule based algorithm could possibly reach the effectiveness of the optimizing algorithm without having the problems caused by the inaccuracy of network model data.

The optimizing algorithm had few problems too, especially when it faced a situation where it could no longer return the voltages within the allowed limits. This could be corrected by changing the hard optimization limits to soft limits implemented as part

of the target function or by adding a part that uses less strict limits when unsolvable situation is detected. Other problem was the optimizing algorithm displaying some hunting behaviour by continuously changing between two set points, but this could probably be corrected by implementing the target function value change limiter that has already been designed but not implemented.

The test model construction had some small problems which should be corrected for the possible further tests, but generally these did not invalidate the results gained. Some of the sequences could also have been slightly improved, but the end results of these simulations did satisfy the expectations: proper operation of the algorithms was confirmed and suggestions for the future development of the algorithms were made.

REFERENCES

[1] Leisse, I.; Samuelsson, O.; Svensson, J., "Electricity meters for coordinated voltage control in medium voltage networks with wind power," *Innovative Smart Grid Technologies Conference Europe (ISGT Europe), 2010 IEEE PES*, pp.1-7, 11.-13. October 2010

[2] Kulmala, A.; Mutanen, A.; Koto, A.; Repo, S.; Järventausta, P., "RTDS verification of a coordinated voltage control implementation for distribution networks with distributed generation," *Innovative Smart Grid Technologies Conference Europe (ISGT Europe), 2010 IEEE PES*, pp.1-8, 11.-11. October 2010

[3] Adine project home page, http://www.hermia.fi/in_english/services/coordination-of-programmes-and-p/adine/, [accessed on 5.4.2013]

[4] SGEM program home page, http://www.cleen.fi/en/sgem, [accessed on 5.4.2013]

[5] Grenard, S.; Pudjianto, D.; Strbac, G., "Benefits of active management of distribution network in the UK," *18th International Conference and Exhibition on Electricity Distribution, CIRED 2005*, pp.1-5, 6.-9. June 2005

[6] Bignucolo, F.; Caldon, R.; Prandoni, V.; Spelta, S.; Vezzola, M., "The Voltage Control on MV Distribution Networks with Aggregated DG Units (VPP), "*Proceedings of the 41st International Universities Power Engineering Conference, UPEC '06.*, vol.1, pp.187-192, 6.-8. September 2006

[7] Kiprakis, A.E.; Wallace, A.R., "Maximising energy capture from distributed generators in weak networks," *Generation, Transmission and Distribution, IEE Proceedings-* , vol.151, no.5, pp.611-618, 13. Sept. 2004

[8] Liew, S. N.; Strbac, G., "Maximising penetration of wind generation in existing distribution networks," *Generation, Transmission and Distribution, IEE Proceedings-* , vol.149, no.3, pp.256-262, May 2002

[9] Kulmala, A.; Mäki, K.; Repo, S.; Järventausta, P., "Including active voltage level management in planning of distribution networks with distributed generation," *PowerTech, 2009 IEEE Bucharest*, pp.1-6, June 28. 2009 - July 2. 2009

[10] Van Thong, V.; Belmans, R., "Maximum penetration level of distributed generation with safety criteria." *European transactions on Electrical Power*, vol.20, no.3, pp.367-381, April 2010

References

[11] Chowdhury, S. P.; Chowdhury, S.; Ten, C.F.; Crossley, P.A., "Operation and control of DG based power island in Smart Grid environment," *20th International Conference and Exhibition on Electricity Distribution - Part 1, 2009. CIRED 2009*, pp.1-5, 8.-11. June 2009

[12] Richardot, O.; Viciu, A.; Besanger, Y.; Hadjsaid, N.; Kieny, C., "Coordinated Voltage Control in Distribution Networks Using Distributed Generation", *Transmission and Distribution Conference and Exhibition* 2005/2006, IEEE PES, pp. 1196-1201, 21.-24. May 2006

[13] Xu, T.; Wade, N.; Davidson, E.; Taylor, P.; McArthur, S.; Garlick, W., "Case-Based Reasoning for Coordinated Voltage Control on Distribution Networks", *Electric Power Systems Research* 81(12): pp. 2088-2098, Year 2011

[14] Mummert, C. R., "Models for Var and power factor controllers added to IEEE 421.5," *Power Engineering Society General Meeting, 2005. IEEE* , pp. 977-979 Vol. 1, 12.-16. June 2005

[15] "IEEE Recommended Practice for Excitation System Models for Power System Stability Studies," IEEE Std 421.5-2005 (Revision of IEEE Std 421.5-1992) pp.14-15, 2006

[16] Gómez-Expósito, A.; Conejo, A.; Cañizares, C., "Electric Energy Systems Analysis and Operation" pp. 387-392, CRC Press 2008, ISBN: 978-0-8493-7365-7 (eBook: ISBN: 978-1-4200-0727-5)

[17] Donald, F.; Beaty, W., "Standard Handbook for Electrical Engineers, Fifteenth Edition" Chapter 10.1, McGRAW-HILL 2006, ISBN: 9780071441469

[18] Dawei, G.; "A novel thyristor assisted diverter switch for on load transformer tap changer", *Transmission and Distribution Conference and Exhibition 2002: Asia Pacific*, IEEE/PES, vol.1, pp. 297- 300, 6.-10. October 2002

[19] Kulmala, A.; Repo, S.; Järventausta, P., "Active voltage control — From theory to practice," *Integration of Renewables into the Distribution Grid, CIRED 2012 Workshop*, pp.1-4, 29.-30. May 2012

[20] Raipala, O.; Mäkinen, A.; Repo, S.; Järventausta, P., "The effect of different control modes and mixed types of DG on the non-detection zones of islanding detection," *Integration of Renewables into the Distribution Grid, CIRED 2012 Workshop*, pp.1-4, 29.-30. May 2012

References

[21] Kiprakis, A.E.; Wallace, A.R., "Maximising energy capture from distributed generators in weak networks," *Generation, Transmission and Distribution, IEE Proceedings*, vol.151, no.5, pp.611-618, 13. Sept. 2004

[22] Vovos, P.N.; Kiprakis, A.E.; Wallace, A.R.; Harrison, G.P., "Centralized and Distributed Voltage Control: Impact on Distributed Generation Penetration," *IEEE Transactions on Power Systems*, vol.22, no.1, pp.476-483, February 2007

[23] Mutanen, A.; Ruska, M.; Repo, S.; Järventausta, P., "Customer Classification and Load Profiling Method for Distribution Systems," *IEEE Transactions on Power Delivery*, vol.26, no.3, pp.1755-1763, July 2011

[24] Pakonen, P.; Vehmasvaara, S.; Pikkarainen, M.; Siddiqui, B.A.; Verho, P., "Experiences on narrowband powerline communication of automated meter reading systems in Finland" *Electric Power Quality and Supply Reliability Conference (PQ), 2012*, pp.1-6, 11.-13. June 2012

[25] Barker, P.; de Mello, R., "Determining the Impact of Distributed Generation on Power Systems: Part 1 - Radial Distribution Systems" *Power Engineering Society Summer Meeting, 2000. IEEE* , vol.3, pp.1645-1656, July 2000

[26] Mutanen, A.; Repo, S.; Järventausta, P., "AMR in distribution network state estimation", *8th Nordic Electricity Distribution and Asset Management Conference, Bergen, Norway*, September 8.-9. 2008

[27] Mutanen, A.; Koto, A.; Kulmala, A.; Järventausta, P., "Development and Testing of a Branch Current Based Distribution System State Estimator," *Proceedings of 2011 46th International Universities' Power Engineering Conference (UPEC),* pp. 1-6, 5.-8. September 2011

[28] Kulmala, A, SGEM Deliverable "D6.6.7: Specification of coordinated voltage control method for practical implementation", CONFIDENTIAL

[29] Matlab online help, http://www.mathworks.se/help/optim/ug/constrained-nonlinear-optimization-algorithms.html#brnpd5f [accessed on 7.3.2013]

[30] RTDS Technologies official webpage, www.rtds.com, [accessed on 9.1.2013]

[31] Lewis, W., "PCDA / Test", Part 2: Overview of Testing Techniques, Auerbach Publications, November 30. 1998, ISBN: 978-0-8493-9980-0 (eBook ISBN: 978-1-4200-4813-1)

References

[32] Demers, S.; Gopalakrishnan, P.; Kant, L., "A Generic Solution to Software-in-the-Loop," *Military Communications Conference, 2007, MILCOM 2007, IEEE*, pp.1-6, 29.–31. October 2007

[33] Adine project Deliverable 45: "Demonstration report on the use of new coordinated voltage control method", CONFIDENTIAL

[34] Dietrich, W.; "An international survey on failures in large power transformers in service", *Elctra*, (88): pp. 21-48, 1983

[35] Franzén, A.; Bertling, L.; "State of the art - life time modeling and management of transformers", pp. 7-8, Royal Institute of Technology, KTH, School of Electrical Engineering, RCAM, Stockholm, Sweden, August 2007,TRITA-EE 2007:041

[36] Matlab online help, http://www.mathworks.se/help/optim/ug/fmincon.html, [accessed on 7.3.2013]

[37] Tuominen, J., SGEM Deliverable "D6.6.12 RTDS simulation data of coordinated voltage control methods" CONFIDENTIAL